

AN EXPERIMENTAL STUDY OF THE SPIN-UP OF A
STRATIFIED FLUID

Kim David Saunders

B.S., Rose Polytechnic Institute
(1966)

SUBMITTED IN PARTIAL FULFILLMENT OF THE
REQUIREMENTS FOR THE DEGREE OF
DOCTOR OF PHILOSOPHY

at the

MASSACHUSETTS INSTITUTE OF TECHNOLOGY

and the

WOODS HOLE OCEANOGRAPHIC INSTITUTION

June, 1971

Signature of Author.....

Joint program in Oceanography,
Massachusetts Institute of Technology -
Woods Hole Oceanographic Institution,
and Department of Earth and Planetary
Sciences, and Department of Meteorology,
Massachusetts Institute of Technology,
June, 1971

Certified by..... Thesis supervisor

Accepted by.....

Chairman, Joint Oceanography Committee in the
Earth Sciences, Massachusetts Institute of
Technology - Woods Hole Oceanographic Institution

Archives





Room 14-0551
77 Massachusetts Avenue
Cambridge, MA 02139
Ph: 617.253.5668 Fax: 617.253.1690
Email: docs@mit.edu
<http://libraries.mit.edu/docs>

DISCLAIMER OF QUALITY

Due to the condition of the original material, there are unavoidable flaws in this reproduction. We have made every effort possible to provide you with the best copy available. If you are dissatisfied with this product and find it unusable, please contact Document Services as soon as possible.

Thank you.

Page 67 does not exist. A mis-numbering error by the author.

AN EXPERIMENTAL STUDY OF THE SPIN-UP OF A STRATIFIED FLUID

Kim David Saunders

Submitted to the Department of Meteorology on June 7, 1971 in

partial fulfillment of the requirements for the degree of

Doctor of Philosophy

A simple model of the spin-up of a continuously stratified fluid is examined both theoretically and experimentally. The geometry of the system is a right circular cylinder, bounded on the top and bottom by planes. A linearly stratified fluid is contained between the planes, rotating at an angular velocity $\Omega(1 - \epsilon)$. At $t = 0$, the rate of rotation is changed to Ω . The problem is to determine the way in which the fluid adjusts to the new angular velocity and how this differs from homogeneous spin-up. The theory is studied for the cases where the Rossby number is small, the Froude number is small, the Burger number is $O(1)$ and the side walls partially conducting. The results of previous investigators are compared and it is shown that Holton's theory for the interior flow is a special case of partially conducting side walls.

Experiments testing the validity of the linear theory were conducted. The Froude number was small, the Rossby number $O(E^{\frac{1}{2}})$, and the Burger number was $O(1)$. The side wall conditions were found to be effectively insulating. The experiments confirmed the qualitative aspect of the theory, showing that the fluid attains a quasi-steady state after a time of $O(\Omega^{-1}E^{-\frac{1}{2}})$, but not reaching a state of solid body rotation on that time scale. Quantitatively, it was shown that the first modal spin-up times are smaller than predicted, the discrepancy depending on the local Rossby number (the Rossby number based on the $E^{\frac{1}{2}}L$ length scale). This suggests non-linear effects in boundary layers of that length scale.

Thesis supervisor: Professor Robert C. Beardsley

TABLE OF CONTENTS

Title page	1
Abstract	2
Table of contents	4
List of tables	6
List of figures	7
List of plates	9
Acknowledgements	10
Dedication	12
Biographical note	13
1. Introduction	14
1.1 Geophysical motivation	14
1.2 Purpose of the thesis and description of the problem	14
1.3 Discussion of previous theory	16
1.4 Previous experiments	17
1.5 Outline for the remainder of the thesis	18
2. The linear theory	20
2.1 Formulation of the problem	20
2.2 Conventions	23
2.3 The linear problem	24
2.4 Solution of the interior problem	27
2.4.1 The quasi-steady Ekman layer condition	27
2.4.2 The $E^{\frac{1}{2}}$ buoyancy layer conditions on the interior flow	28
2.4.3 The form of the interior solutions	31
3. Description of the experiments	33

3.1 Description of the apparatus	33
3.2 The experimental method	37
3.3 Data analysis	38
4. Experimental results	41
4.1 Experimental parameters	41
4.2 Detailed description of one experiment (No.24)	42
4.3 General discussion of the temperature data	45
4.4 Conclusions and recommendations	48
Bibliography	51
Tables	54
Figures	60
Plates	102
Appendix I	110
Appendix II	116
Appendix III	124
Appendix IV	130

LIST OF TABLES

Table No.	Title	Page
1	Experimental Parameters	54
2	Data Usage	56
3	Temperature Perturbation Data for Experiment 24	57
4	Experimental Parameters which do not vary from experiment to experiment	59

LIST OF FIGURES

Figure No.	Title	Page
1	Geometry of the Problem	60
2	Thermistor Locations	61
3	Location of the Experiments in Rossby number - Burger number space	62 63
4	Location of the experiments in Ekman number - Burger number space	64
5	Temperature data for thermistor 1, Expt. 24	65
6	" 2 "	66
7	" 4 "	67
8	" 5 "	68
9	" 6 "	69
10	" 7 "	70
11	" 8 "	71
12	" 10 "	72
13	" 11 "	73
14	" 12 "	74
15	" 13 "	75
16	" 14 "	76
17	" 15 "	77
18	" 16 "	78
19	" 17 "	79
20	" 18 "	80
21	" 19 "	81

Figure no.	Title	Page
22	Temperature data for thermistor 20, Expt. 24	82
23	Angular position of a float at $r=1.08$	83
24	Angular velocity of a particle at $r=1.08$	84
25	Vertical Structure of the reciprocal spin-up times, Experiment 24	85
26	Vertical Structure of mode 1, Expt. 24	86
27	Integrated amplitude for all experiments	87
28	Reciprocal spin-up times vs. B for all experiments	88
29	Plot of the relative deviations from the linear theory vs. the local Rossby number	89
30	Schematic diagram of the test cell	90
31	Schematic diagram of the temperature control system	91
32	Camera control	92
33	Temperature measurement system	93
34	Typical interface circuit	94
35	Bias and impedance matching circuitry	95
36	Frequency changer	96
37	60 Hz band reject filter	97
38	Low pass filter	98
39	Camera driving circuitry	99
40	Perturbation density field at an early stage of spin-up, computed from a numerical model	100
41	A typical fit of the perturbation temperature field	101

LIST OF PLATES

Plate No.	Description	page
1	Photograph of the apparatus	102
2	Detail of the test section	103
3	Detail of the table drive	104
4	The mercury slip rings	105
5	Photograph of the camera interface	106
6	Photograph of the camera trigger	107
7	Photograph of the frequency changer	108
8	Photograph of the filter board	109

ACKNOWLEDGEMENTS

I would like to thank Professor Robert C. Beardsley for his support and encouragement over the past few years. His availability and the many discussions we had were greatly appreciated. I would also like to thank the other members of my committee: Professors MØllø-Christensen and Howard and Dr. McKee for their help and advice. I also found discussions with Professors Greenspan, Barcilon and Malkus very helpful. The nine months spent in Professor Baker's laboratory were invaluable. Professor Edmond was kind enough to give me the use of GAUSHA.

Dr. J.C. Van Leer taught me a great deal about practical engineering design, and Al Bradley and Dave Nergaard taught me almost all I know about electronics. Their help was inestimable and I thank them all.

I would like to acknowledge the work done by the Athbro company of Sturbridge in building the turntable and the fine jobs of building equipment by Ed Bean of the Meteorology Department machine shop and the people of the Earth and Planetary Sciences Department machine shop.

Discussions with Drs. Cacchione and Knox and Bruce Magnell, Chris Welch and John Festa were useful and appreciated.

My wife, Barbara, is especially to be thanked for her help and patience with my thesis work while she was working on her own. My dog, Schnapps, is also thanked for her encouragement every evening when I came home.

This work was supported under National Science Foundation Grant GP 5053. Their support is gratefully acknowledged.

This thesis is dedicated to the memory of my grandfather,
Hugh Keough and to my mother and father. They gave me a thirst
for knowledge which I hope will never be quenched.

BIOGRAPHICAL NOTE

The author was born in Chicago, Illinois on January 21, 1945. He attended the Flossmoor Public Schools, the Homewood-Flossmoor High School and Rose Polytechnic Institute, from which he received his B.S. degree in 1966. He married Barbara Breidenbach in 1968.

1. INTRODUCTION

1.1 Geophysical motivation

The process where a rotating fluid changes from one state of rotation to another is known as "spin-up". Recently, this has been of interest in an astrophysical problem: Is the interior of the sun rotating at a faster rate than the surface? The answer to this question is of vital importance in determining the validity of the Brans-Dicke (1964) scalar-tensor theory of general relativity. This is a spin-down problem with the entire sun initially rotating rapidly and being slowed down by the torque of the solar wind. (See also Dicke, 1970) The spin-up process is of geophysical interest in problems relating to the time response of the oceans, the atmosphere and the earth's core to external forcing.

1.2 Purpose of the thesis and description of the problem

The purpose of this thesis is two-fold:

1. to provide experimental results which describe the time

dependent motion of a rotating, continuously stratified fluid for a simple set of initial and boundary conditions, and

2. to compare the results with a simple linear theory, indicating the limits of validity of the model.

As mentioned in 1.1, stratified, rotating, time dependent fluid motions are of major concern in any study of the oceans or atmospheres. In order to apply mathematical models to these systems, it is necessary to determine the limits of the theory. One useful method is the laboratory experiment. Heretofore, most problems of the stratified, rotating, time dependent type have been studied theoretically as a two layer system with viscosity or a continuously stratified system without viscosity. The problem considered in this thesis incorporates both viscosity and continuous stratification.

The geometry of the problem consists of a right circular cylinder, bounded by two planes at right angles to the axis of symmetry of the cylinder, rotating at an angular velocity $\underline{\Omega}(1-\epsilon)$ coincident with the axis of the cylinder and antiparallel to the gravity vector. This is illustrated in figure 1. A stably, linearly stratified, viscous fluid is contained in the cylinder. At some time, the angular velocity of the container is changed by a small amount from $\underline{\Omega}(1-\epsilon)$ to $\underline{\Omega}$, The problem is to determine the temporal and spatial structure of the flow which this change of rotation causes.

1.3 Discussion of previous theory

Greenspan and Howard (1963) were the first to carefully study the problem of homogeneous spin-up. They found the adjustment time for a homogeneous fluid to reach a new state of solid body rotation was $O(\Omega^{-1}E^{-\frac{1}{2}})$. The spin-up is accomplished by the conservation of angular momentum in the interior as fluid from greater radii replaces fluid removed from the interior by the Ekman suction. Greenspan and Weinbaum (1965) studied the non-linear theory for the homogeneous case. They found the spin-up times were not greatly affected by Rossby number below 0.5 and that the sign of the deviation of the non-linear spin-up time was opposite the sign of the Rossby number.

The stratified problem was first studied by Holton (1965), who derived the correct interior equations and Ekman layer conditions for the linear problem. He chose unrealistic boundary conditions at the side walls for the interior variables, though these are consistent with a special case of partially conducting side walls.

Pedlosky (1967) next published a model for stratified spin-up with an insulating side wall. He rederived the interior equations and obtained the same Ekman layer equations as Holton. He analyzed the $E^{\frac{1}{2}}$ buoyancy layer equations and correctly concluded that the insulating condition prevented this side wall layer from carrying any fluid from the Ekman layers to the interior. From this, he concluded that the Ekman layers could not exist and that the

spin-up must occur on the longer diffusive time scale $\Omega^{-1}E^{-1}$. He was wrong (Holton and Stone,1968) in the sense that a spin-up process does take place near the horizontal boundaries by a return flow through the interior. He was right in that the full spin-up to a new state of solid body rotation does occur on the diffusive time scale and that on the homogeneous spin-up time scale, any constant height level of fluid conserves its circulation. A part of this problem is the need for a precise definition of what is meant by " spin-up time " for a stratified fluid. This will be discussed at the end of chapter 2.

Walin (1969) and Sakurai (1970) published careful treatments of the linear, insulated wall spin-up problem on the homogeneous spin-up time scale. Their results were identical with the earlier, unpublished results of Siegmann (1967). Their solutions use the same Ekman layer conditions on the interior as Holton and Pedlosky and the same buoyancy layer conditions as Pedlosky. They applied both boundary conditions to the interior and obtained a result similar to Holton's, but differing in detail. This linear theory will be referred to henceforth as the "Walin" theory (as he published the result first) to avoid confusion.

1.4 Previous experiments

Holton (1965), MacDonald and Dicke (1967), and Modisette and Novotny (1969) conducted experiments on the stratified spin-up problem. These experiments were not carefully performed and will

not be discussed here. (See Buzyna and Veronis, 1971, for more discussion.)

The only careful experiments to date have been those of Buzyna and Veronis (1971). They studied the problem using salt stratification and dye-wire techniques to measure the azimuthal velocity at four levels. The salt stratification ensured a perfectly insulating condition and a high Schmidt number. They found some apparently paradoxical results. Near the mid-plane of the cylinder, they found the angular velocity agreed well with that predicted by Walin's theory, and near the bottom, the angular measurements showed a more rapid adjustment than predicted, but a derived "spin-up" time showed the opposite results at both levels. They explained the faster response as a possible effect of a non-linear interaction in the " corner " regions where the Ekman transport is returned (or removed for spin-down) to (from) the interior.

1.5 Outline for the remainder of the thesis

The second chapter discusses the linear theory. This is not presented in chronological order of publication, but in a form unifying all the previous theory in a common notation. In a real experiment, perfectly insulating walls cannot exist for thermally stratified fluids. Therefore, the previous theory was enlarged to include the case of partially insulating walls to determine the proper theory for the experiment. It was found that

the experiments presented in this thesis were in good approximation to the insulating side wall, and it was shown that Holton's boundary condition on the interior flow at the side wall was a special case of a partially conducting side wall. The extension of the theory also reproduced Pedlosky's boundary condition for a perfectly conducting side wall. Chapter 3 discusses the experimental apparatus, method and technique of data analysis. The results of the experiments are discussed in chapter 4. One experiment is considered in detail and the rest are discussed in relation to this experiment.

In the text to follow, the parameter, B , is called a Burger number. This is not quite correct, as the aspect ratio also enters into the definition of the Burger number in its usual meaning.

2. THE LINEAR THEORY

2.1 Formulation of the problem

Most of this chapter is concerned with a presentation of the linear theory, parts of which have been discussed by Holton (1965), Siegmann (1967), Pedlosky (1967), Walin (1969), and Sakurai (1970). Each of these authors has used different conventions concerning the scaling parameters and basic variables. The scaling has been chosen to be consistent with Walin's in order that the solutions derived in this chapter may be compared to his and the basic variable has been chosen to be the stream function to reduce the order of the equation governing the interior field.

The basic equations used are the Navier-Stokes equations for an incompressible fluid. The Boussinesq approximation has been made and axial symmetry is assumed. The scaling, as mentioned above, is consistent with Walin's. It should be noted that the time scaling is $\frac{1}{2}\Omega^{-1}E^{-\frac{1}{2}}$ rather than $\Omega^{-1}E^{-\frac{1}{2}}$, and that L is the half-height of the container.

The variables are scaled as follows:

$$(r_*, z_*) = L (r, z),$$

$$\begin{aligned}
 t_* &= (2\Omega)^{-1} E^{-\frac{1}{2}} t, \\
 (u_*, v_*, w_*) &= \epsilon \Omega L (u, v, w), \\
 p_* &= 2\Omega^2 L^2 \epsilon \rho_0 p, \\
 \rho_* &= 2\Omega^2 L \epsilon \rho_0 g^{-1} \rho, \\
 \rho_{s_*} &= Q_s \rho_s,
 \end{aligned}$$

where

$$\begin{aligned}
 P_* &= \text{real, total pressure} = p_{s_*}(r_*, z_*) + p_*(r_*, z_*, t_*), \\
 p_{s_*} &= \text{real, static pressure} = \rho_0 (-gz_* + \frac{1}{2} \Omega^2 r_*^2), \\
 \rho_{\text{total}_*} &= \text{real, total density} = \rho_{s_*}(z_*) + \rho_*(r_*, z_*, t_*),
 \end{aligned}$$

and

$$Q_s = \alpha \Delta T.$$

Other parameters used in the analysis are

- ϵ = the Rossby number = $\Delta\Omega/\Omega$,
- Ω = the final angular velocity of the system,
- $\Delta\Omega$ = the change in angular velocity,
- $L = \frac{1}{2}$ the height of the cylinder,
- ρ_0 = the average density of the fluid,
- ΔT = the temperature difference between the upper and lower boundaries,
- ν = the average kinematic viscosity,
- κ = the average thermometric conductivity,
- E = the Ekman number = $\nu / 2\Omega L^2$,
- F = the Froude number = $\Omega^2 L / g$,
- B = the Burger number = $N / 2\Omega$,
- N = the Brunt-Väisälä frequency = $Q_s g / 2L$,
- σ = the Prandtl number = ν / κ ,

α = the coefficient of thermal expansion.

If we define the operator

$$\mathcal{L} = \nabla^2 - \frac{1}{r^2} = \frac{\partial}{\partial r} \frac{1}{r} \frac{\partial}{\partial r} r + \frac{\partial^2}{\partial z^2},$$

the scaled equations of motion, heat and continuity are

$$E^{\frac{1}{2}} u_t + \frac{1}{2}\epsilon(\underline{u} \cdot \nabla u - v^2/r) - v = -p_r + E \mathcal{L} u + \frac{1}{2}Fr(\rho + B^2 \rho_s),$$

$$E^{\frac{1}{2}} v_t + \frac{1}{2}\epsilon(\underline{u} \cdot \nabla v + uv/r) + u = E \mathcal{L} v$$

$$E^{\frac{1}{2}} w_t + \frac{1}{2}\epsilon(\underline{u} \cdot \nabla w) = -p_z + E \nabla^2 w - \rho$$

$$E^{\frac{1}{2}} \rho_t + \frac{1}{2}\epsilon(\underline{u} \cdot \nabla \rho) + w \frac{\partial \rho_s}{\partial z} B^2 = \frac{E}{\sigma} \nabla^2 \rho,$$

and,

$$\nabla \cdot \underline{u} = 0.$$

The incompressibility condition allows the introduction of a stream function ψ such that $(u, w) = (\psi_z, -(r\psi)_r/r)$.

In the theory to follow, the Rossby number and the Froude number will be neglected. Although the existence of an initial state of solid body rotation is precluded in any rotating, stratified fluid whose Froude number is not identically zero (see Barcilon and Pedlosky, 1967), such a state will be assumed, arguing that the superposed Sweet-Eddington flow can be separated from the spin-up in the linear theory. The further assumption of a linear basic density gradient will be made: $\frac{\partial \rho_s}{\partial z} = -1$. The full equations, after eliminating the pressure field, are

$$\begin{aligned}
(E^{\frac{1}{2}} \frac{\partial}{\partial t} \mathcal{L} - E \mathcal{L}^2) \psi - v_z - \rho_r &= \frac{1}{2} \epsilon \left(\psi_z \left((\mathcal{L}\psi)_r - \frac{1}{r} \mathcal{L}\psi \right) - \right. \\
&\quad \left. \frac{1}{r} \frac{\partial}{\partial z} (\mathcal{L}\psi) (r\psi)_r - 2v_z/r + \right. \\
&\quad \left. \frac{1}{2} \Gamma_r \left(\rho_z - B^2 \right) \right), \\
(E^{\frac{1}{2}} \frac{\partial}{\partial t} - E \mathcal{L}) v + \psi_z &= \frac{1}{2} \frac{\epsilon}{r} \left(v_z (r\psi)_r - \psi_z (rv)_r \right), \\
(E^{\frac{1}{2}} \frac{\partial}{\partial t} - \frac{E}{\sigma} \nabla^2) \rho + B^2 (r\psi)_r / r &= \frac{1}{2} \epsilon \left(((r\psi)_r / r) \rho_z - \rho_r \psi_z \right).
\end{aligned}$$

The initial condition for the problem is $v = r$ at $t = 0$, and the boundary conditions are $\underline{u} = 0$ on all boundaries, and

$$\frac{\partial \rho}{\partial n} = \Gamma_n \left(\rho - \rho_n \right),$$

where

$\frac{\partial}{\partial n}$ is the derivative normal to a boundary

and Γ_n and ρ_n depend on the boundary and the specific case under study. Physically, this condition is an approximation to partial heat conduction through a thin wall. See appendix II for the derivation of this condition.

2.2 Conventions

The convention used in the perturbation expansion follows.

Let Y be any dependent variable. Then

$$Y = Y^{(0)} + E^{\frac{1}{4}} Y^{(1)} + E^{\frac{1}{2}} Y^{(2)} + \dots$$

No expansion in powers of $E^{1/3}$ are needed for the problem when B is $O(1)$. See appendix II for details.

The boundary layer variables will be denoted by diacritical marks above the dependent variable. The stretched coordinates will be represented by lower case Greek letters and "x".

The conventions for the boundary layer independent and dependent variables are

Ekman layer, $\zeta = E^{-\frac{1}{2}} (1 + (-1)^j z)$, $j = 0$ on the bottom

$j = 1$ on the top,

$Y \rightarrow \bar{Y}$,

$E^{\frac{1}{4}}$ horizontal layer, $\eta = E^{-\frac{1}{4}} (1 + (-1)^j z)$, $Y \rightarrow \bar{\bar{Y}}$,

$E^{\frac{1}{2}}$ buoyancy layer, $\xi = E^{-\frac{1}{2}} (r_0 - r)$, $Y \rightarrow \hat{Y}$,

$E^{\frac{1}{2}}$ Stewartson layer, $x = E^{-\frac{1}{4}} (r_0 - r)$, $Y \rightarrow \hat{\hat{Y}}$.

Other conventions will be introduced as needed.

2.3 The linear problem

For the linear problem, $\epsilon = 0$ and $F = 0$. The variables are expanded in a perturbation expansion in powers of $E^{\frac{1}{4}}$.

Interior equations

$O(1)$

$$v_z^{(0)} + \rho_r^{(0)} = 0$$

$$\psi_z^{(0)} = 0$$

$$(r\psi^{(0)})_r = 0$$

$O(E^{\frac{1}{4}})$

The equations for the $E^{\frac{1}{4}}$ terms are the same as the $O(1)$ equations.

 $O(E^{\frac{1}{2}})$

$$v_z^{(2)} + \rho_r^{(2)} = 0$$

$$v_t^{(0)} + \psi_z^{(2)} = 0$$

$$\rho_t^{(0)} + \frac{B^2}{r} (r\psi^{(2)})_r = 0$$

Ekman layer equations

 $O(1)$

$$\bar{\psi}^{(0)} = \bar{\rho}^{(0)} = 0$$

 $O(E^{\frac{1}{4}})$

$$\bar{\psi}^{(1)} = \bar{\rho}^{(1)} = 0$$

 $O(E^{\frac{1}{2}})$

$$\bar{\psi}_{\zeta\zeta\zeta\zeta}^{(2)} + (-1)^j \bar{v}_{\zeta}^{(0)} = 0$$

$$\bar{v}_{\zeta\zeta}^{(0)} - (-1)^j \bar{\psi}_{\zeta}^{(2)} = 0$$

$$B^2 (r\bar{\psi}^{(2)})_r / r - \sigma^{-1} \bar{\rho}_{\zeta\zeta}^{(2)} = 0$$

$E^{\frac{1}{4}}$ horizontal thermal boundary layer equations

 $O(1)$

$$\left(\frac{\partial}{\partial t} - \sigma^{-1} \frac{\partial^2}{\partial \eta^2} \right) \bar{\rho}^{(0)} = 0$$

$$O(E^{\frac{1}{4}})$$

The same equations hold to this order.

$E^{\frac{1}{2}}$ buoyancy layer equations

$$O(1)$$

$$\hat{\psi}^{(0)} = 0$$

$$O(E^{\frac{1}{4}})$$

$$\hat{\psi}^{(1)} = 0$$

$$O(E^{\frac{1}{2}})$$

$$\hat{\psi}_{\xi\xi\xi\xi}^{(2)} - \hat{\rho}_{\xi}^{(0)} = 0$$

$$\hat{\rho}_{\xi\xi}^{(0)} + \sigma B^2 \hat{\psi}_{\xi}^{(2)} = 0$$

$E^{\frac{1}{4}}$ Stewartson layer equations

$$O(1)$$

$$\hat{\psi}^{(0)} = 0$$

$$\hat{\rho}^{(0)} = 0$$

$$O(E^{\frac{1}{4}})$$

$$\hat{\psi}^{(1)} = 0$$

$$\hat{\rho}^{(1)} = 0$$

$$O(E^{\frac{1}{2}})$$

$$\hat{\psi}^{(2)} = 0$$

$$\hat{v}_t^{(0)} - \hat{v}_{xx}^{(0)} = 0$$

$$\hat{\rho}_x^{(2)} - \hat{v}_z^{(1)} = 0$$

2.4 Solution of the interior problem

From the interior equations, a single equation may be obtained for $\psi^{(2)}$:

$$\frac{\partial}{\partial r} \frac{1}{r} \frac{\partial}{\partial r} r \psi^{(2)} + B^{-2} \psi_{zz}^{(2)} = 0.$$

This is clearly separable for the geometry of the problem and solutions obtained in terms of Bessel and hyperbolic functions. The boundary conditions on the interior fields must be derived from the boundary layer equations.

2.4.1 The quasi-steady Ekman layer condition

The quasi-steady Ekman layer conditions are used as the Ekman layers do not change rapidly with time after the initial spin-up on the $O(1)$ time scale. This condition is consistent with the scaling on the $E^{-\frac{1}{2}}$ time scale.

The non-slip conditions at the top and bottom demand $\bar{\psi}_{\zeta}^{(2)} = 0$, $\bar{\psi}^{(2)} + \psi^{(2)} = 0$, and $\bar{v}^{(0)} + v^{(0)} = 0$ on $z = \pm 1$ and $\zeta = 0$.

From the Ekman layer equations, the Ekman layer azimuthal velocity and stream function are found to be

$$\bar{v}^{(0)} = -v_B \exp(-2^{-\frac{1}{2}}\zeta) \cos 2^{-\frac{1}{2}}\zeta,$$

$$\bar{\psi}^{(2)} = (-1)^j 2^{-\frac{1}{2}} v_B \exp(-2^{-\frac{1}{2}}\zeta) (\cos 2^{-\frac{1}{2}}\zeta + \sin 2^{-\frac{1}{2}}\zeta),$$

where $v_B = v^{(0)}(z = \pm 1)$. From these equations, we have

$$\bar{\psi}^{(2)}(\zeta = 0) = (-1)^j 2^{-\frac{1}{2}} v_B = -\psi^{(2)}(z = \pm 1).$$

These conditions, with the interior equations give

$$\psi_t^{(2)} - (-1)^j 2^{-\frac{1}{2}} \psi_z^{(2)} = 0 \text{ at } z = \pm 1$$

as the boundary conditions on the interior flow at the horizontal boundaries.

2.4.2 The $E^{\frac{1}{2}}$ buoyancy layer conditions on the interior flow

The non-slip and thermal boundary conditions give

$$\psi^{(2)} + \hat{\psi}^{(2)} = 0,$$

$$\psi_\xi^{(2)} = 0,$$

$$\hat{\rho}_\xi^{(0)} = -\Gamma' (\hat{\rho}^{(0)} + \rho^{(0)}) \text{ at } r = r_0, \xi = 0,$$

where

$$\Gamma' = E^{\frac{1}{2}} \Gamma,$$

$$\rho_n = 0.$$

After the tangential velocity condition is applied, it is

found that

$$\hat{\rho}^{(0)} = b \exp(-h\xi) \cos h\xi,$$

$$\hat{\psi}^{(2)} = \frac{hb}{\sigma B^2} \exp(-h\xi) (\sin h\xi + \cos h\xi),$$

where

$$h = \left(\frac{1}{2}B\right)^{\frac{1}{2}} \sigma^{\frac{1}{4}}.$$

From the thermal boundary condition

$$(\Gamma' - h) b = -\Gamma' \rho^{(0)} \quad \text{at } r = r_0,$$

and hence

$$\frac{\sigma B^2 (\Gamma' - h)}{\Gamma' h} \hat{\psi}^{(2)}(\xi=0) = -\rho^{(0)}.$$

As $\psi^{(2)} + \hat{\psi}^{(2)} = 0$ at $r=r_0, \xi=0$, we have

$$\frac{\sigma B^2 (\Gamma' - h)}{\Gamma' h} \psi^{(2)} = \rho^{(0)},$$

or

$$\frac{\sigma B^2 (\Gamma' - h)}{\Gamma' h} \psi_t^{(2)} = \rho_t^{(0)},$$

and as

$$\rho_t^{(0)} = -\frac{B^2}{r} (r\psi^{(2)})_r,$$

the boundary condition on $\psi^{(2)}$ at $r = r_0$ is

$$\psi_t^{(2)} + \frac{\Gamma' h}{\sigma(\Gamma' - h)} \frac{1}{r} (r \psi^{(2)})_r = 0.$$

This condition, the Ekman conditions, and the requirement that all fields remain finite at $r = 0$, define the boundary value problem.

The side wall boundary condition may be studied in a number of cases. In the first case, where the coefficient $K = h\Gamma'/\sigma(\Gamma' - h)$ is $O(E^{\frac{1}{2}})$, the side wall boundary condition reduces to $\psi^{(2)} = 0$ at $r = r_0$ (as $\psi^{(2)}$ goes to zero as t increases without bound). This is just the insulating condition $\rho_r = 0$ at $r = r_0$. When this condition is used, it should be noted that the buoyancy layer ceases to exist and thus cannot transport fluid from the Ekman layers to the interior. This condition may be created by either an insulating wall or a large Prandtl number.

The next interesting case occurs when $\Gamma' = h$. This requires that $(r\psi^{(2)})_r = 0$ at $r = r_0$. This is the equivalent of Holton's boundary condition, expressed in terms of the stream function.

The last special case of interest occurs as Γ' becomes infinite. This corresponds to a side wall held at constant temperature, or a perfectly conducting side wall. This gives a boundary condition which is equivalent to Pedlosky's side wall condition, expressed in terms of the stream function.

Both Holton's and Pedlosky's boundary conditions would be very difficult and expensive to produce in a laboratory experiment. This is mostly due to problems in constructing side walls of

sufficient conductivity and maintenance of the outer wall temperature.

2.4.3 The form of the interior solutions

The initial condition for the interior fields is $v^{(0)} = -r, \rho^{(0)} = 0$, at $t = 0$. The solution of the problem is then quite straightforward (see appendix II) and is given by

$$\psi^{(2)} = \sum_n -2^{-\frac{1}{2}} r_o C_n e^{-\beta_n t} \frac{\sinh m_n z}{\sinh m_n} J_1(\alpha_n r/r_o),$$

$$v^{(0)} = -r + \sum_n r_o C_n (1 - e^{-\beta_n t}) \frac{\cosh m_n z}{\cosh m_n} J_1(\alpha_n r/r_o),$$

$$\rho^{(0)} = \sum_n r_o^B C_n (1 - e^{-\beta_n t}) \frac{\sinh m_n z}{\cosh m_n} J_0(\alpha_n r/r_o),$$

where

$$m_n = B\alpha_n/r_o, \quad \beta = 2^{-\frac{1}{2}} m_n \coth m_n,$$

and the α_n satisfy the equation

$$\frac{J_1(\alpha_n)}{J_0(\alpha_n)} + \frac{2^{\frac{1}{2}} h \Gamma'}{B\sigma (\Gamma' - h)} \tanh \frac{B\alpha_n}{r_o} = 0.$$

The C_n are defined by

$$r = \sum_n C_n J_1(\alpha_n r).$$

For the insulating case, $C_n = \frac{2}{\alpha_n J_0(\alpha_n)}$. For the non-insulating

cases, the solutions for the C_n are obtained by numerical methods (see appendix II).

From these solutions, we can now define a precise "spin-up time ". The modal coefficients, β_n , are of the form of reciprocal times. The n-th modal spin-up time will be defined as $1/\beta_n$. It should be noted that these spin-up times are independent of position or time.

For the experiments described in this thesis, the coefficient in the second term of the eigenvalue equation is $O(E^{\frac{1}{2}})$ and thus, the theory that will be used for comparison with the experiments will be the insulating side wall walin theory.

3. DESCRIPTION OF THE EXPERIMENTS

3.1 Description of the apparatus

The apparatus was designed to test the theory discussed in the previous chapter. The basic geometry of the test section was a right circular cylinder, made of plexiglass, 8.89 cm high, 10.03 cm inner radius, with all walls approximately 1 cm thick. This cylinder was bounded on the top and bottom by 0.6 cm thick glass plates, flat to better than 0.002 cm. Glass was chosen for its relatively high thermal conductivity, clarity and mechanical strength. The walls and the glass plates were made rather thick for reasons of rigidity. The cylinder and the glass plates were sealed inside a large plexiglass box. Spaces were provided above and below the glass plates for the heating and cooling water. The interior of the cylinder was filled with Dow-Corning 200 silicone oil, 1 cs viscosity grade. This was chosen as the working fluid for its large coefficient of thermal expansion and high resistivity. The low surface tension of the oil made removal of air bubbles particularly easy. The space around the cylinder, between the glass plates was filled with Dow-Corning 200 silicone

oil, 500 cs viscosity grade. The surrounding oil served the purpose of providing a thermal isolation from the room and a medium for viewing the interior of the cylinder from the side with little distortion. The high viscosity was used to ensure that the spin-up by side wall diffusion would be at least as important as the Ekman pumping mechanism. The purpose was to preserve the temperature field outside the cylinder as much as possible. An even higher viscosity would have been used, but the problems involved in working with such high viscosity oils prevented this.

The plastic box was mounted on a three point leveling system on the turntable and provided with clamps which allowed leveling and centering of the test section. Before the experiments were performed, the tank was leveled to better than 30" of arc and centered to within ± 0.02 cm of the rotation axis of the turntable. The centering was needed to make the flow axisymmetric and to avoid problems of variation of the centrifugal acceleration on the fluid. The centrifugal effect could be neglected for a homogeneous fluid, but not for a stratified fluid. When the turntable's rate of rotation is changed to give the initial condition, the centering must be accurate.

The turntable was the MIT/GFDL Air Bearing Turntable. The details of construction of this turntable are described in Saunders (1970). The axis of rotation of the table was adjusted to within 3" of the vertical. (This is the same order as the tilt of the building due to differential heating at the 6th floor. See Simon and Strong, 1968) The rate of rotation of the turntable was

very stable. Under very good conditions, stabilities of several parts in a million have been obtained. For most experiments, however, the stability was of the order of a few parts in 10^4 .

The density gradient in the test section was maintained by heating the upper plate and cooling the lower plate by running hot and cold water through the spaces above and below the plates, respectively. Temperature was used instead of salt to maintain the density field because of diffusive problems near the boundaries with salt and the ease of monitoring the density field when temperature was used. The temperature of the water was controlled by two water temperature controllers to better than 0.05°C . The temperature on the top and bottom plates varied by less than 0.02°C during the experiments.

The density field was measured by sensing the temperature at a number of thermistors placed in the interior of the cylinder. Twenty thermistors were originally available for determining the temperature field, but two ceased to function, leaving eighteen. The location and numbering system of the thermistors is shown in figure 2. The locations of the thermistors were chosen to increase the density of thermistors near the boundaries where the temperature field would be changing most rapidly. The arrangement of putting the thermistors at half the distance from the wall as the previous thermistors made the data reduction easy.

The temperature sensing was done by measuring the out of null voltage of a Wheatstone bridge in which the thermistors constituted one of the resistors. Thirty bridges were available, but not all

were used. A stepping switch from a guidance system testing computer was used to sequence the bridge's output. This was amplified by a high input impedance amplifier before the signal left the turntable. Mercury slip rings were used for electrically connecting the turntable to the stationary laboratory reference frame to keep slip ring noise low. The signal was then filtered to remove 60 Hz hum and higher frequency noise. The voltage was then converted into a digital format and read into the memory of a computer.

The computer used in these experiments was a Digital Equipment Corporation P.D.P. 8/S computer. All the sequencing and data sampling operations in the experiments were performed under the control of this computer.

The sequence of operations in a typical experiment began with starting the computer. This was followed by a five second wait state for the operator to set a series of switches which could not be set before the run, due to possible accidental triggering of some of the circuitry. After the five second wait period was over, the stepping switch was set to the first position and the speed changed. A photograph was taken and the stepping switch sequenced and the temperature taken for all the thermistors. The photograph-thermistor sequencing cycle took about 4.5 seconds to sample all the thermistors. About twenty five pictures were taken and fifty full cycles of thermistor readings taken for each experiment.

The velocity field data was measured by photographing neutrally buoyant particles at the mid-plane of the cylinder. The particles

were polystyrene spheres, about 0.05 cm in diameter. The camera used was an automatic Nikon F (35 mm), The film used was Kodak Tri-X, developed in Diafine. The light source was a G.E. projector lamp and the beam was collimated by two slits. The thickness of the beam at the mid-plane was about 1 cm, approximately 10% of the cylinder height.

The apparatus is described in more detail in appendix I.

3.2 The experimental method

A typical experiment began by turning on the water temperature controllers and the pumps on the table and letting the system equilibrate for two to three hours. This time was necessary for the system to reach thermal equilibrium and to make sure the flow rates and pressures were balanced to avoid breaking the apparatus. During this time, the equipment was checked and the computer tested. The camera was loaded and the experiment number and date photographed. The turntable was then turned on and the speed checked. If the rate was constant to better than one part in 10^4 , the system was left to settle for another two hours. This allowed the large initial spin-up transients to die out and the temperature field to adjust by diffusion. The temperature was measured during this time to determine when it had reached steady state and linearity. These measurements were performed at a lower amplification than used during the actual experiments. This allowed checking the absolute temperature field. After these measurements were made,

the amplification was increased to allow the use of differential measurements of higher precision. The experimental parameters were set into the computer and the apparatus readied for the run.

The sampling during the run was conducted in the sequence described in the previous section. The sampling time usually covered two to five homogeneous spin-up times.

3.3 Data analysis

The temperature data from the thermistors were taken sequentially. In order to analyze the time dependence of the temperature field, it was necessary to interpolate the output of each thermistor to the beginning of the sampling sequence. A linear interpolating routine was used, as the temperature data seemed smooth enough to warrant it.

After the data were synchronized, the initial readings were subtracted from the later readings to give the perturbation temperatures. This put the data into a form which could be readily compared to the theory. As the Sweet-Eddington flow is essentially a steady phenomenon, this subtraction of the initial readings from the time-dependent readings eliminated the effect of this superposed circulation to $O(\epsilon)$.

In order to analyze the temperature field, it was first necessary to obtain a representation of the field from the measurements at specific points in space and time. A least squares technique, using Bessel functions in the radial direction

was found to be inadequate, due to the large oscillations produced in the fit. The representation of the field finally decided upon was a double polynomial expansion in the radial and vertical coordinates. If $T'(r,z;t)$ is the fitted field, then

$$T'(r,z;t) = \sum_{\substack{j=N-1 \\ i=N \\ i=1 \\ j=1}} a_{ij} r^{2(i-1)} z^{2j-1} .$$

In the actual analyses, N was taken as either 3 or 4. This polynomial was fitted to the data by a standard least squares technique. The fitted field was computed and contoured. If the contours indicated a bad fit, the standard deviation of the fit was checked. This was usually more than 15 digitizing intervals (one digitizing interval = 0.0026°C). If the contour plot indicated a good fit, the standard deviation was usually no more than 2 to 4 digitizing intervals. There was never any question whether the fit was good or bad. The fits which were not reliable were not used. This fitting program is listed in appendix IV.

In order to compare the observed results with the theory, it was decided to try to analyze the modal behavior of the temperature field. This was accomplished by decomposing the polynomial into its Bessel modes in the radial direction, based on $J_0(\alpha_n r)$ where the α_n are the eigenvalues of the previous chapter. This is quite easy to do, as the even powers of r are easily Fourier-Bessel analyzed by recursion methods. These are discussed in appendix II. Once these have been found, the modal structure of the flow is known at any time.

According to the linear theory, the modal structure of the temperature field has the general form $A_n(z)(1 - e^{-\beta_n t})$, where the β 's are the reciprocal spin-up times. The fitted field, after the Fourier-Bessel decomposition, was fitted to this functional form with a non-linear fitting routine, GAUSHA, which is listed in appendix IV. The $A_n(z)$ and β_n were determined for sixteen equally spaced values of z and $n=1$, and for the field integrated in z from 0 to -1 . Only the first mode was computed.

The accuracy of the analysis procedure was checked by generating theoretical data according to the linear theory and analyzing them in the same manner as the observed data. The first mode was reproduced to within a few percent, but the second mode was in error by more than twenty percent. Because of this, the second mode was not used.

An attempt was made to determine the modal spin-up times by fitting the observed angular positions of the particles with the theoretical form. It was found that this method was not feasible, as it was too sensitive to random errors in the data. This will be discussed in more detail in the next chapter.

4. EXPERIMENTAL RESULTS

4.1 Experimental parameters

One of the original purposes of this thesis was to study the stratified spin-up problem over a wide range of parameter space. The way in which the experiment was constructed limited the number of parameters which could be varied. The length and height scales, the viscosity, coefficient of thermal expansion and the thermometric conductivity were all held constant for all the experiments. In order to avoid changing the settings of the thermistor bridges and to keep the effect of the viscosity stratification constant, the temperature difference between the top and bottom plates was kept approximately constant. This required that changes in the Burger number could be produced only by changing the rotation rate, hence making the Burger number proportional to the Ekman number and to the square root of the reciprocal of the Froude number. The Rossby number was independent of the other non-dimensional parameters of the system. The values of the non-dimensional parameters and some of the more important dimensional parameters are given in table 1.

Not all the data were used. Some were not reliable due to errors committed during the runs. The temperature data from the first nine experiments could not be used as the electrical noise from the pumps on the turntable was too large. After that experiment, electronic filters were introduced to remove this noise. The data usage is given in table 2.

4.2 Detailed description of one experiment (No. 24)

Before looking at the data from all the experiments, it is worthwhile to consider one experiment in detail. Experiment 24 was chosen because it was representative of the stratified spin-up experiments, lying in the mid-range in both the Burger and Rossby numbers, and being rather free from noise.

The velocity data for experiment 24 had the least noise of any of the velocity data. The angular position of one particle at an average non-dimensional radius of 1.08 is plotted in figure 23. The non-dimensionalized angular velocity for the same particle is plotted in figure 24. The solid lines in both figures are the theoretical curves predicted by the Walin theory with insulating side walls. At first glance, it appears that the agreement of the data with the theory is good. It would be easy to conclude that the experiment agrees well with the theory for the mid-plane. This is actually not warranted. If the spin-up time for the first mode is determined by fitting the angular position with the theoretical functional form, it is

found that the precision of the experiment is not great enough to determine the spin-up time to any reasonable degree of accuracy. With ten points, a value of 2.0 is found instead of the theoretical value of about 1.2. If eight points are used, the value changes to 1.6. If the data were reliable, there would have been no significant change when two points out of ten were deleted. Another indication of the precision needed is that the large deviations occurred even though the positions agree with the theory to within a few thousandths of a radian. Unfortunately, this is the limit of resolution for these experiments. The fitting procedure has shown that the spin-up time is shorter than predicted, even though the exact value is in doubt. The other experiments were more subject to noise and this procedure was not used for them. The causes of the noise were mostly in the copying and digitizing of the photographs.

The temperature data offer much better hope for experimentally determining the modal spin-up times. The interpolated temperature perturbations, in terms of absolute digitizing intervals are presented in figures 5 - 22 versus time. It may be seen that the actual results show the same trends as the theory, but exact agreement is not very good. In most cases, the perturbation temperatures start out with larger amplitudes than the theoretical temperatures and have a greater curvature. In some cases, they cross the theoretical curves, and in others, they show a tendency to cross outside the time range. Another feature is the values of the perturbation temperatures at the mid-plane (i.e., thermistors

whose numbers are even multiples of four) are not exactly zero, as predicted. This is especially evident in figures 14, 18, and 22.

In all cases, the perturbation temperature was lower than predicted. The experiment was a spin-down, and therefore, the Ekman pumping would have been upward for fluid near the lower boundary. The viscosity of the fluid is greater there, due to the lower temperature, resulting in a larger local Ekman number than assumed for the whole flow. This would have resulted in a larger Ekman pumping for the bottom than for the top. The fluid below the mid-plane would have been expected to penetrate some distance above the mid-plane and cool the thermistors there. This is exactly what was observed. The thermistors were observed to be warmer for the cases where the fluid was spun-up.

The temperature data from this experiment were analyzed by the method discussed in 3.3. A typical fit of the temperature field is shown in figure 41. (For a qualitative comparison with contoured data from a numerical model of stratified spin-up, see figure 40.) The fits are generally good, the standard deviation being one or two digitizing intervals. The Fourier-Bessel decomposition and fitting the time dependent functional form was carried out for seven levels in z and for the vertically integrated polynomial. The reciprocal spin-up time for the first mode are shown in figure 25 as a function of depth. The non-linear fitting routine computes the confidence limits assuming a linear hypothesis on the other variables for the input data. These are

the error bars indicated in the figure. At the 95% confidence level, the reciprocal spin-up times are not significantly different from being constant with depth. They are all slightly greater than the integrated result, but this is probably a result of the fitting procedure. The integrated results and the results at the different heights do not differ on the 95% confidence level. Both the value from the vertically integrated data and the values at the various levels are significantly greater than the values predicted by the linear theory. This feature has been found in all the experiments which have been analyzed. The asymptotic coefficient for the first Bessel mode are plotted in figure 26 as a function of depth.

4.3 General discussion of the temperature data

The temporal coefficients for the first mode are plotted in figure 28 versus the Burger number. It may be seen that as the Burger number increases, the coefficients also increase, about as rapidly as predicted by the theory. However, the values of the computed coefficients are all greater than those predicted by the linear theory. This means that for all the experiments considered, the spin-up times are smaller than predicted.

A smaller spin-up time would be expected for several reasons. The wires which support the thermistors exert a certain amount of drag on the interior flow. This drag would cause the interior to spin-up more rapidly than predicted and must be considered in

any explanation of the increase in the reciprocal spin-up time. Another possible cause is the increased Ekman pumping near the bottom boundary which would increase the value of the coefficient in the bottom half of the tank, where the thermistors are located. Non-linear effects could be another possible cause.

The effect of the wires may be estimated by comparing the rates of energy dissipation of the wire drag to that of the spin-up process. The simple case where the wires are all on diameters of the cylinder and the spin-up is homogeneous is discussed in appendix II. It is found that the rate of dissipation is less than 5% of the spin-up process. This eliminates the effect of the wire drag as a major source of the smaller spin-up times. (The case where the fluid is stratified has also been studied and the same result found.)

The viscosity varies by about 10% from the bottom to the top of the tank. The difference in viscosity, and hence the Ekman number, from the average value is about 5%. The implied difference in the Ekman suction and hence, the decrease in the spin-up time for the lower half of the cylinder would be about $2\frac{1}{2}\%$, which is less than the effect of the wire drag .

There remains the possibility of non-linear interactions. These could occur anywhere in the fluid, but could appear in the lowest order solution in the boundary layers when the local Rossby number (based on the length scale $E^{\frac{1}{2}}L$) becomes $O(1)$, even though the interior Rossby number is small. This effect can be seen when the percentage deviation in the spin-up coefficients

are plotted against the local Rossby number. The magnitude of the discrepancies increases with increasing local Rossby number, though there is a great deal of scatter. The scatter is the same order as the 95% confidence limits determined by the fitting routine. These results are plotted in figure 29. The graph indicates that the effect may be taking place where the length scale is $O(E^{\frac{1}{2}})$. These regions are the Ekman layers, the $E^{\frac{1}{2}}$ buoyancy layer and the $E^{\frac{1}{2}} \times E^{\frac{1}{2}}$ "corner" regions.

The buoyancy layer may be ruled out if it is argued that the non-linear terms are identically zero for the first order, thus the equations for the first non-linear interaction are the same as the linear equations and there is no correction.

The Ekman layers may be ruled out by arguing that the non-linear stratified Ekman layers are not qualitatively different from the non-linear homogeneous Ekman layers. In the homogeneous case, the sign of the deviation from the linear theory depends on the sign of the Rossby number. In these experiments, it does not.

The only regions left are the "corner" regions where the Ekman transport is returned to the interior. This is a singular region in the analytic theory, and it may be expected that the scaling arguments do not hold there. Unfortunately, the solution of the problem in that region requires the solving of the full non-linear Navier-Stokes equations. This is not very tractable analytically, but may be numerically.

The asymptotic coefficients agree well with the linear theory and are presented in figure 27.

4.4 Conclusions and recommendations

From the experiments it may be concluded that the experiment and the theory are in qualitative agreement. The first modal spin-up times are smaller for the stratified fluid than for the homogeneous fluid. The order of magnitude of the temperature and velocity fields are consistent for the theory and experiment. The fluid does not attain a solid body rotation on the $E^{-\frac{1}{2}}$ time scale, but does reach a new quasi-steady state. The insulating wall condition is a good approximation for the experiments.

There is some disagreement with the linear theory. In all cases, the spin-up times are shorter for the first mode than predicted by the linear theory. The discrepancy between the theoretical and observed values increases with increasing local Rossby number. The discrepancy cannot be accounted for by wire drag or viscosity stratification, though they affect it, or by non-linear effects in the Ekman or buoyancy layers. The effect of the corner regions cannot be ruled out.

Buzyna and Veronis (1971) have studied the problem of stratified spin-up in a similar geometry, using salt stratification to obtain the density gradient. They measured the azimuthal velocities at four levels using the Thymol blue dye line technique (Baker, 1966). They compared their results with the theory at the mid-plane and near the lower boundary, above the Ekman layer. The insulating side wall condition was the proper side wall boundary condition for their problem and their Schmidt number

was very large.

From the comparison of the azimuthal positions of the dye lines with the theory, they found that the spin-up was more rapid near the horizontal boundaries, reproducing the qualitative aspects of the theory. This is in agreement with the observation in this thesis.

They also computed some "spin-up times" at two levels. These were defined as the time at which the azimuthal velocity had fallen to within e^{-1} of its final value. Therefore, each point in the fluid has a different "spin-up" time as defined by Buzyna and Veronis. They found that these "spin-up times" were smaller than predicted at the mid-plane and agreed with the "spin-up times" computed from the theory (within the error bounds) for $z = -0.8$ and $r/r_0 = 0.5$. This form of measuring spin-up times is not well suited to a comparison with theory, but for higher values of the Burger number and large time, it approximates the behavior of the first modal spin-up time. At the mid-plane their result is in qualitative agreement with the experiments in this thesis, but it disagrees with the measurements at $z = -0.8$. One of the authors (Buzyna, private communication) has suggested that this discrepancy may be due to the diffusion of the salt near the lower boundary over the time from when the stratification was produced and the time when the experiment was conducted. This would allow greater penetration of the effects of the Ekman layers and tend to result in a larger spin-up time than would be expected for a linear gradient. The observed spin-up time

was that expected from a linear gradient. Thus, if the stratification had been linear, the spin-up time would have been smaller.

Therefore, the results of the experiments of Buzyna and Veronis are qualitatively consistent with the results presented here.

Further experimental work should be performed to study the effects of non-linearity, viscosity and stratification on the deviations from the linear theory. This can be done most easily for the larger Rossby numbers and intermediate stratifications. Small Rossby numbers and small stratifications cannot yield accurate results as the temperature perturbations are too small to resolve.

BIBLIOGRAPHY

- Baker, D.J., " A Technique for the Precise Measurement of Small Fluid Velocities ", J. Fluid Mech 26 (3), 573-575 (1966)
- Buzyna and Veronis, " Spin-up of a Stratified Fluid: Theory and Experiment ", to be published
- Dicke, R.H., " The Sun's Rotation and Relativity ", Nature, 2 May 1964
- Dicke, R.H., " The Solar Oblateness and the Gravitational Quadrupole Moment", Ap.J. 159 , 1-24 (1970)
- Greenspan, H.P., The Theory of Rotating Fluids, Cambridge University Press, Cambridge, 1968
- Greenspan H.P., and Howard, L.N., " On the Time-dependent Motion of a Rotating Fluid", J.Fluid Mech. 17 (3), 385-404 (1963)
- Greenspan, H.P. and Weinbaum, S., " On non-linear Spin-up of a Rotating Fluid", J. Math. and Phys. 44, 66-85 (1965)
- Holton, J.R., " The Influence of Viscous Boundary Layers on Transient Motions in a Stratified Rotating Fluid", J.Atmos. Sci. 22 (4), 402-411 (1965)

Holton, J.R., and Stone, P.H., "A Note on the Spin-up of a Stratified Fluid", J. Fluid Mech.

Lamb, H., Hydrodynamics Dover reprint of the 6th edition, 1932

Pedlosky, J., "The Spin-up of a Stratified Fluid", J. Fluid Mech.
28 (3), 463-479 (1967)

Sakurai, T., "Spin-down of a Rotating Stratified Fluid in Thermally Insulated cylinders", J. Fluid Mech. 37 (4), 689-699 (1970)

Saunders, K.D., The Design and Construction of the MIT Air-bearing Turntable, Report GFD/70-3, July 1970

Siegmann, W.L., Spin-up of a Continuously Stratified Fluid,
M.S. Thesis, MIT, 1967

Simon, I., and Strong, P.F., "Measurement of Static and Dynamic Response of the Green Building at the MIT Campus to Insolation and Wind", Bull. Seis. Soc. Amer. 58 (5)
1631-1638 (1968)

Walsh, G., "Some Aspects of Time-dependent Motion of a Stratified Rotating Fluid". J. Fluid Mech. 36 (2), 289-307 (1969)

Walin, G., "Contained Inhomogeneous Flow Under Gravity, or How
to Produce a Stratified Fluid System", to be published

McDonald and Dicke, Science 158 , 1562 (1967)

Modisette and Novotny, Science 166, 872 (1969)

Table 1
Experimental Parameters

Experiment	$/\epsilon/$	$S = N^2/\Omega^2$	B	$E \times 10^4$	$F \times 10^4$	t_{spin}	ΔT	Ω	$\Delta \Omega$
1	0.106	0.627	0.396	2.12	88.6	24.54	8.3	1.398	-0.148
2	0.038	0.882	0.470	2.12	88.6	24.54	8.35	1.398	-0.053
3	0.038	0.882	0.470	2.12	88.6	24.54	8.35	1.398	-0.053
4	0.038	0.915	0.478	2.13	88.2	24.57	8.64	1.395	-0.053
5	0.037	0.882	0.470	2.05	95.0	24.12	8.64	1.448	+0.053
6	0.038	0.915	0.478	2.13	88.2	24.57	8.64	1.395	-0.053
7	0.029	0.776	0.440	1.90	110.5	23.22	8.20	1.561	-0.045
8	0.029	0.617	0.393	1.90	110.5	23.22	8.30	1.561	-0.045
9									
10	0.041	1.331	0.576	2.92	46.9	28.78	9.32	1.017	-0.041
11	0.000								
12	0.000								
13	0.0082	1.286	0.567	3.05	42.7	29.45	8.20	0.971	-0.0080
14	0.0084	1.250	0.559	3.06	42.7	29.47	7.97	0.970	-0.0081
15	0.0082	1.229	0.554	3.03	43.4	29.36	7.97	0.979	-0.0080
16	0.050	1.292	0.568	3.19	39.3	30.09	8.14	0.932	-0.047
17	0.035	1.293	0.564	3.14	40.5	29.87	8.14	0.946	-0.033
18	0.228	0.865	0.465	3.72	28.8	32.52	9.20	0.798	-0.182
19	0.029	2.808	0.851	4.58	19.1	36.06	8.25	0.649	-0.0185
20	0.081	3.175	0.891	4.81	17.3	36.97	8.18	0.617	-0.0502
21	0.147	3.561	0.944	5.10	15.4	38.07	8.16	0.582	-0.085
22	0.223	4.140	1.017	5.44	13.5	39.31	8.34	0.546	-0.1215
23	0.028	3.827	0.978	5.25	14.5	38.63	8.27	0.565	-0.016
24	0.044	2.053	0.716	3.88	26.6	33.19	8.14	0.766	-0.034
25	0.095	2.131	0.730	3.88	26.6	33.20	8.45	0.766	-0.073
26	0.065	7.363	1.356	7.51	7.08	46.20	7.78	0.395	+0.026
27	0.061	7.450	1.365	7.45	7.19	46.01	8.00	0.398	+0.024
28	0.033	12.711	1.783	9.67	4.27	52.43	8.10	0.307	+0.010
29	0.047	16.60	2.037	11.1	3.24	56.17	8.03	0.267	+0.013

44

Table 1 (continued)

Experiment	$/\epsilon/$	S	B	$E \times 10^4$	$F \times 10^4$	t_{spin}	ΔT	Ω	$\Delta \Omega$
30	0.057	18.87	2.172	11.90	2.82	58.15	7.95	0.250	+0.014
31	0.055	22.41	2.367	12.9	2.42	60.43	8.09	0.231	+0.013
32	0.098	12.779	1.787	9.70	4.24	52.51	8.09	0.306	+0.030
33	0.083	17.323	2.081	11.2	3.16	56.53	8.17	0.264	+0.022
34	0.047	9.202	1.517	8.3	5.87	48.41	8.07	0.360	+0.017
35	0.048	9.956	1.577	8.52	5.50	49.21	8.17	0.348	+0.017
36	0.090	9.800	1.565	8.53	5.48	49.25	8.02	0.348	+0.031
37	0.056	11.754	1.714	9.28	4.64	51.35	8.14	0.320	+0.018
38	0.032	11.759	1.715	9.28	4.64	51.35	8.14	0.320	+0.010

Table 2
Data Usage

Experiment	Temperature Data	Photographic Data
1	N*	N
2	N*	N
3	N*	N
4	N*	-
5	N*	-
6	N*	-
7	N*	N
8	N*	-
9	-	-
10	N	N
11	-	N
12	-	N
13	-	N
14	N	N
15	+B	N
16	-	+
17	+G	N
18	+G	N
19	+B	+
20	+B	+
21	+G	+
22	+G	N
23	+D	+
24	+G	+
25	+G	N
26	+B	N
27	+G	+
28	+B	N
29	+G	N
30	+B	+
31	+G	+
32	+D	+
33	+G	+
34	+G	+
35	+B	+
36	+G	+
37	+G	N
38	N	+

Key:

+ taken and reduced
- not taken
N taken but not reduced

* no filtering
B too large fitting error
D result of doubtful quality
G fit seems reliable

TABLE 3

Temperature Perturbation Data for Experiment 24

Series	t	Thermistor										
		1	2	4	5	6	7	8	10	11	12	
0	0.000	0.0	0.0	0.0	0.0	0.0	0.0	0.0	0.0	0.0	0.0	0.0
1	0.042	-1.0	-2.2	0.0	-0.5	-2.3	-1.4	1.0	1.6	2.5	3.0	
2	0.180	-19.0	-12.3	0.0	-5.6	-5.6	-4.6	1.0	4.2	4.0	3.5	
3	0.318	-25.0	-26.1	0.0	-11.6	-10.5	-8.6	1.0	5.0	4.0	4.7	
4	0.456	-34.0	-32.1	0.0	-17.6	-14.2	-12.3	1.0	5.0	4.0	4.0	
5	0.594	-39.0	-38.1	-0.1	-24.5	-16.5	-14.8	0.8	4.8	3.8	4.0	
6	0.732	-43.0	-42.0	-1.9	-29.4	-20.3	-20.0	0.0	3.6	3.0	4.0	
7	0.870	-46.0	-43.1	-0.1	-33.2	-23.2	-20.4	0.0	1.8	2.5	4.0	
8	1.008	-52.0	-46.0	-0.9	-35.4	-26.0	-23.1	0.0	0.6	0.8	4.0	
9	1.146	-53.0	-46.0	-0.1	-39.1	-26.2	-24.4	0.0	-1.4	0.0	4.0	
10	1.284	-53.0	-48.0	-0.9	-40.1	-28.2	-27.0	0.0	-3.2	-0.2	3.3	
11	1.422	-53.0	-48.0	-0.0	-41.1	-29.9	-27.1	0.0	-4.4	-1.0	3.7	
12	1.560	-53.0	-47.0	-0.1	-42.0	-29.1	-28.0	0.0	-6.0	-1.2	3.3	

TABLE 3 (continued)

Series	Thermistor							
	13	14	15	16	17	18	19	20
0	0.0	0.0	0.0	0.0	0.0	0.0	0.0	0.0
1	5.4	5.1	3.3	3.3	6.2	6.8	3.7	3.0
2	10.7	11.8	7.0	4.0	12.2	12.6	7.7	3.0
3	16.1	16.9	10.3	4.0	18.2	17.2	11.2	3.0
4	20.4	19.9	13.6	4.0	23.5	22.0	14.2	3.4
5	24.6	22.9	15.3	4.0	27.5	25.8	16.8	3.6
6	26.8	25.9	16.6	4.3	31.1	28.6	18.8	3.0
7	29.6	28.6	18.0	4.7	34.1	31.8	20.8	3.0
8	31.6	30.0	18.6	4.0	37.1	34.6	22.0	3.0
9	33.0	30.6	20.3	4.0	40.1	37.8	23.2	3.0
10	33.3	32.0	20.7	4.0	42.4	39.8	25.4	3.0
11	34.0	32.0	20.3	4.0	43.4	41.8	26.0	3.0
12	33.7	32.3	21.0	3.7	45.1	43.0	26.8	3.0

TABLE 4

Experimental parameters which do not vary from experiment to experiment.

$$\nu = 0.01172 \text{ cm}^2 \text{ sec}^{-1}$$

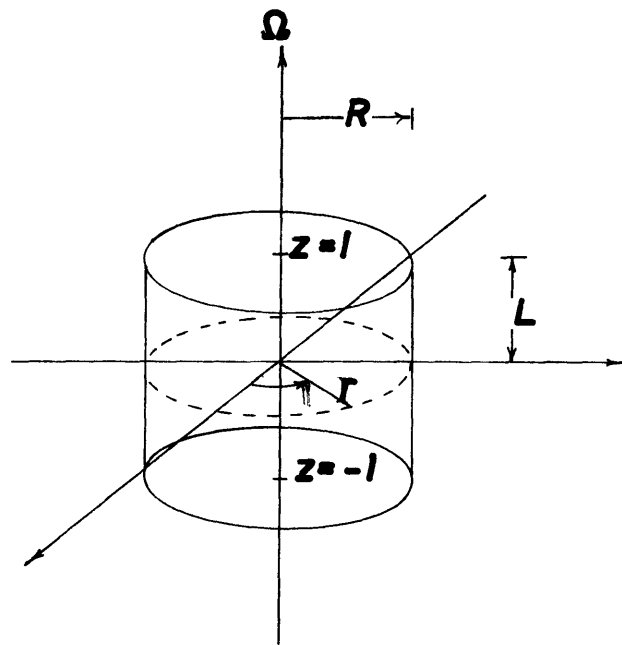
$$\kappa = 0.000837 \text{ cm}^2 \text{ sec}^{-1}$$

$$L = 4.445 \text{ cm}$$

$$\alpha = 0.00134 \text{ } ^\circ\text{C}^{-1}$$

$$\sigma = 14.0$$

$$\rho_0 = 0.818 \text{ gm cm}^{-3}$$



**GEOMETRY OF THE
PROBLEM**

FIGURE 1

THERMISTOR LOCATIONS

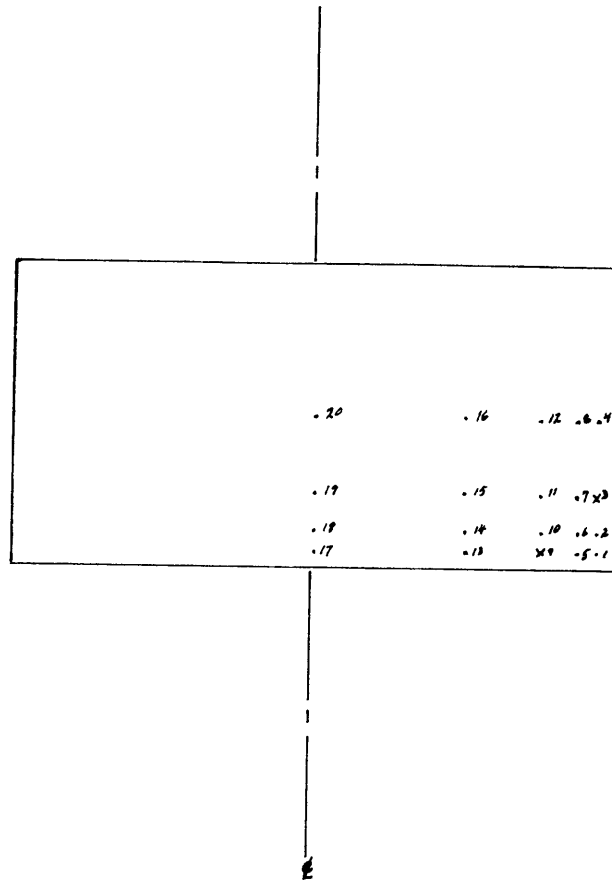


FIGURE 2

LOCATION OF THE EXPERIMENTS
IN ROSSBY NUMBER - BURGER
NUMBER SPACE

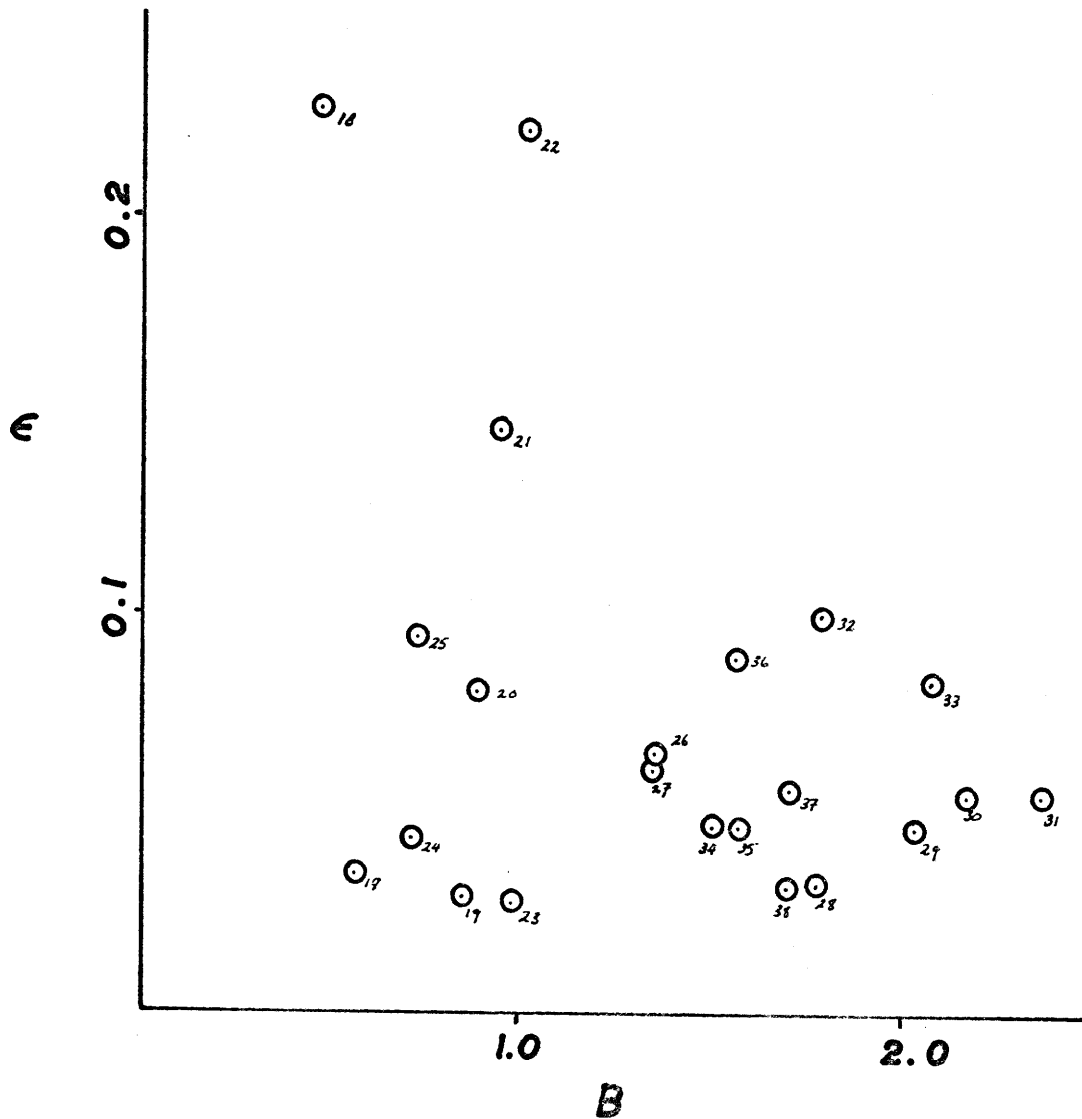


FIGURE 3

63
LOCATION OF THE EXPERIMENTS
IN EKMAN NUMBER - BURGER
NUMBER SPACE

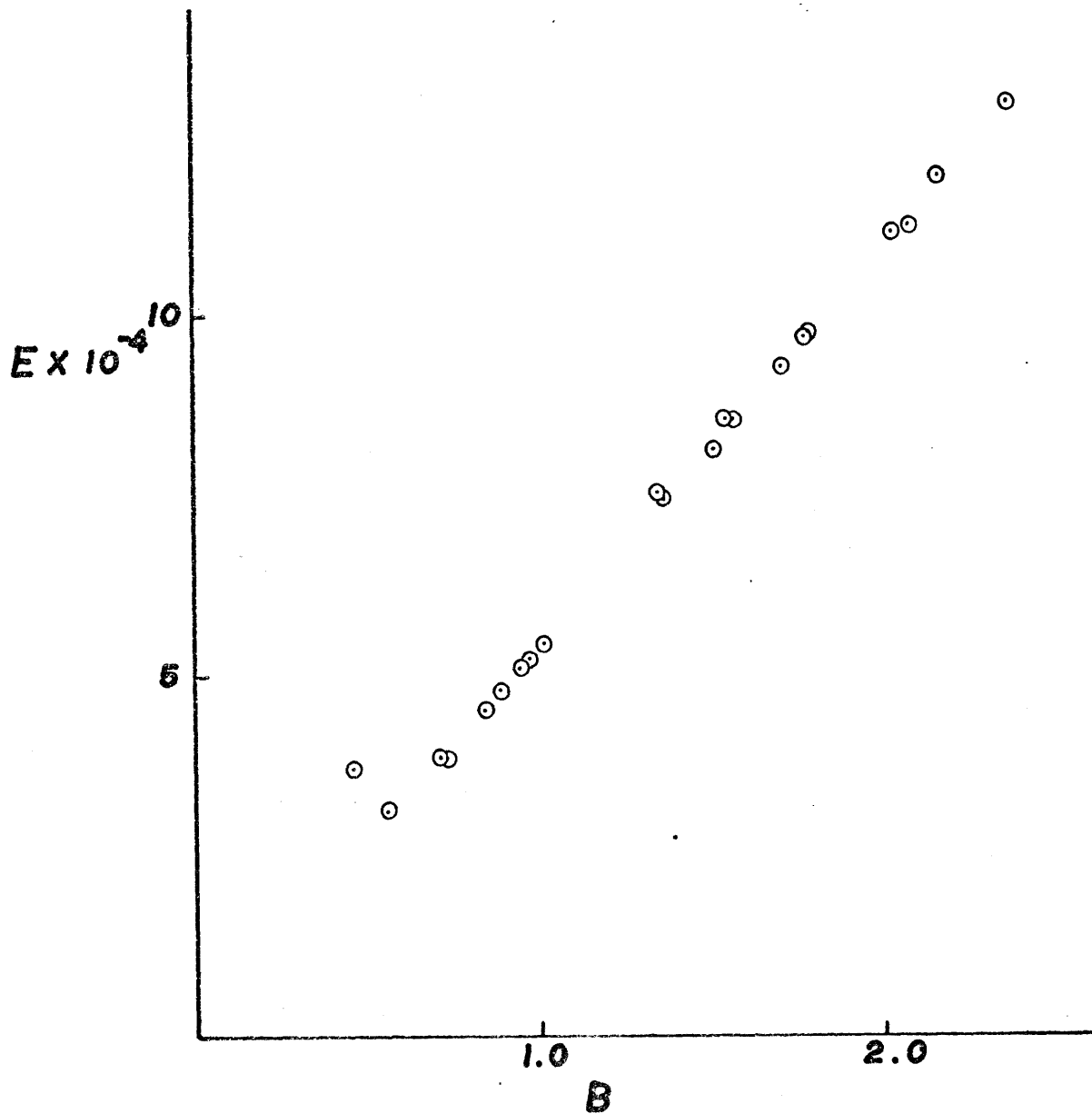


FIGURE 4

FIGURES 5-22 ARE ALL FOR EXPT. 24 THERMISTOR 1
THE SOLID CURVE IS THE WALIN THEORY
THE TEMPERATURE IS GIVEN IN ABSOLUTE
DIGITIZING UNITS

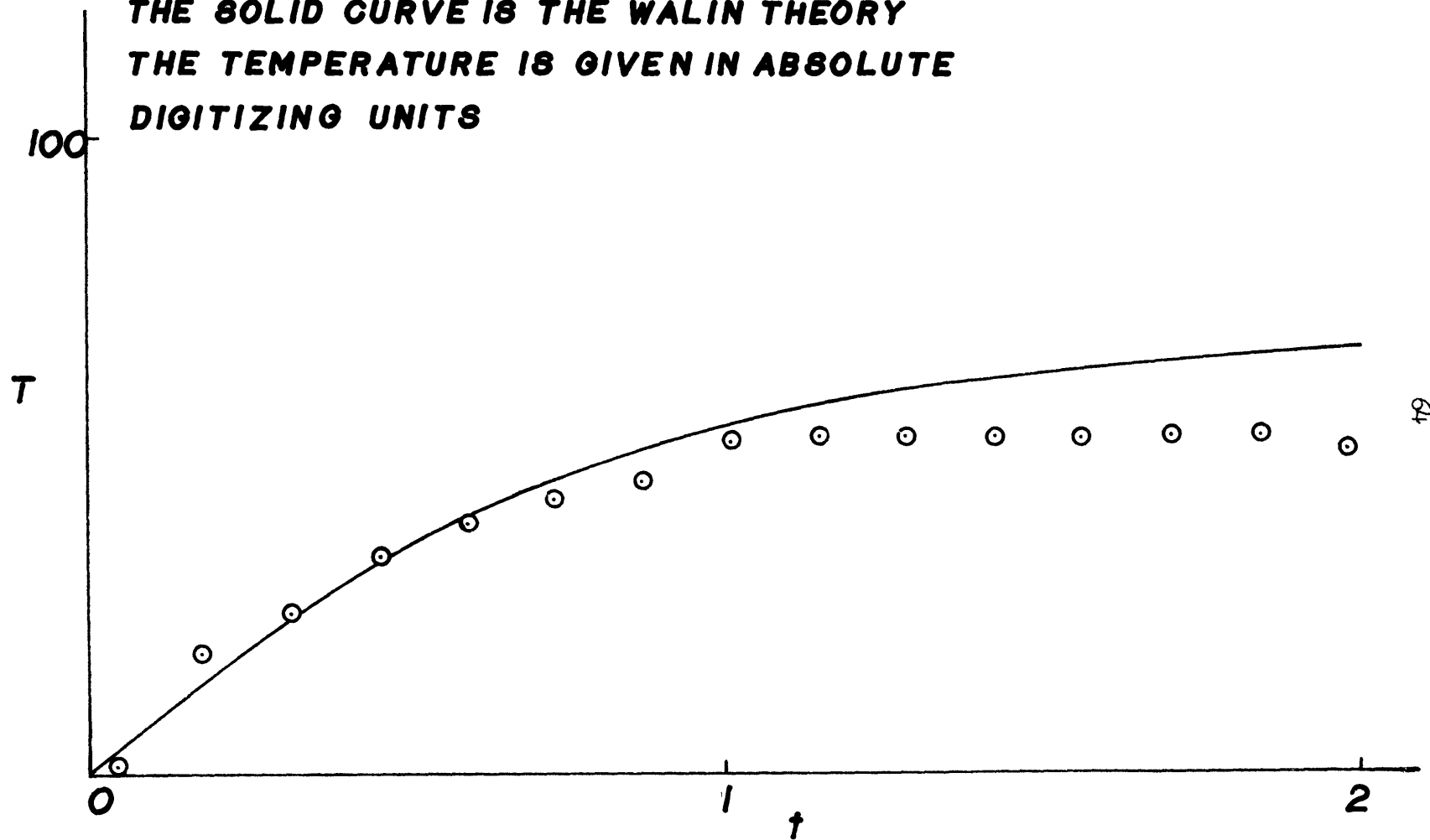


FIGURE 5

THERMISTOR 2

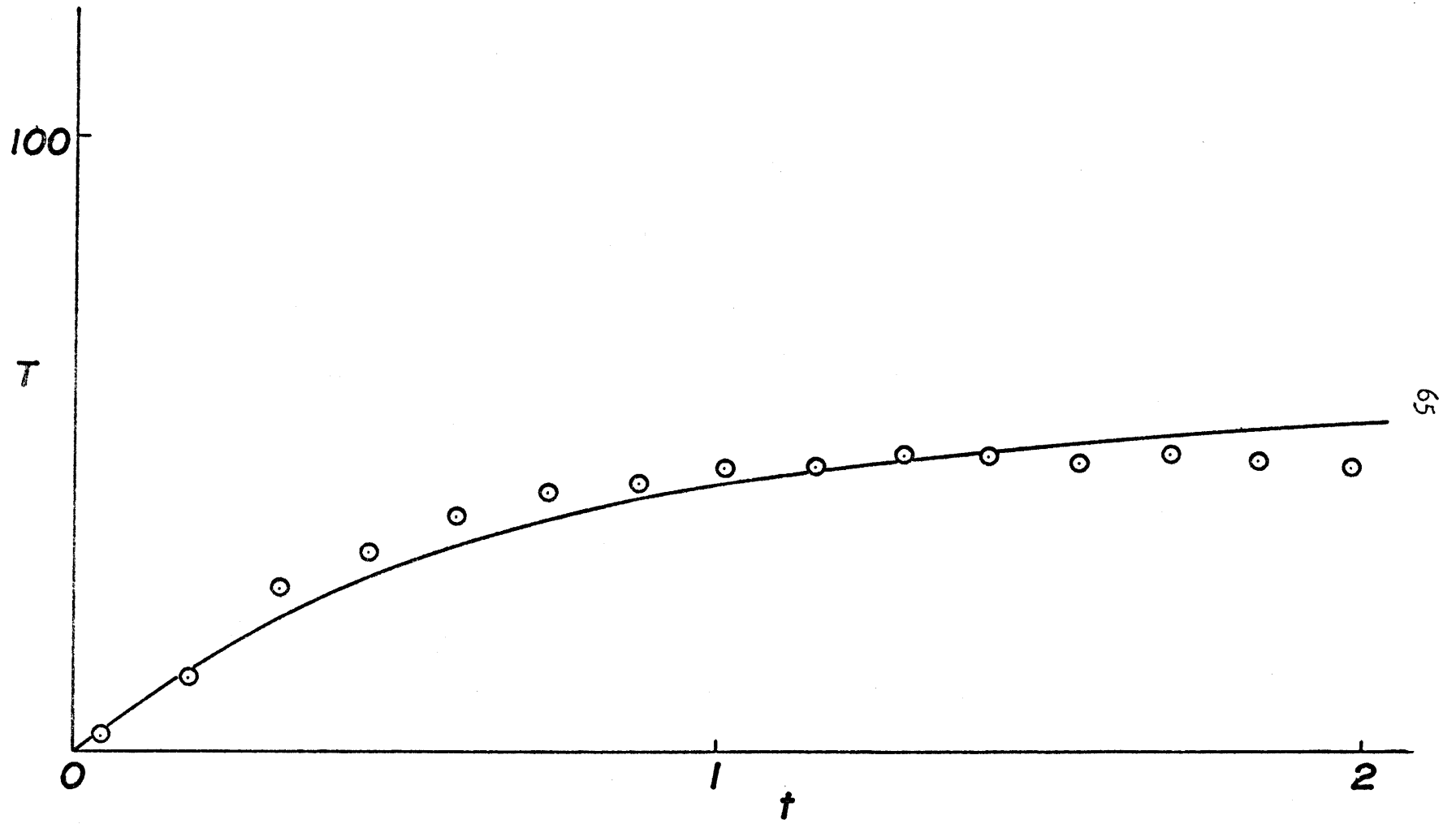


FIGURE 6

THERMISTOR 4

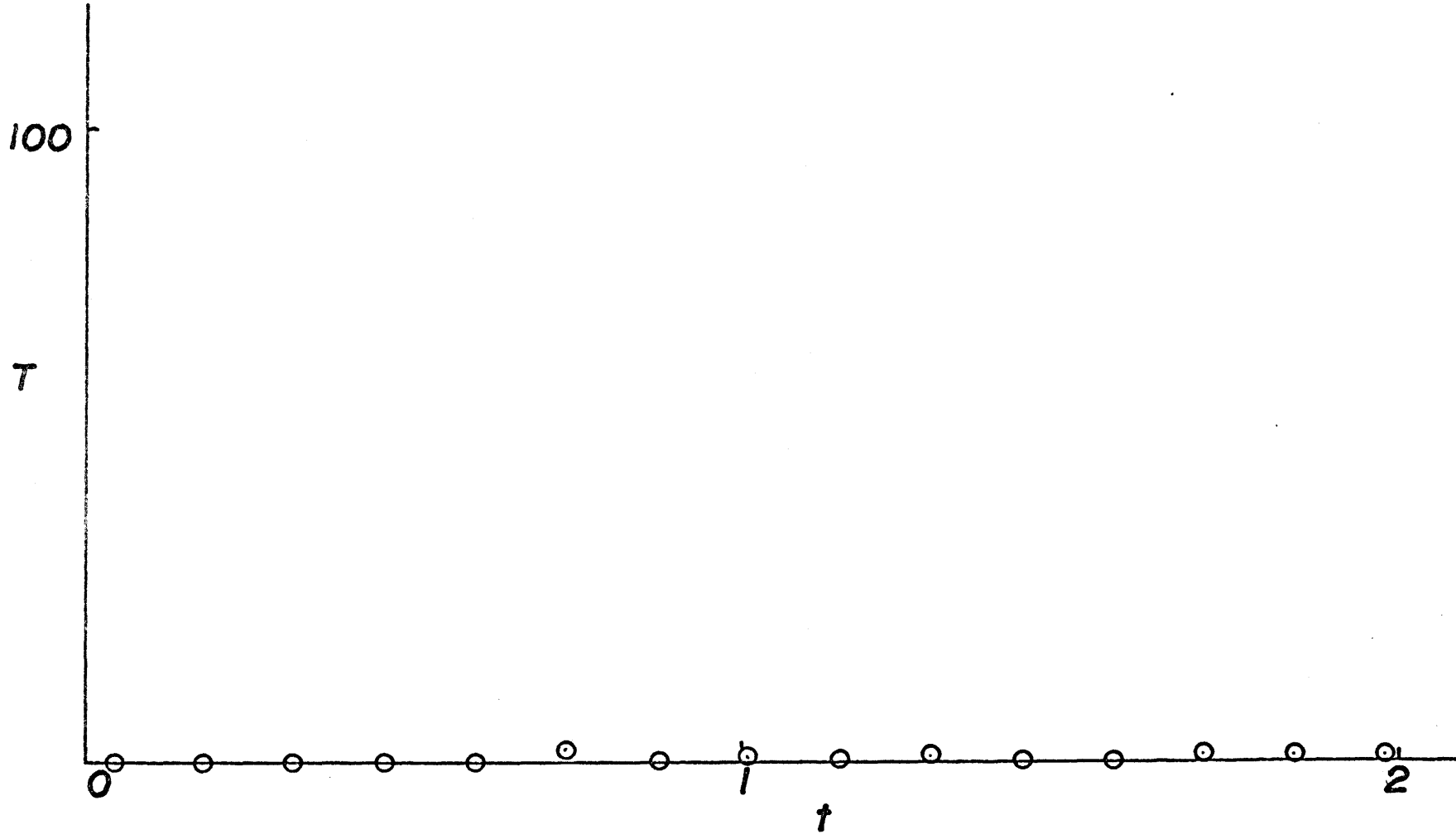


FIGURE 7

THERMISTOR 5

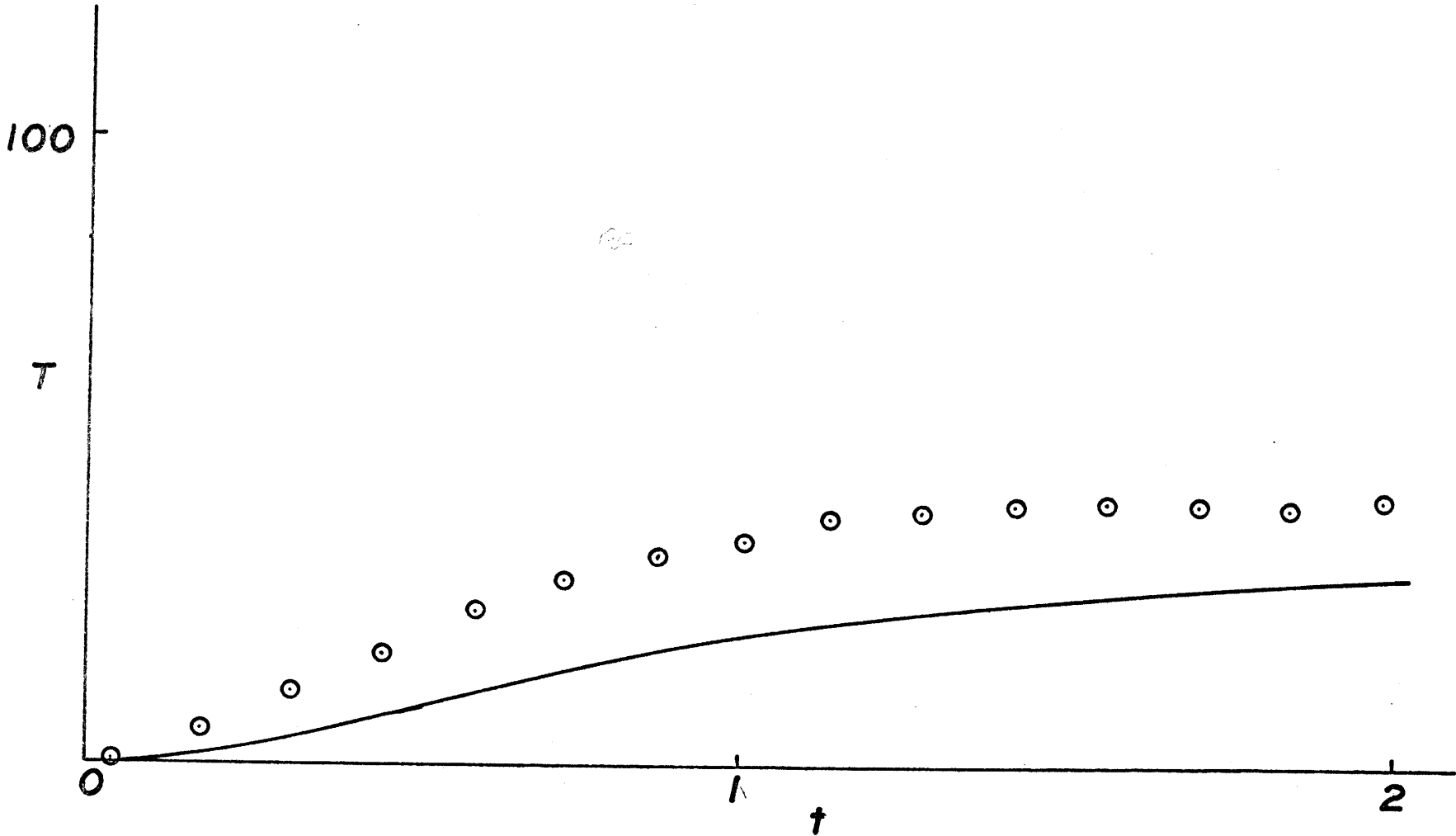
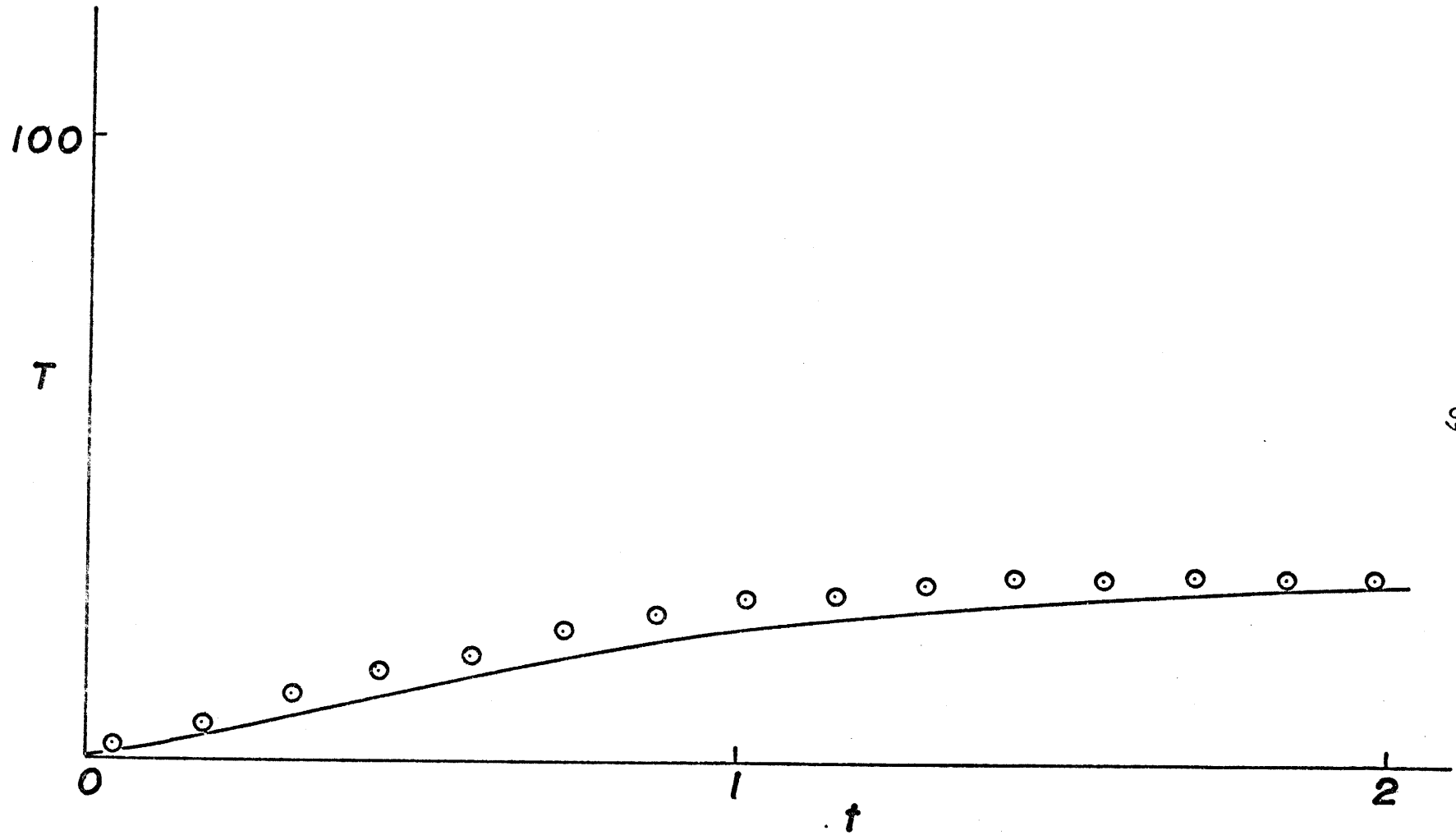


FIGURE 8

THERMISTOR 6



69

FIGURE 9

THERMISTOR 7

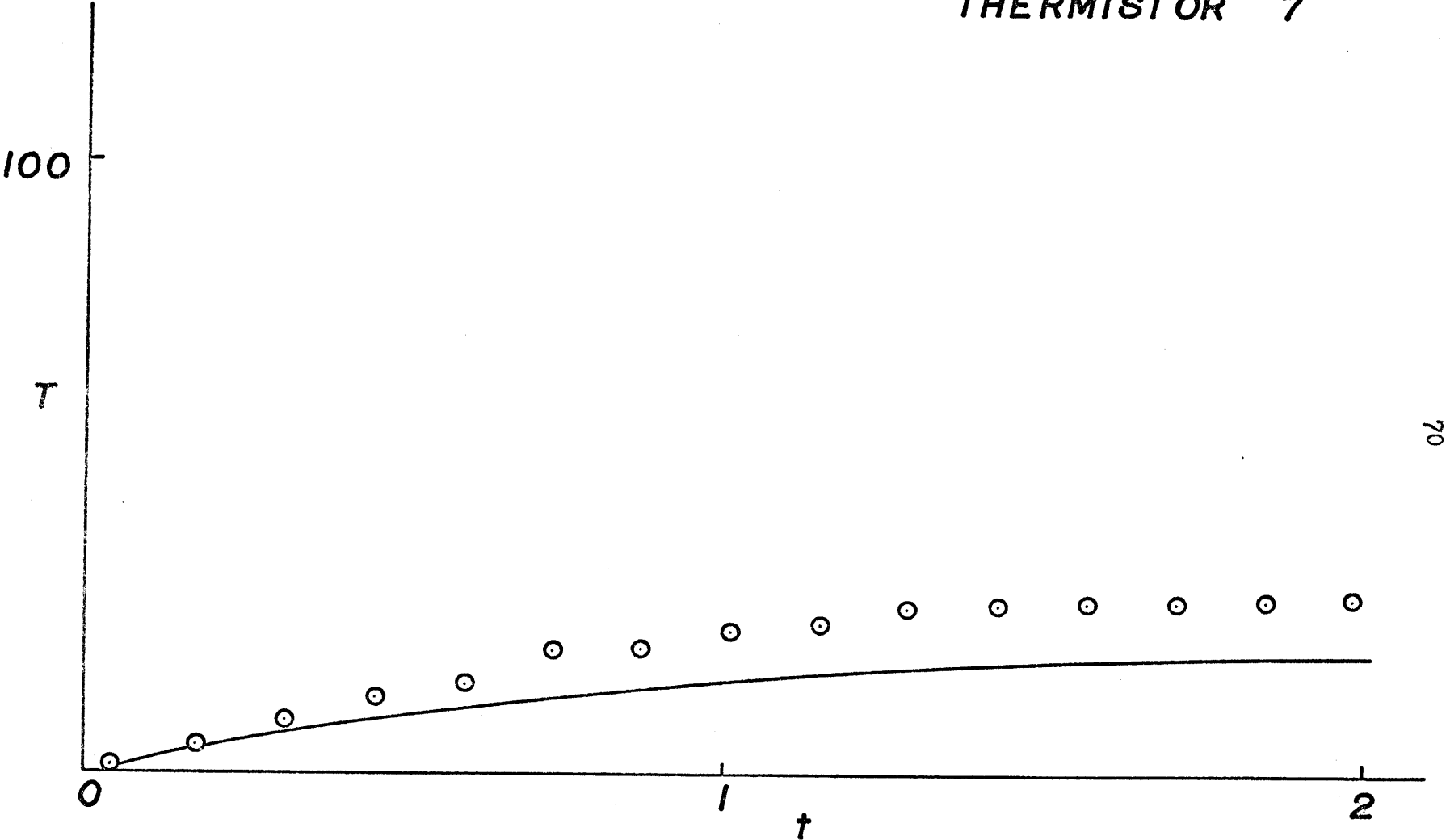
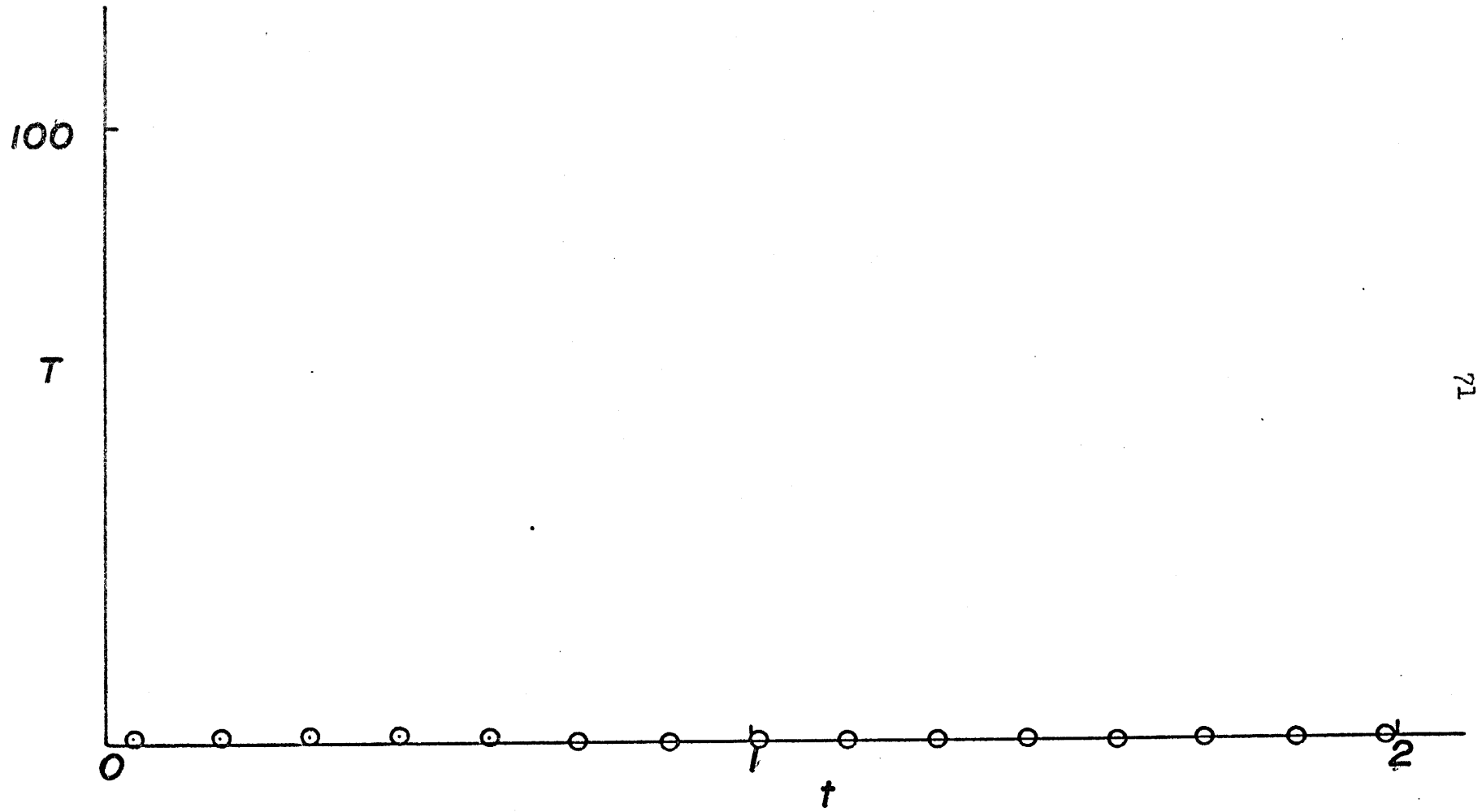


FIGURE 10

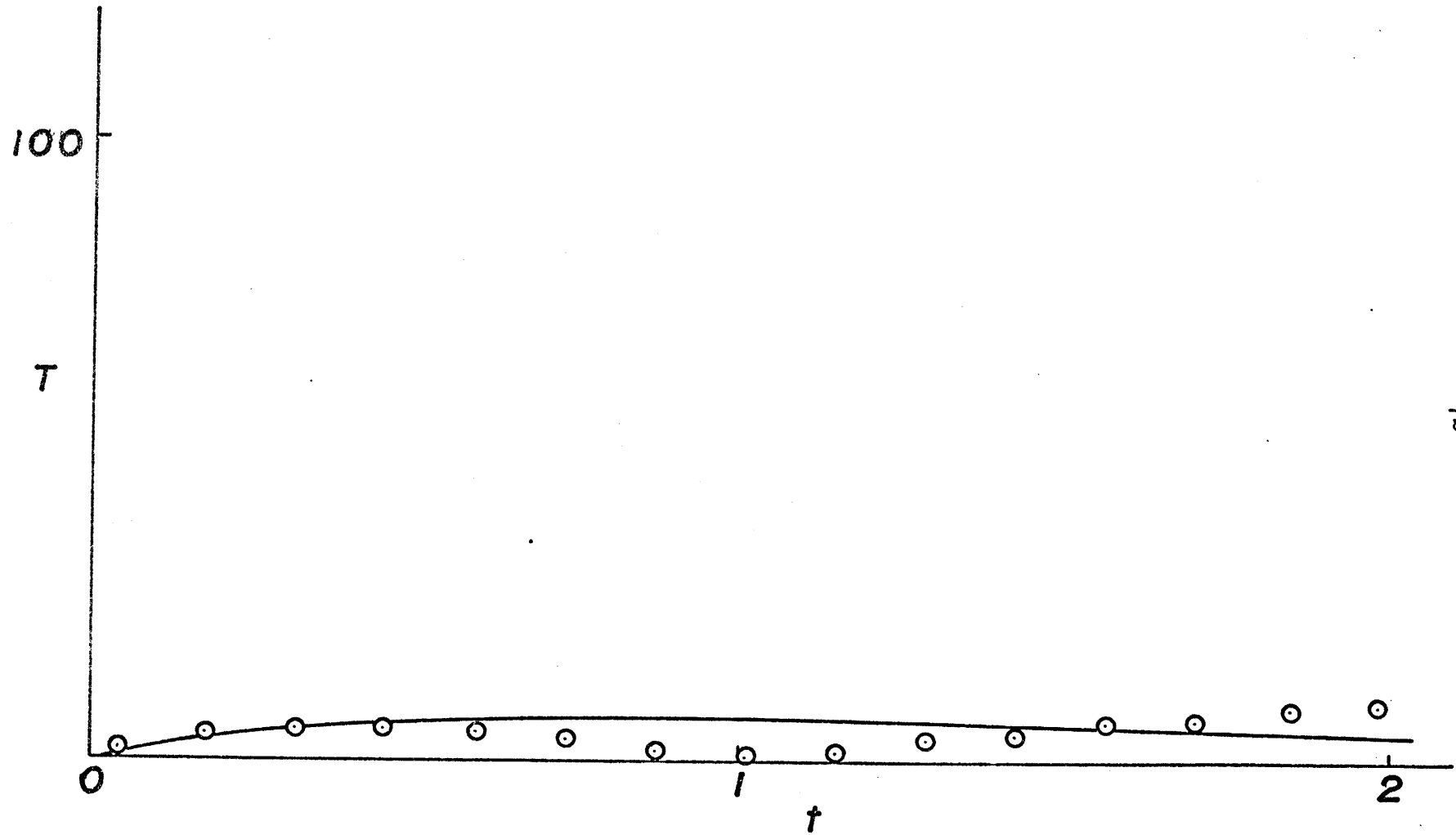
THERMISTOR 8



71

FIGURE 11

THERMISTOR 10



72

FIGURE 12

THERMISTOR 11

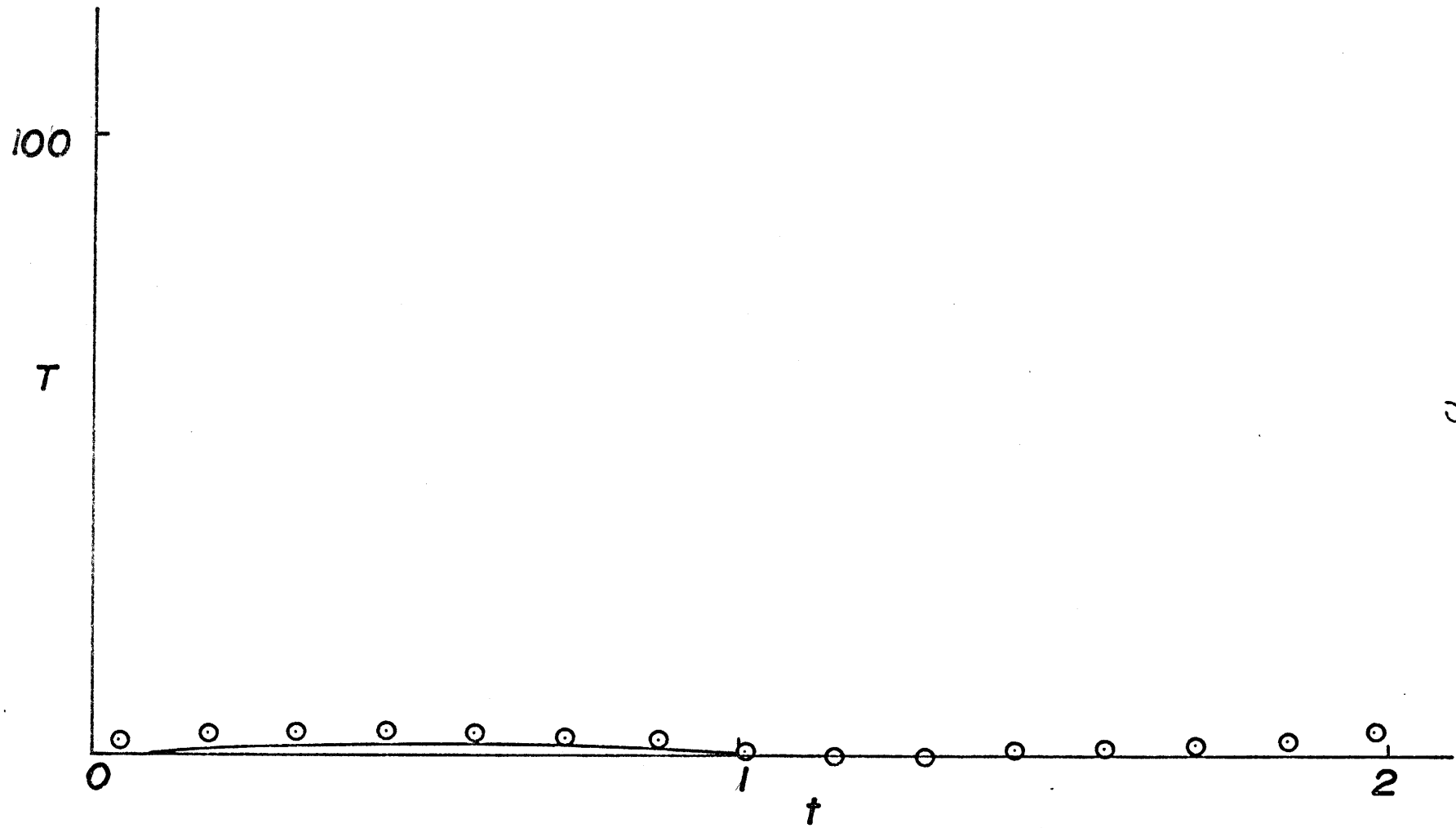
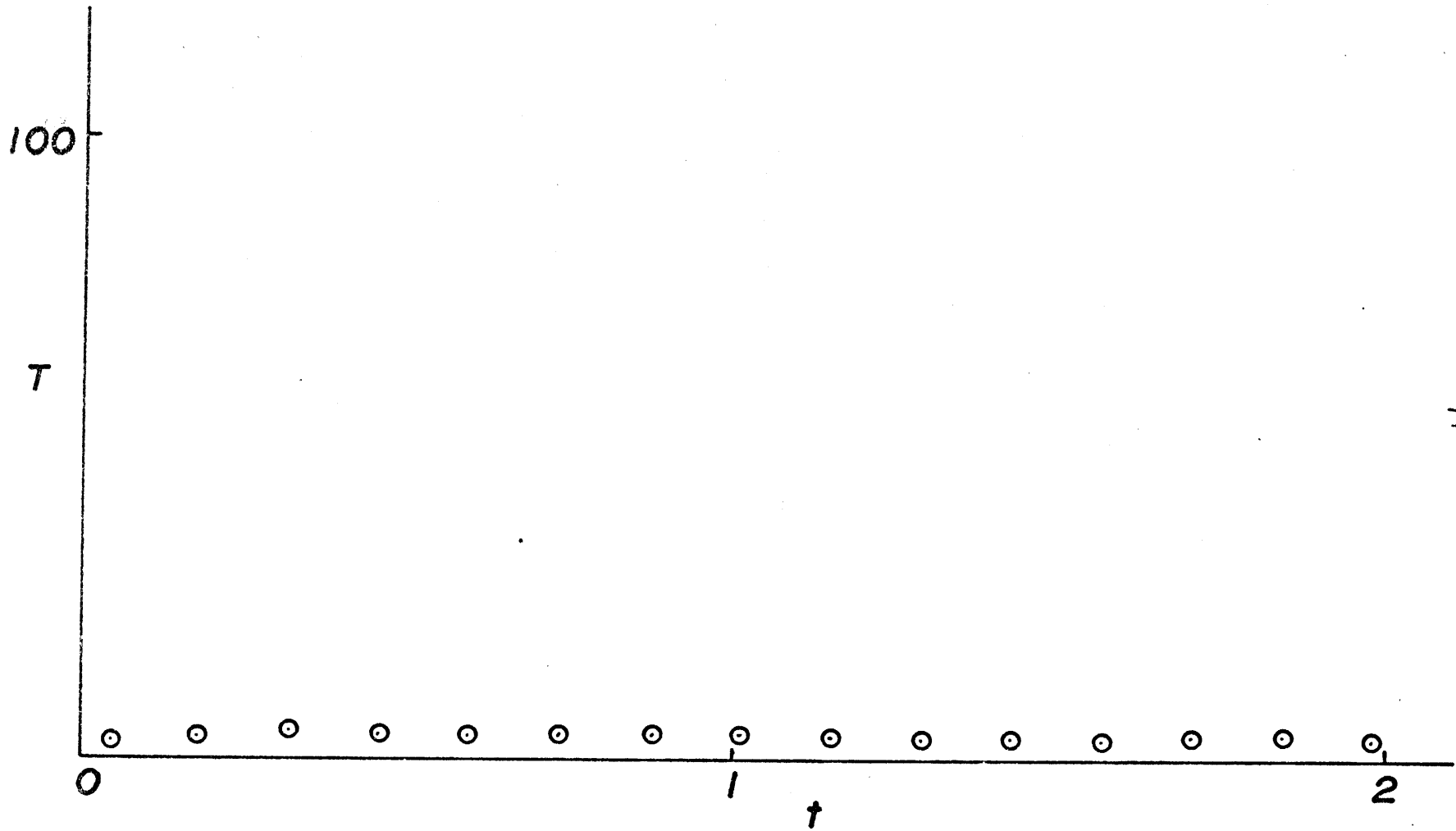


FIGURE 13

THERMISTOR 12



76

FIGURE 14

THERMISTOR 13

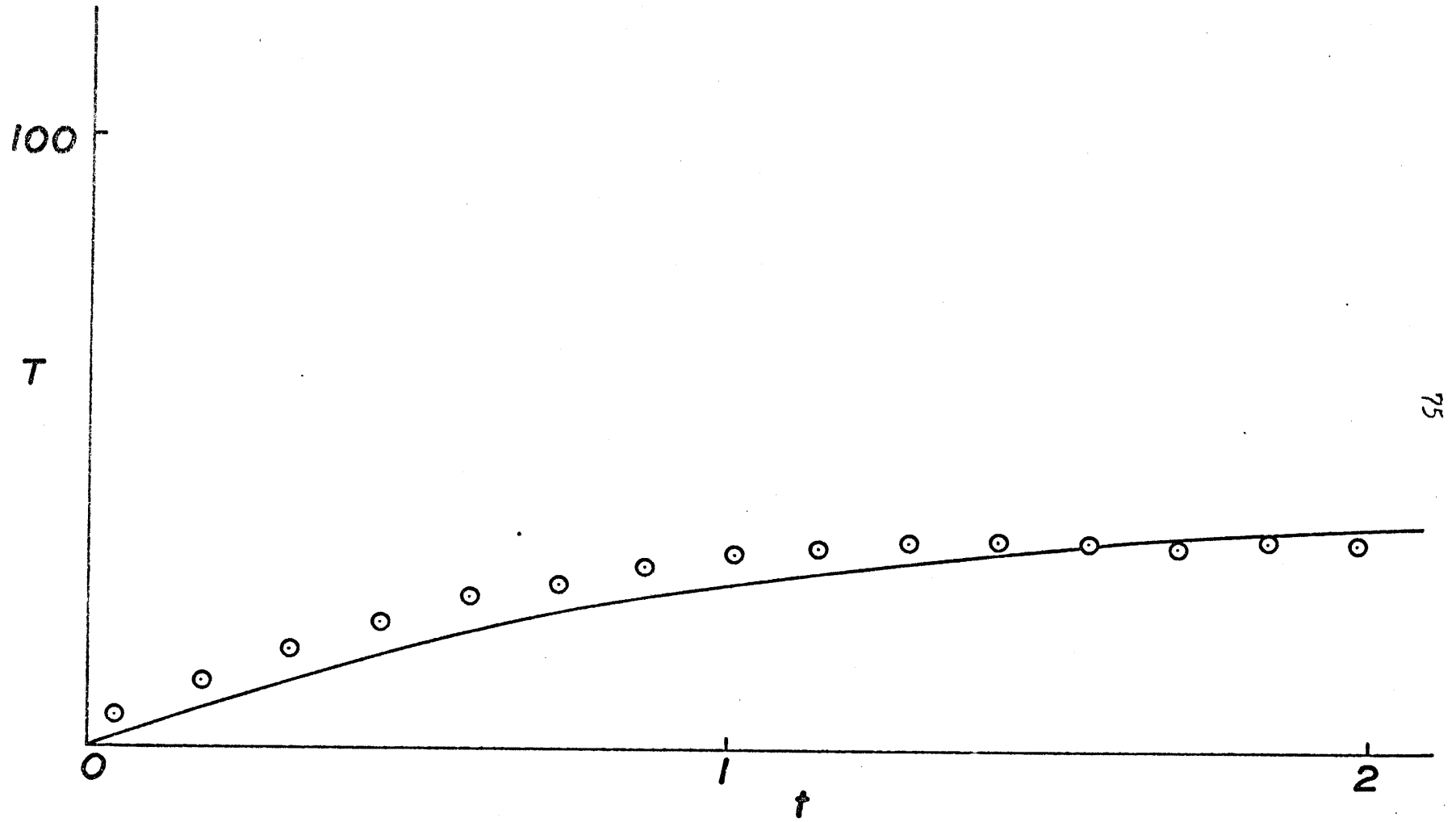
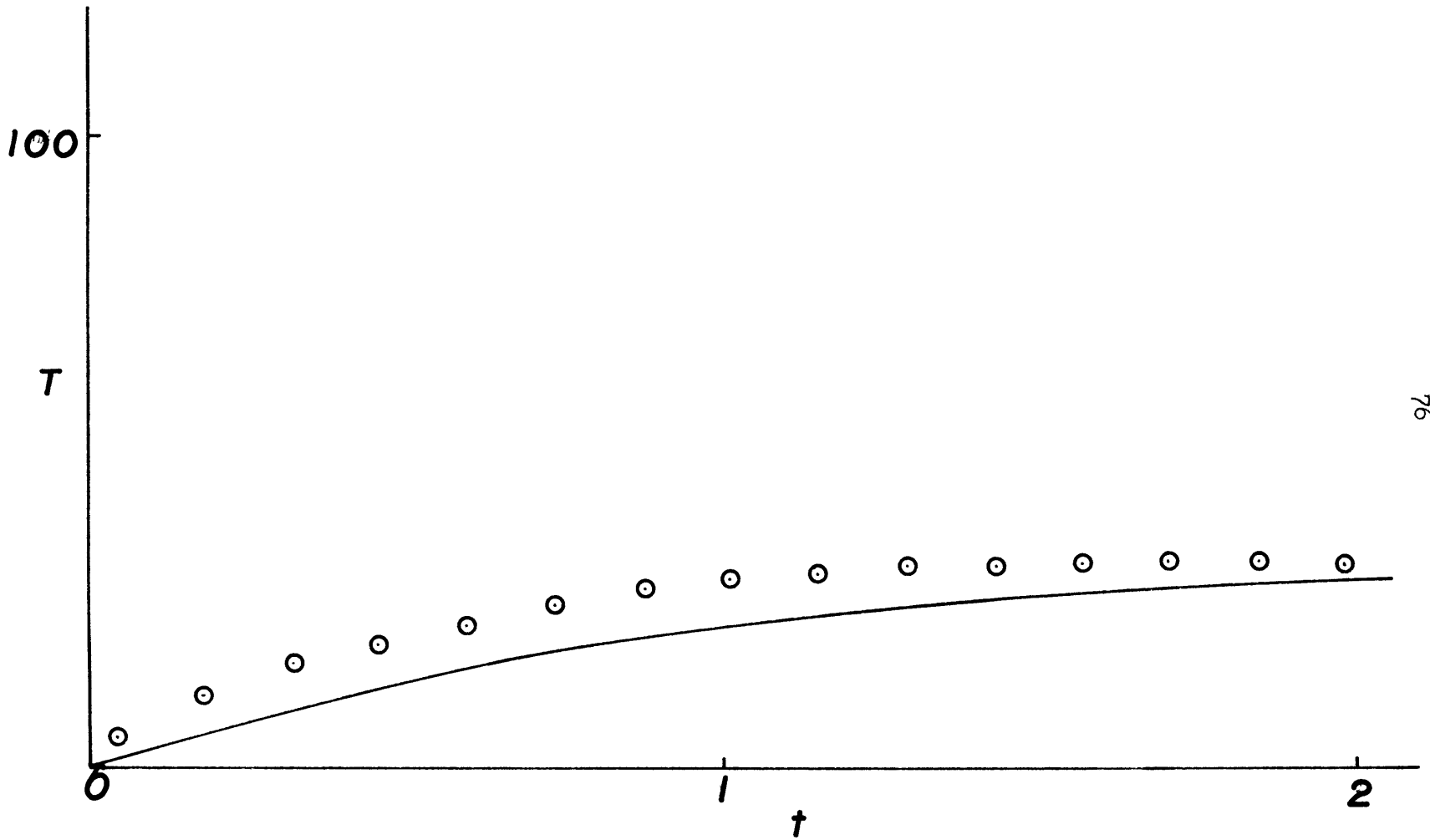


FIGURE 15

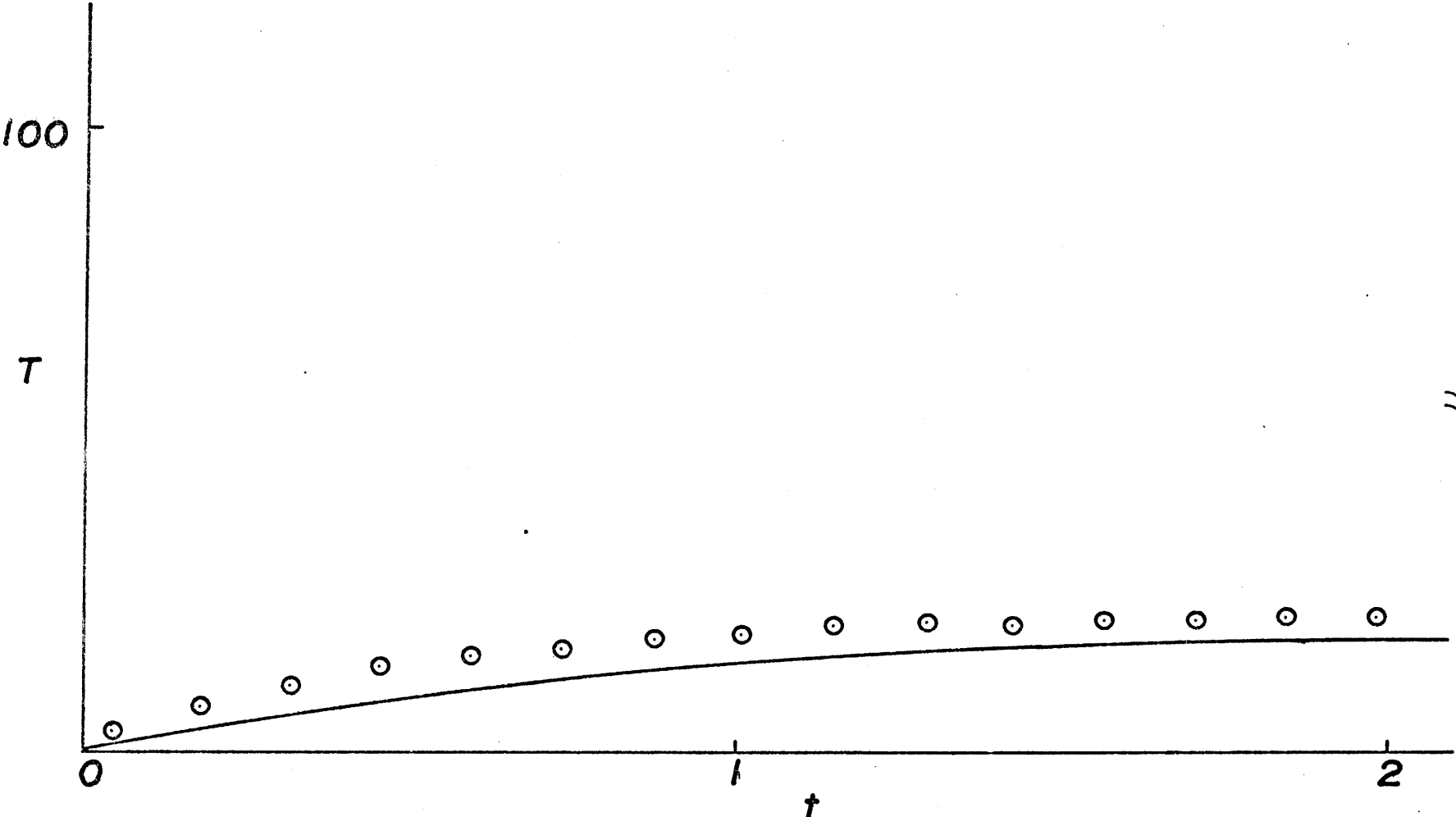
THERMISTOR 14



76

FIGURE 16

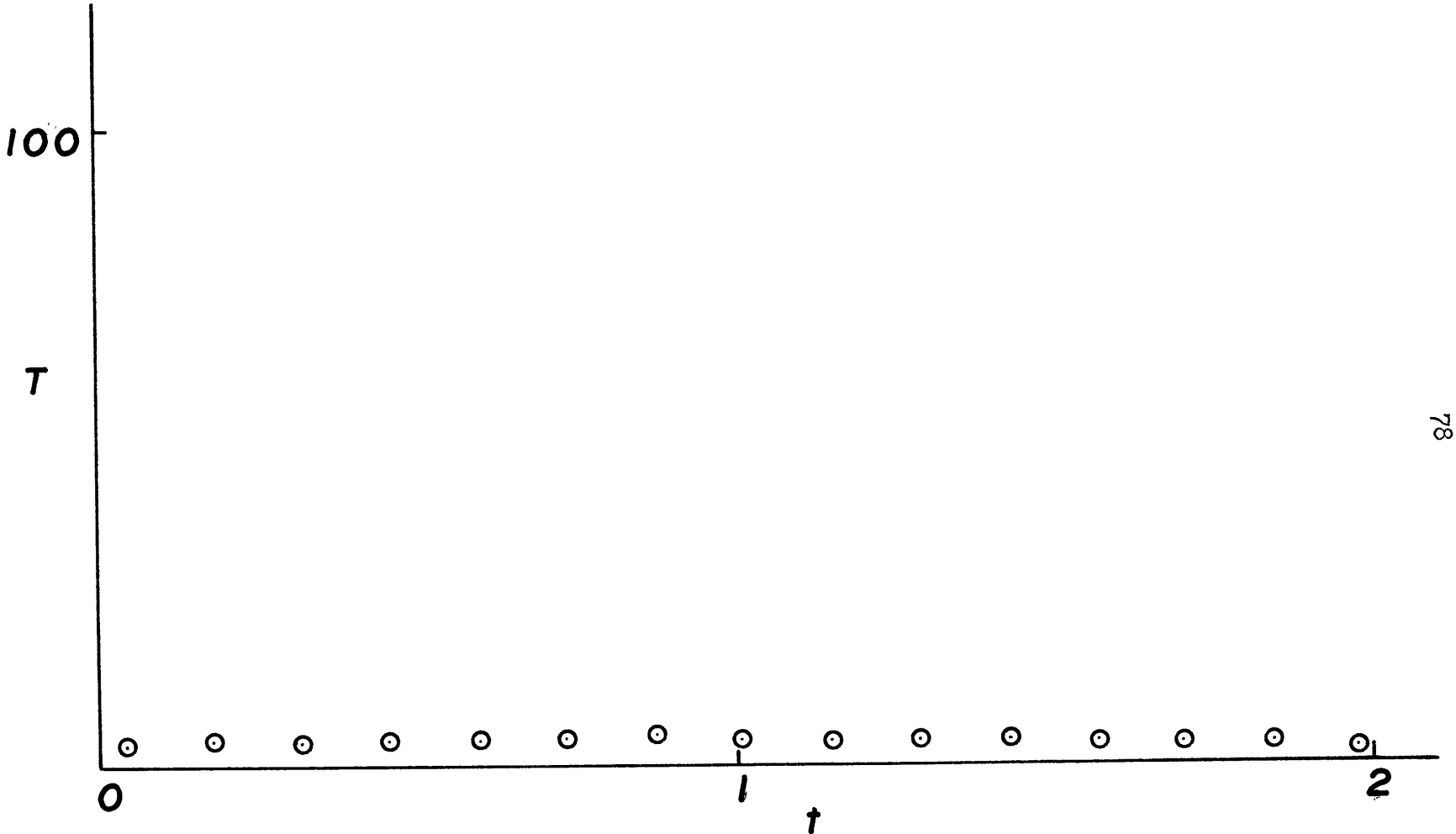
THERMISTOR 15



77

FIGURE 17

THERMISTOR 16



78

FIGURE 18

THERMISTOR 17

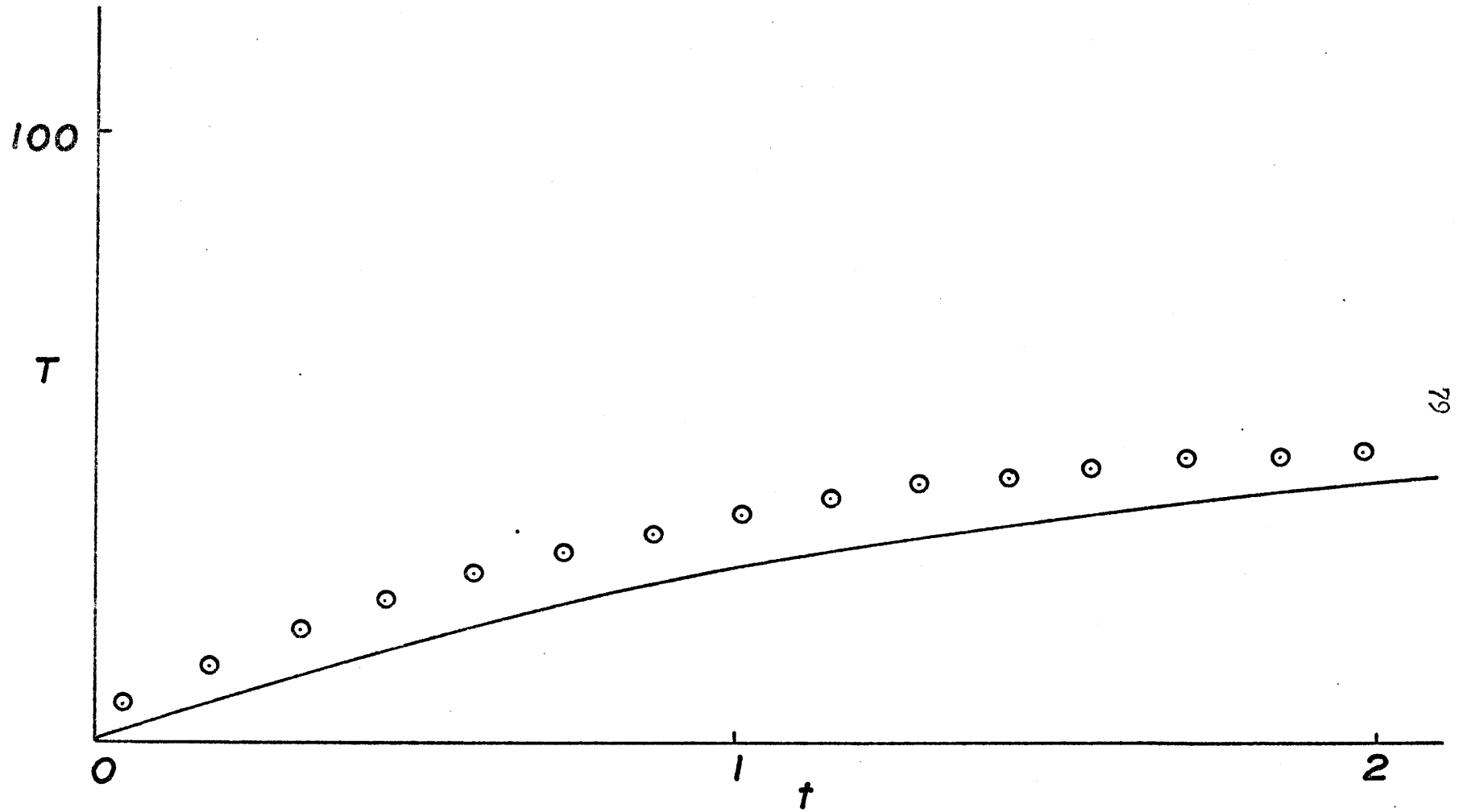


FIGURE 19

THERMISTOR 18

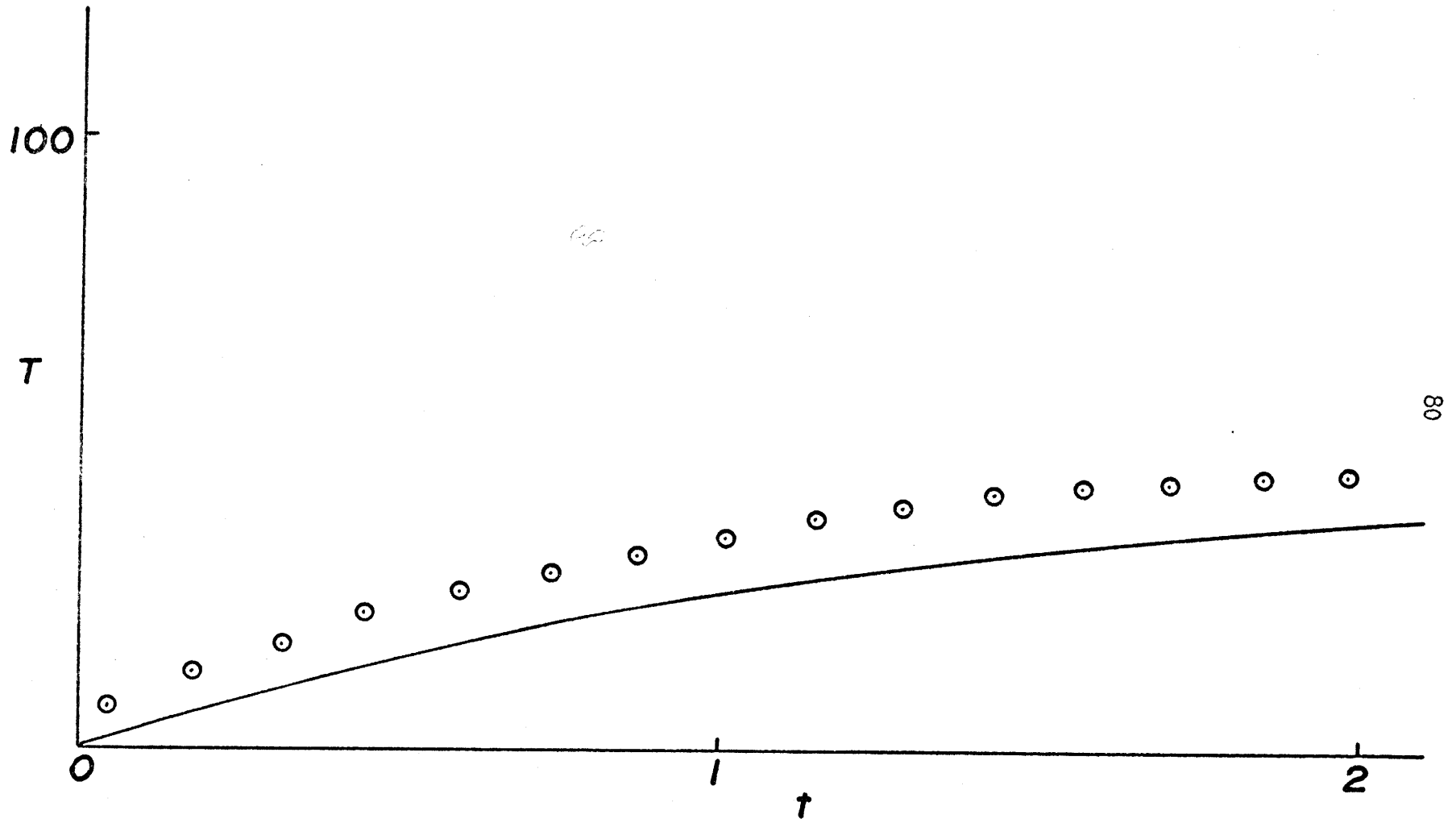
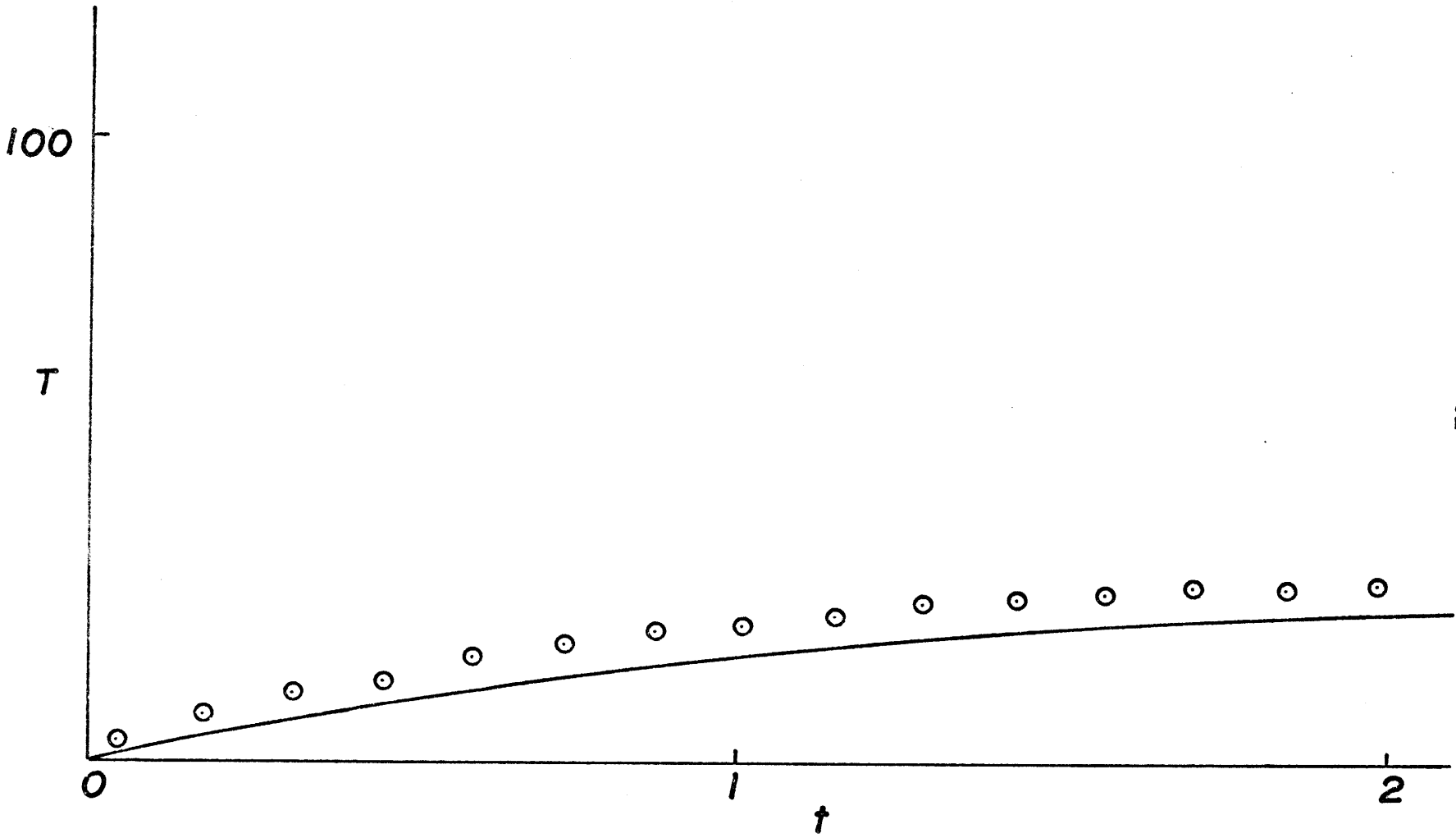


FIGURE 20

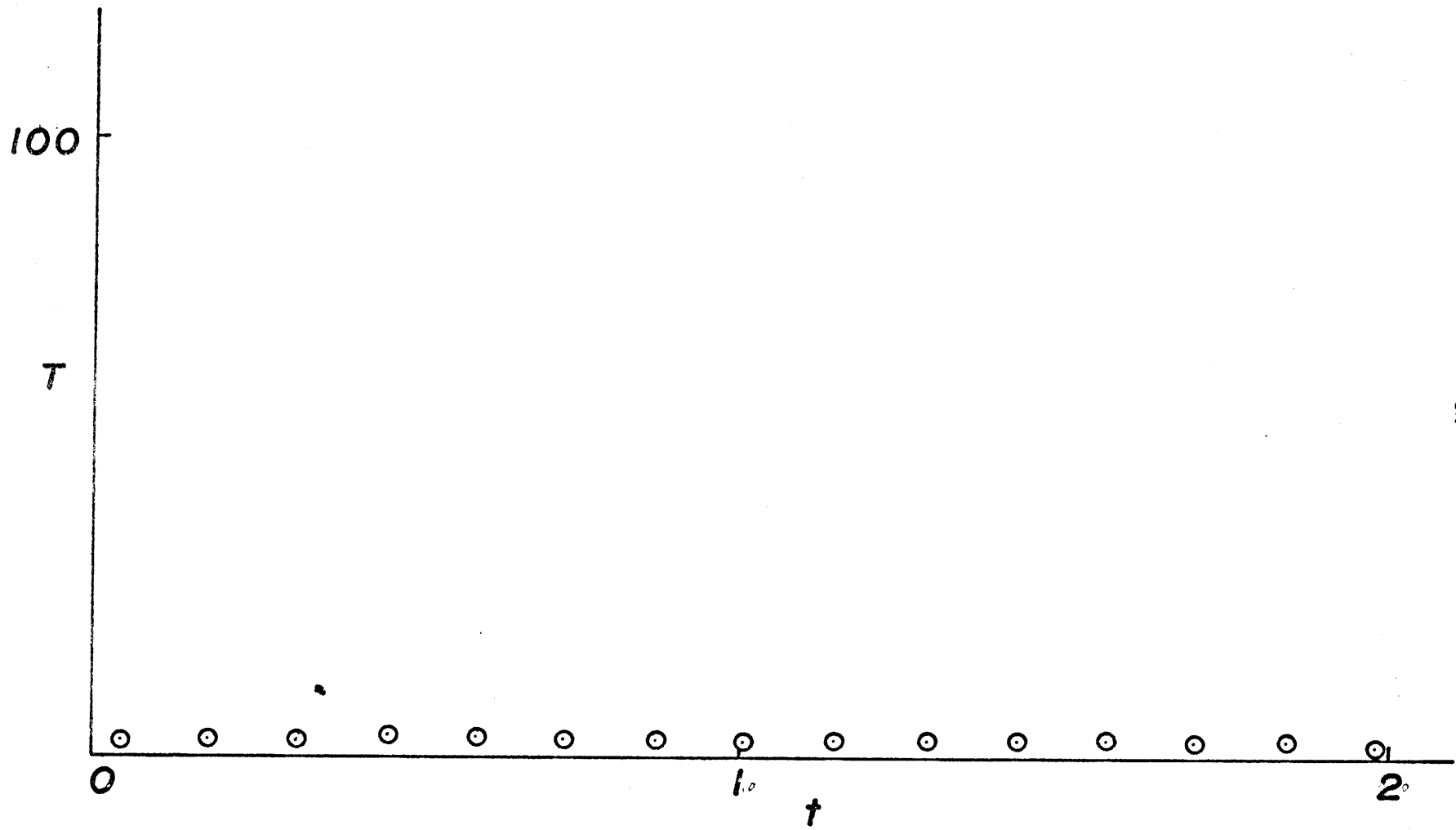
THERMISTOR 19



81

FIGURE 21

THERMISTOR 20



82

FIGURE 22

ANGULAR POSITION
OF A FLOAT AT
 $R = 1.08$
EXPT. 24

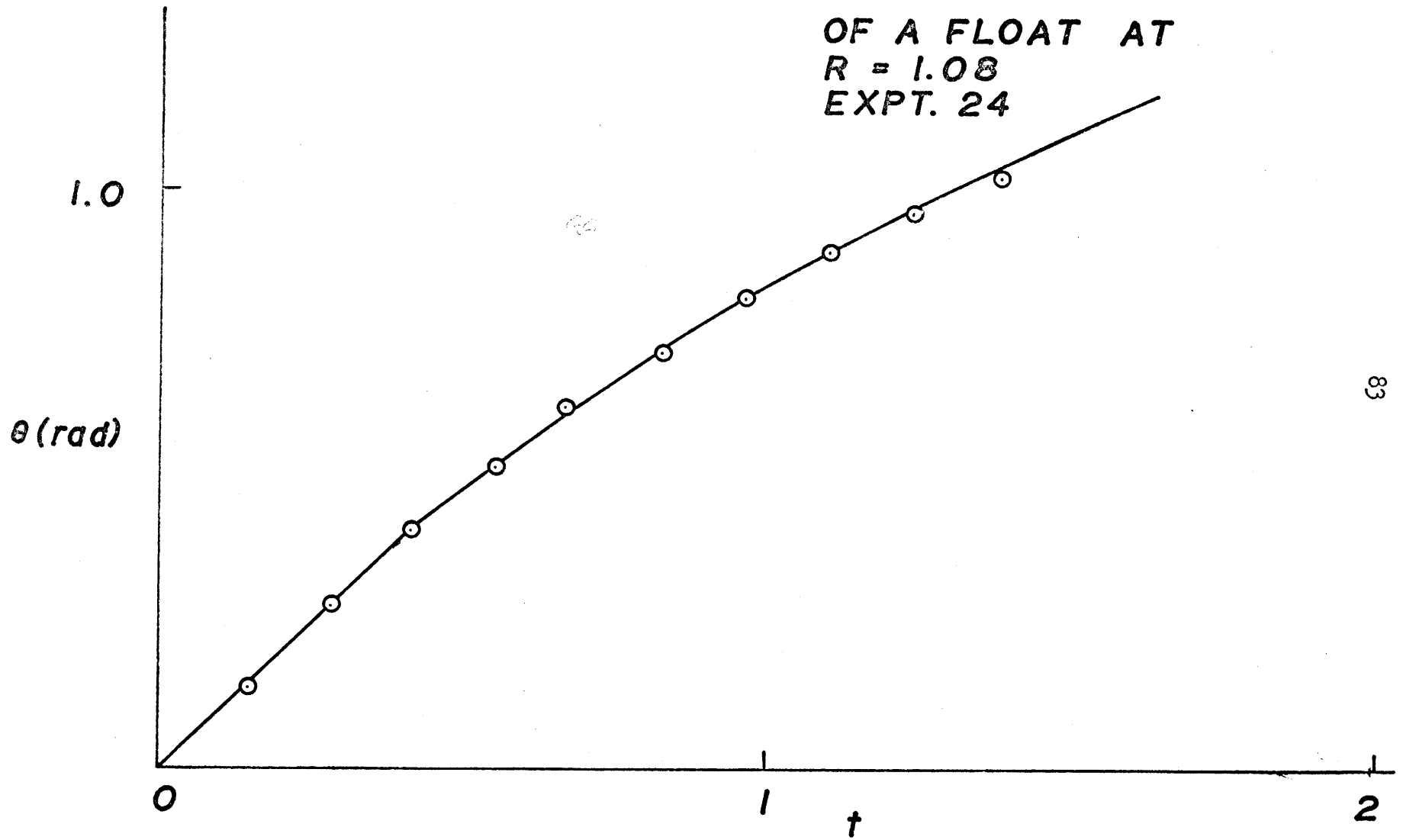
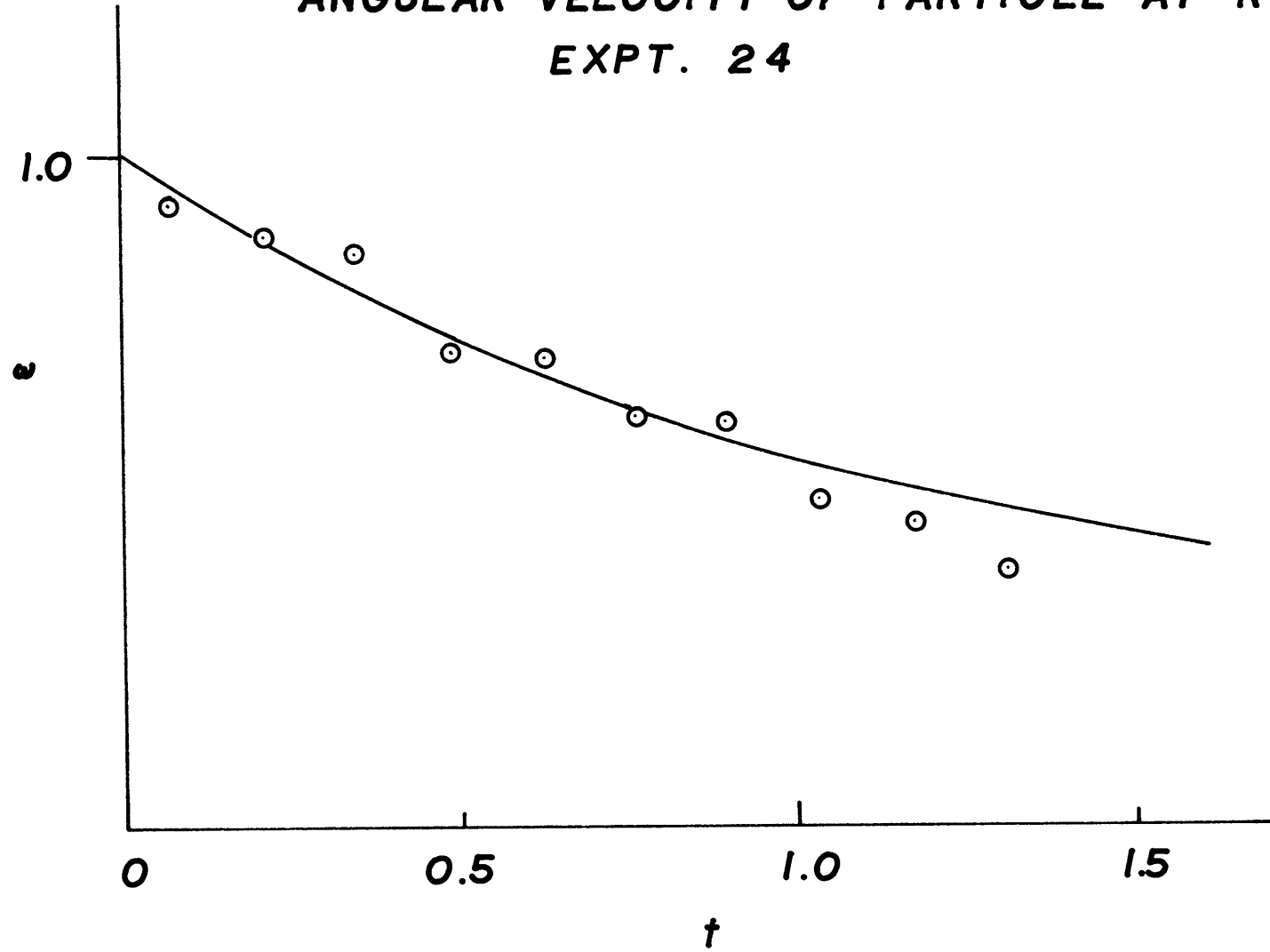


FIGURE 23

ANGULAR VELOCITY OF PARTICLE AT R=1.08
EXPT. 24



84

FIGURE 24

VERTICAL STRUCTURE OF THE
RECIPROCAL SPIN-UP TIMES
EXPERIMENT 24

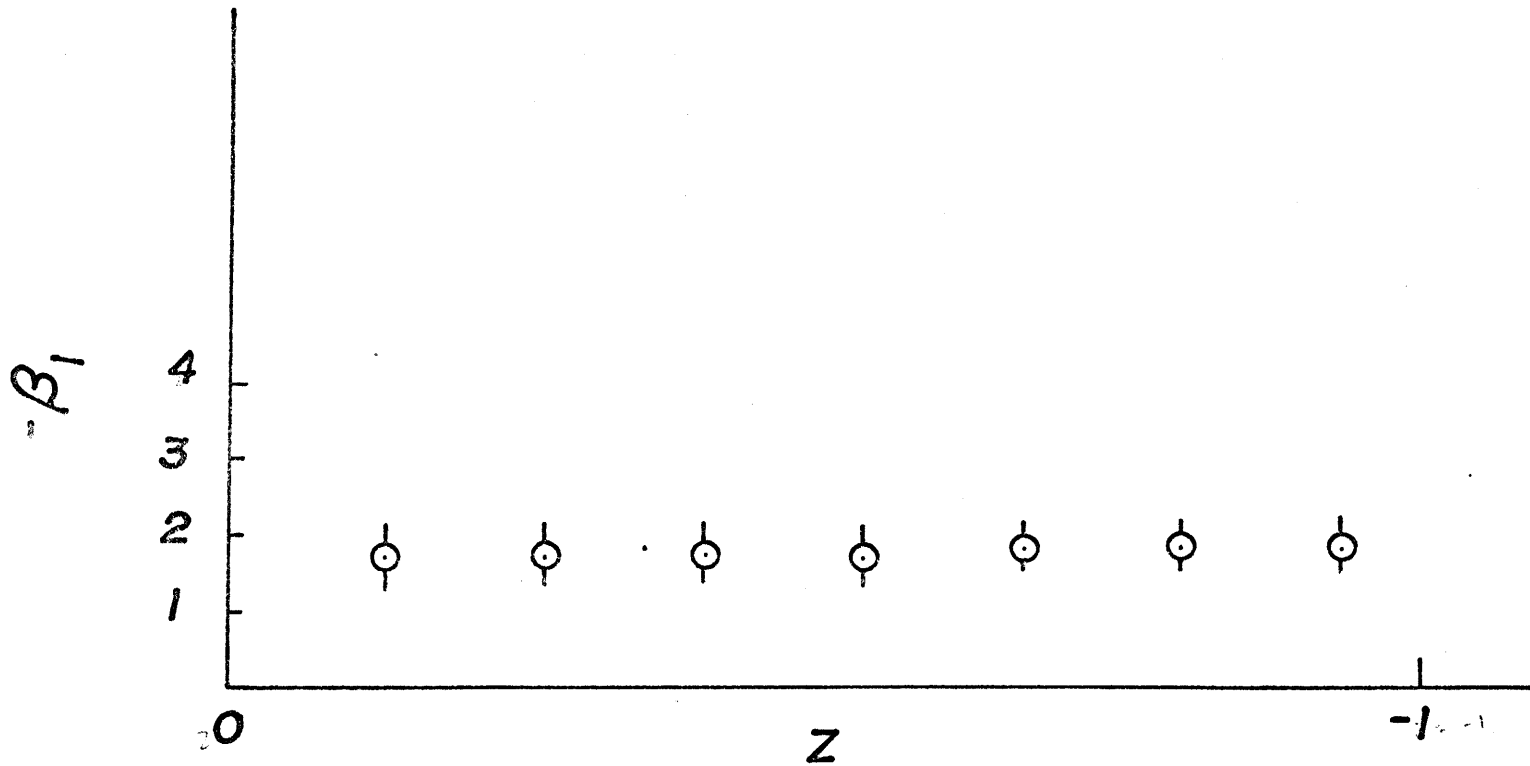


FIGURE 25

**VERTICAL STRUCTURE
OF MODE 1
EXPT. 24**

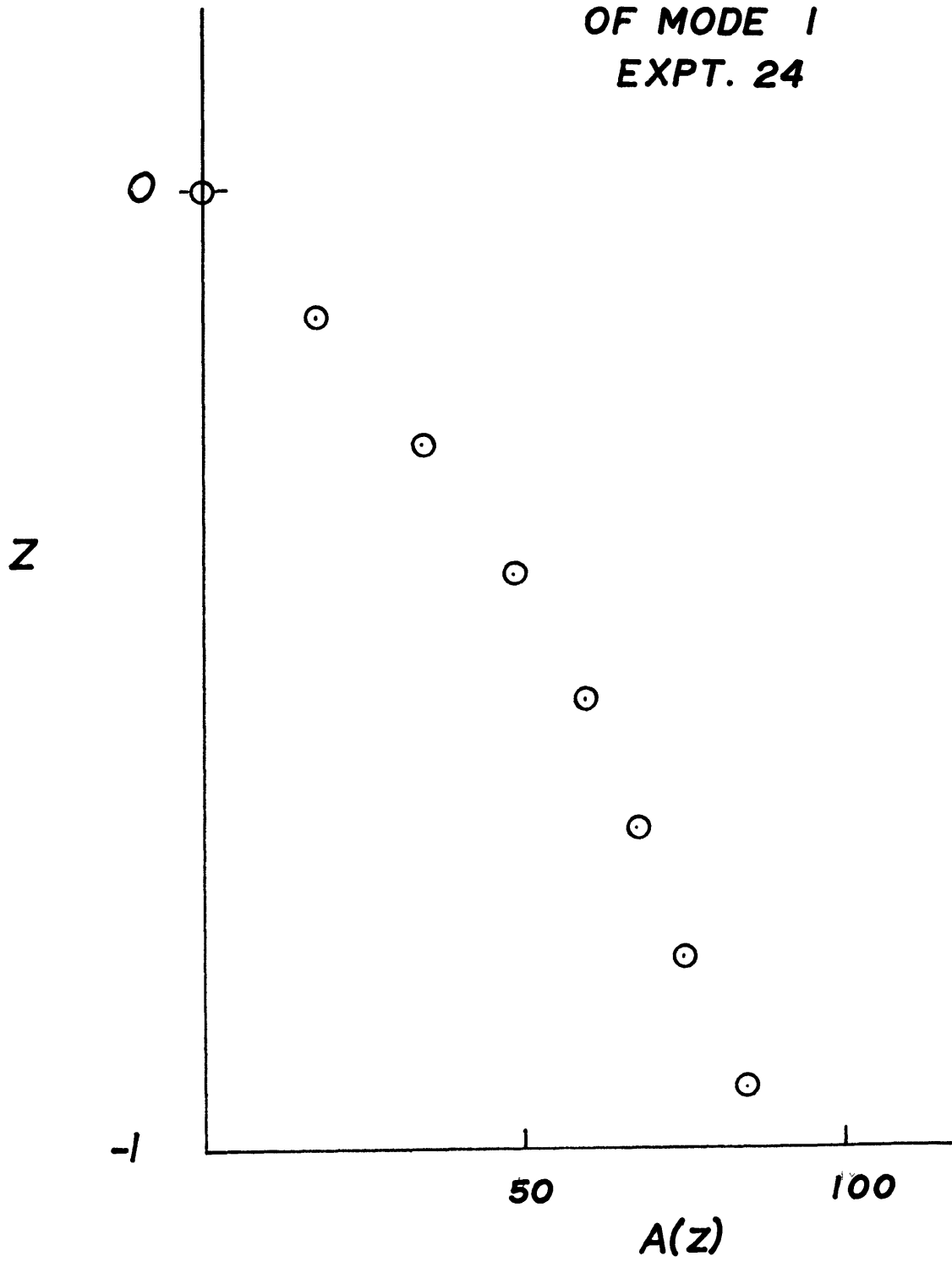


FIGURE 26

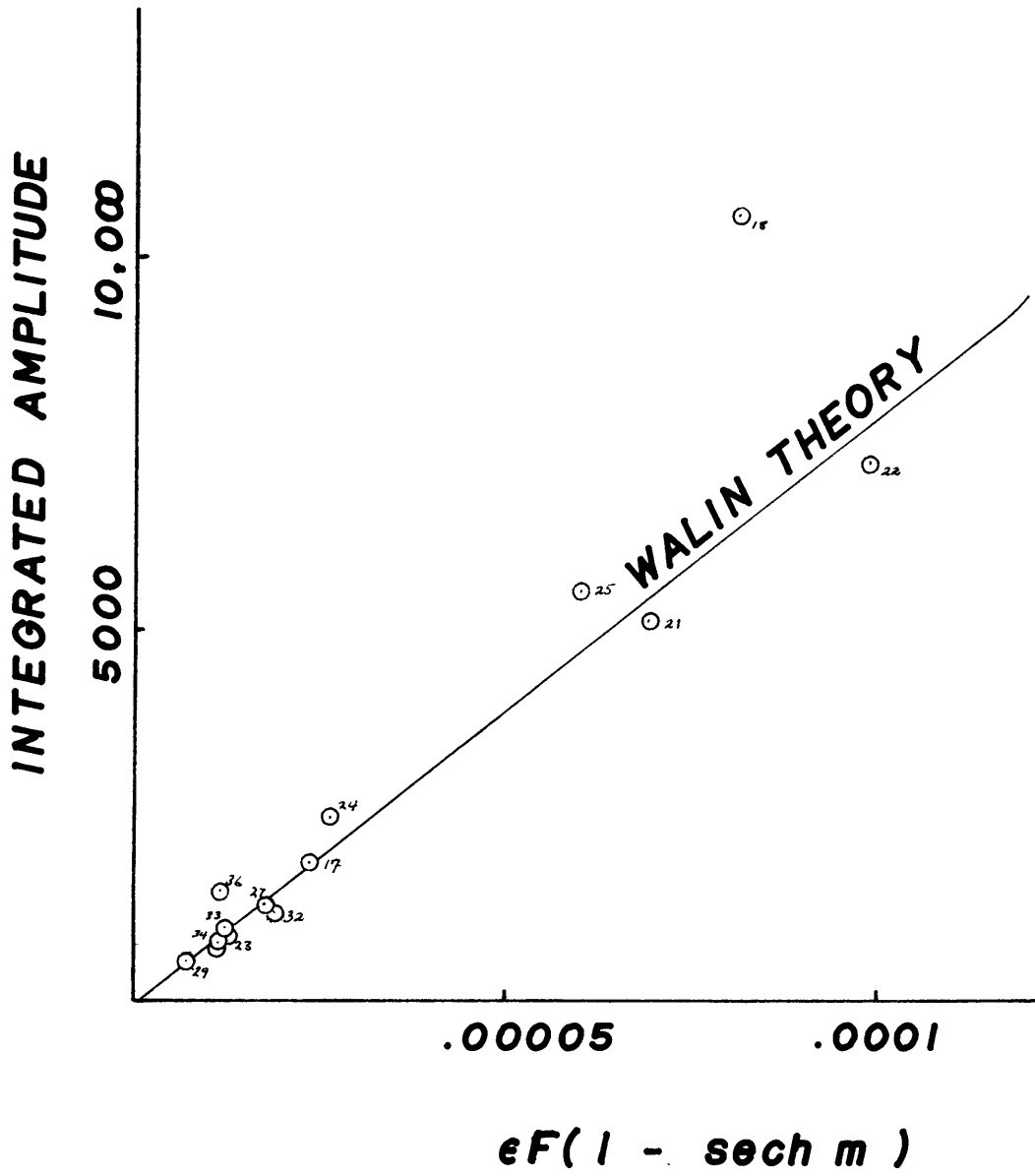


FIGURE 27

RECIPROCAL SPIN-UP TIMES

VS. m_1

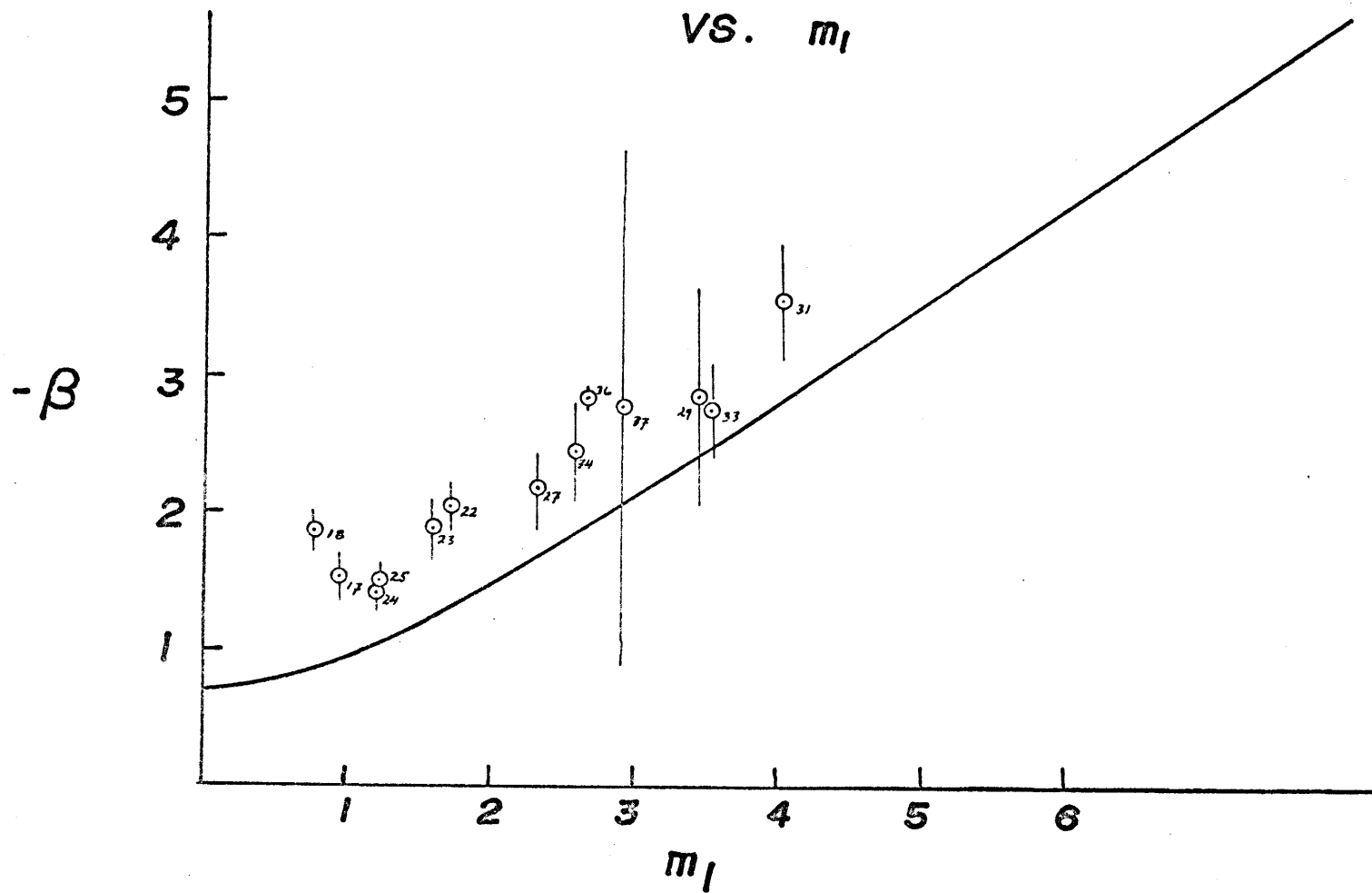


FIGURE 28

DEVIATION OF RECIPROCAL
SPIN-UP TIME FROM THE
WALIN THEORY VERSUS
LOCAL ROSSBY NO.

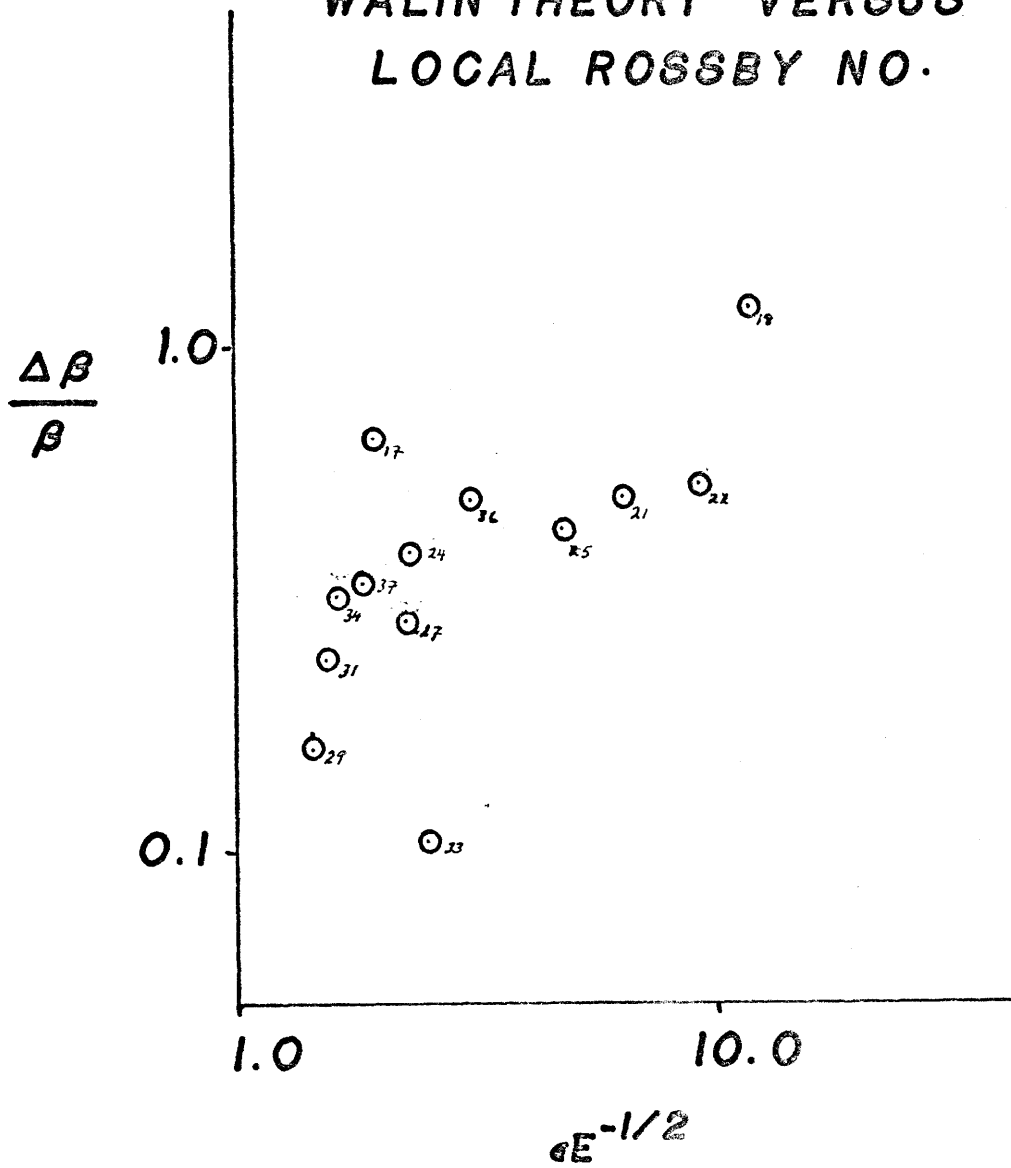
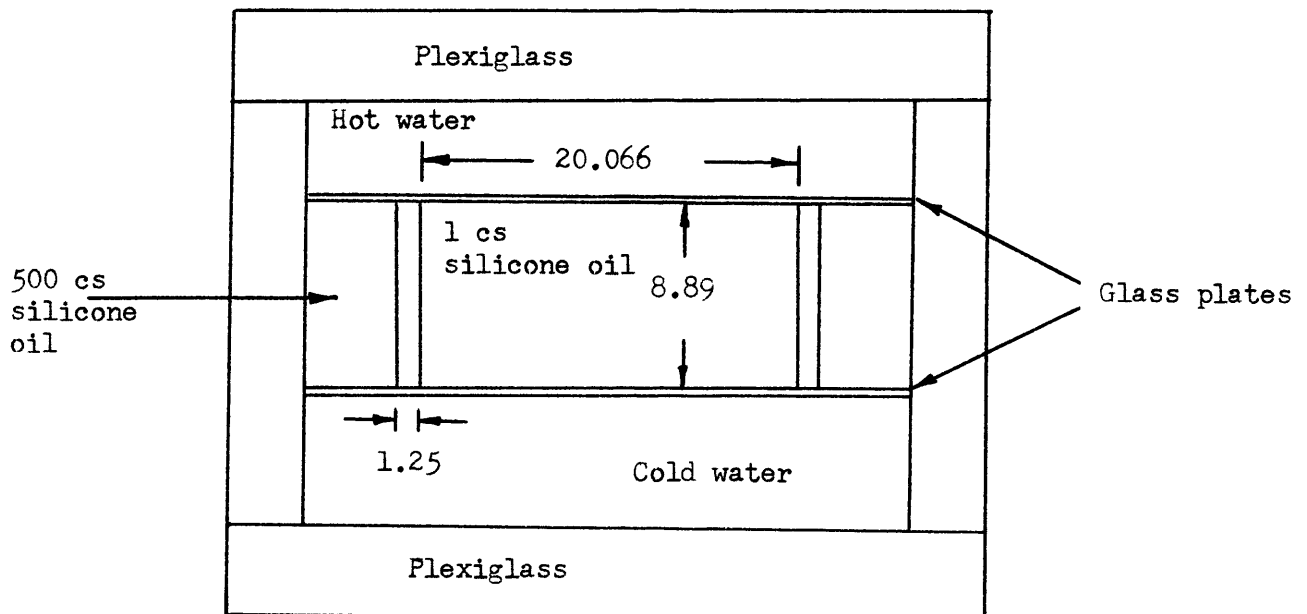
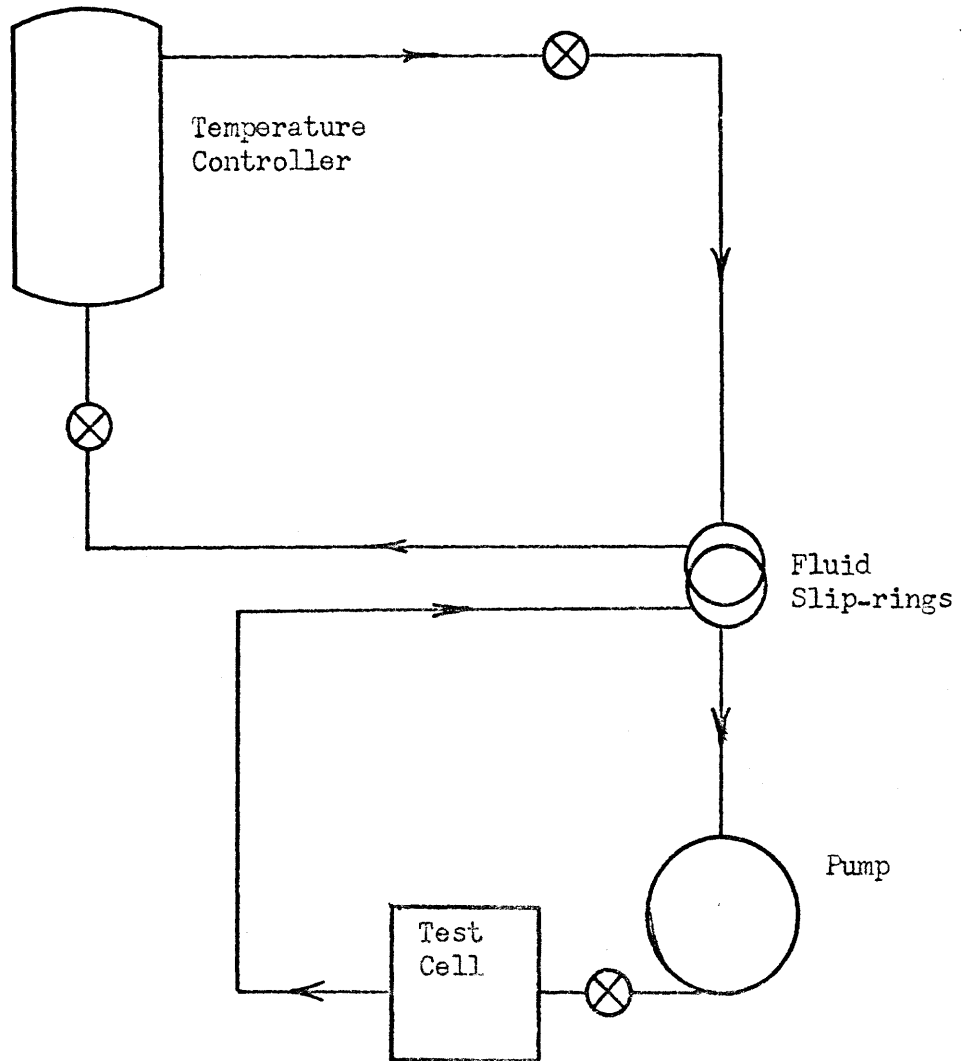


FIGURE 29



Schematic Diagram of Test Cell
(Dimensions in cm)

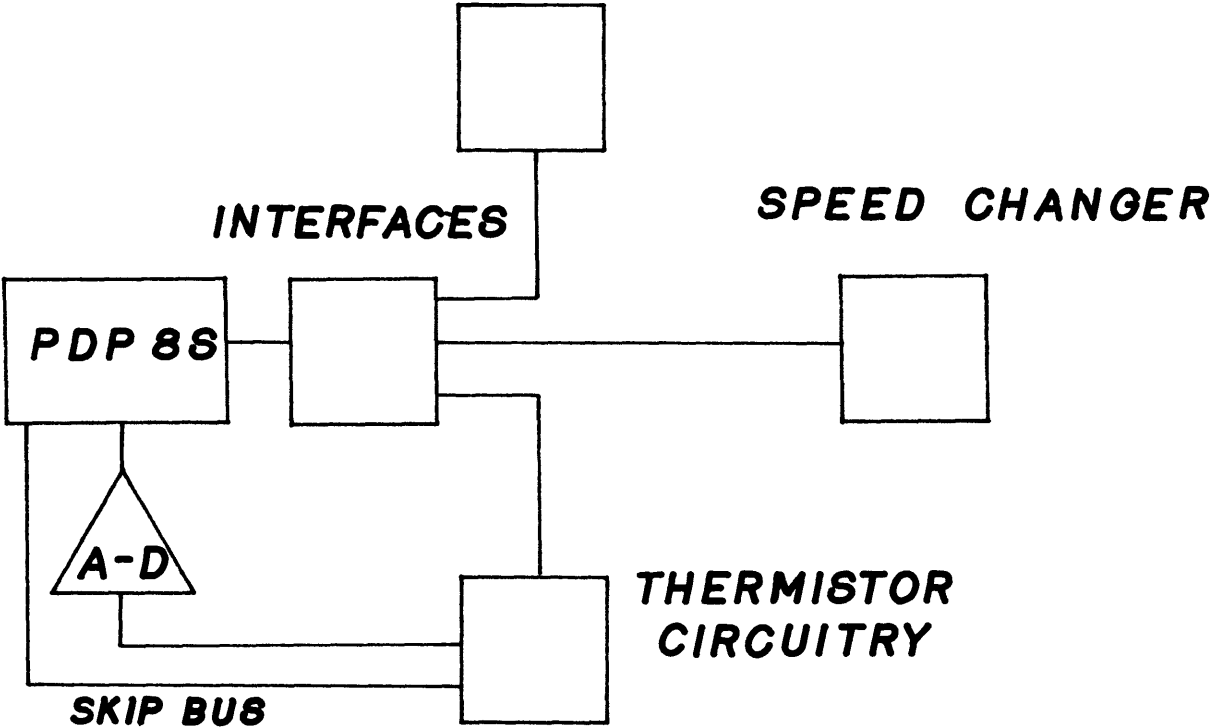
FIGURE 30



Schematic Diagram of Temperature Control System

FIGURE 31

CAMERA CONTROL



COMPUTER CONTROL

FIGURE 32

TEMPERATURE MEASUREMENT SYSTEM

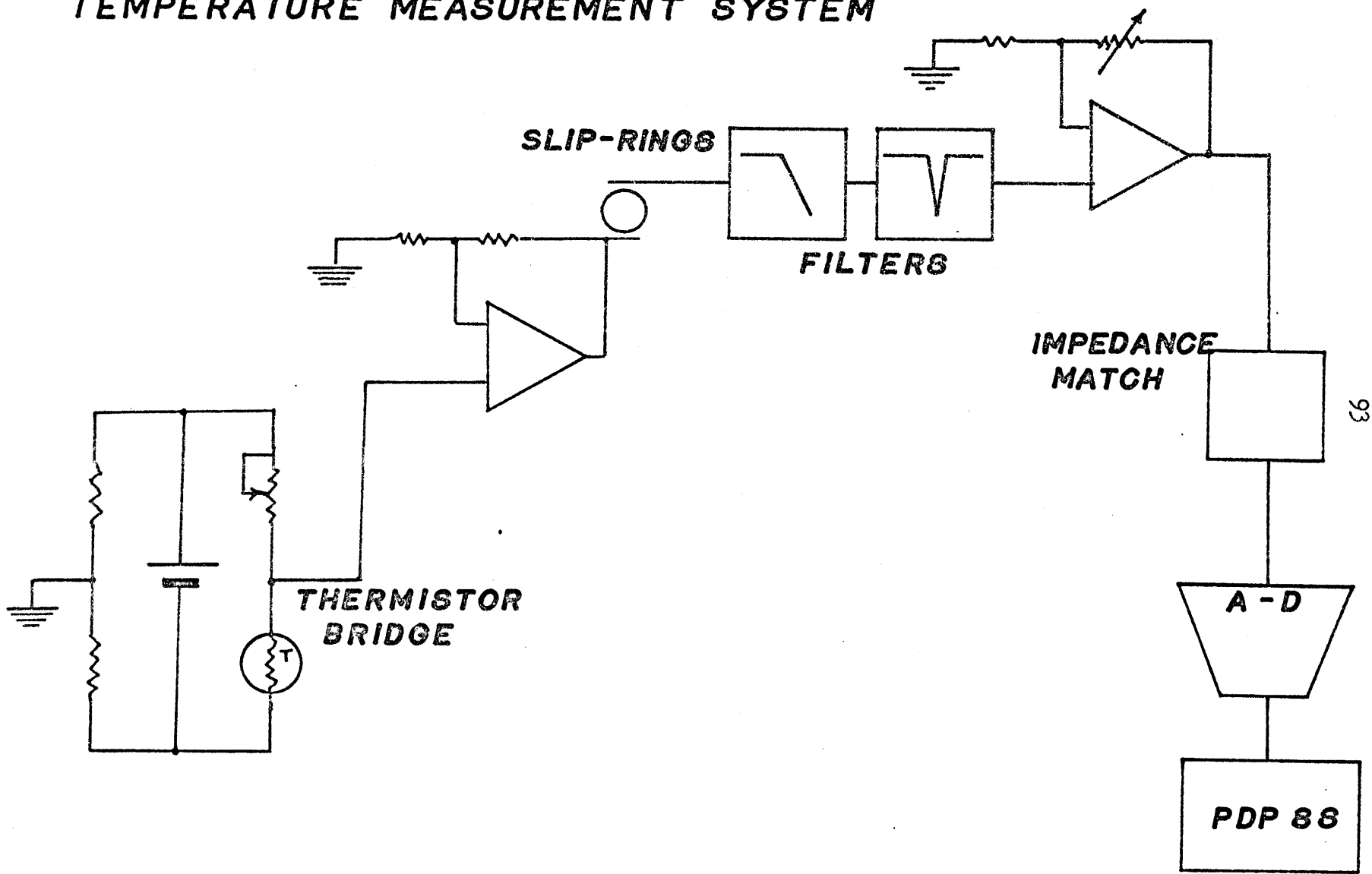


FIGURE 33

TYPICAL INTERFACE CIRCUIT

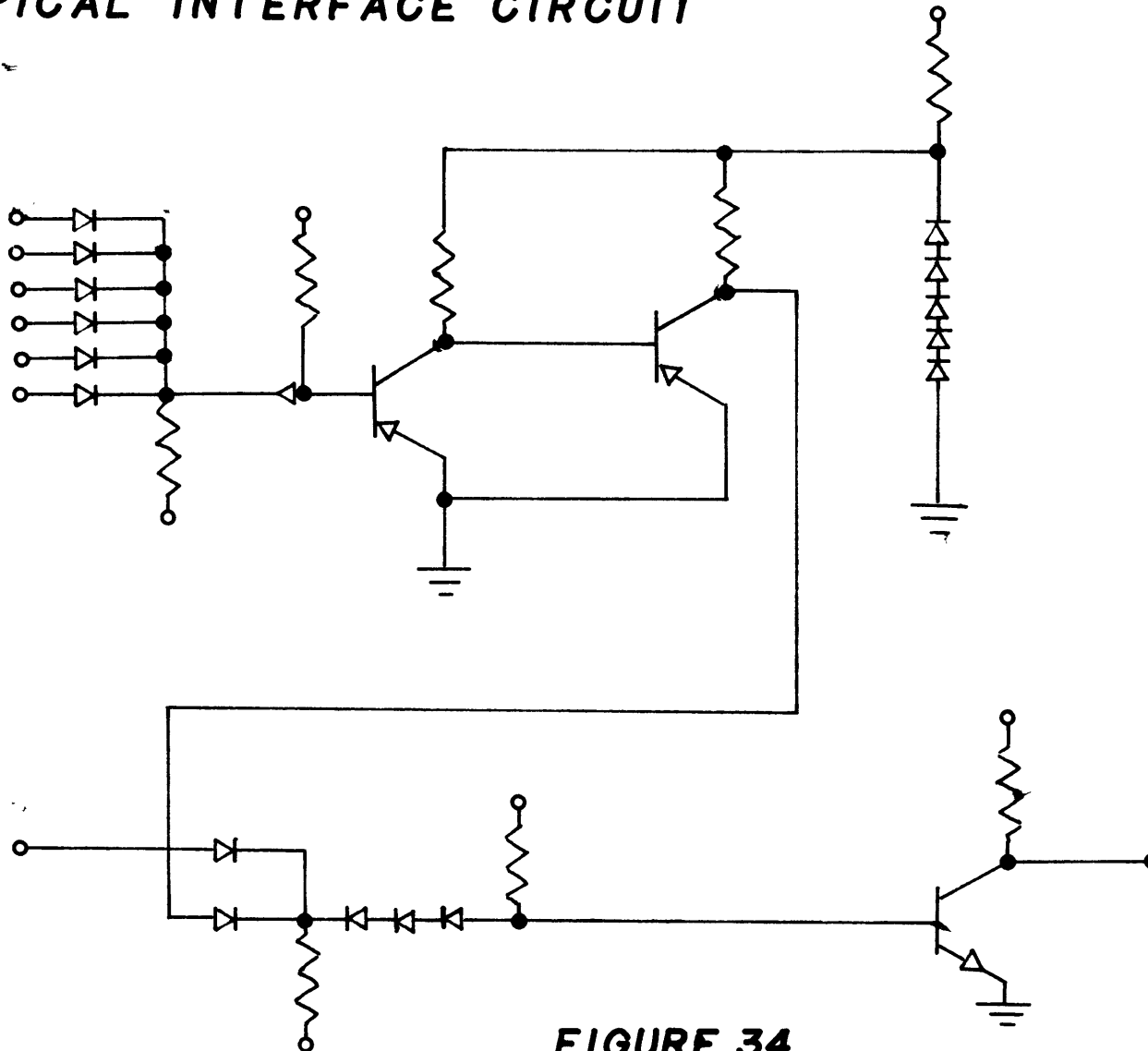


FIGURE 34

BIAS AND IMPEDANCE MATCHING CIRCUITRY

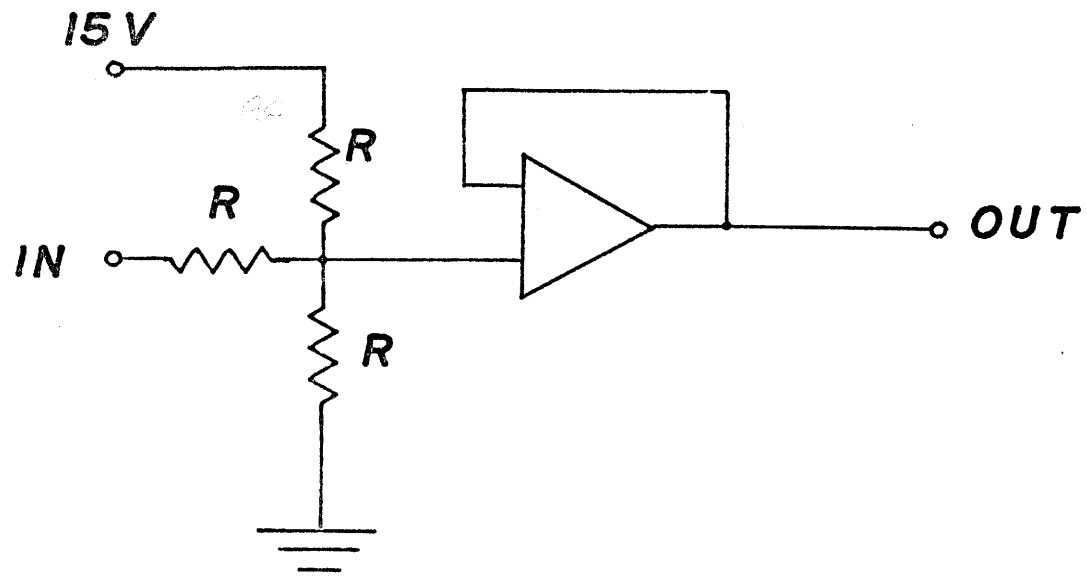


FIGURE 35

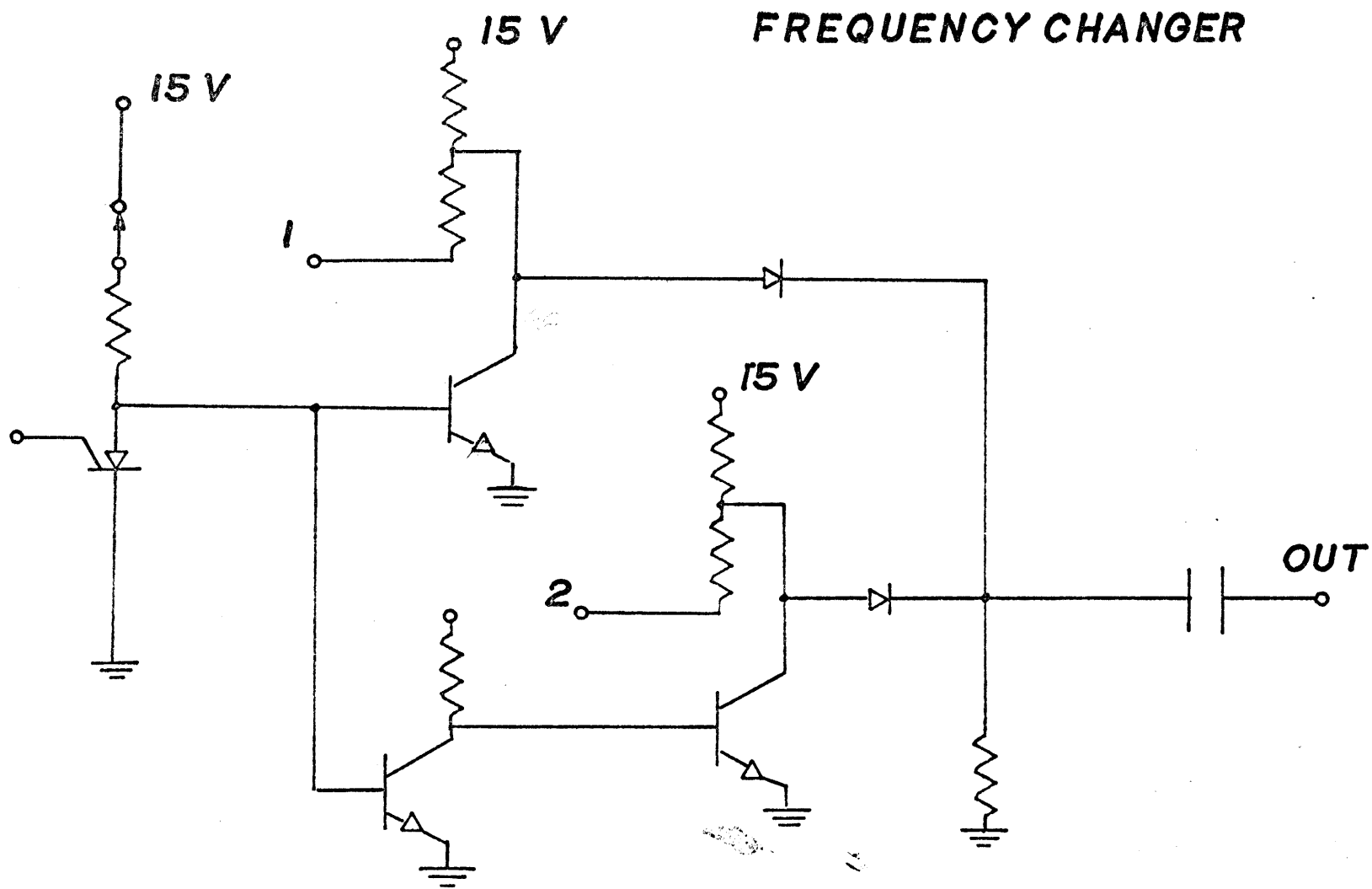


FIGURE 36

60 HZ BAND REJECT FILTER

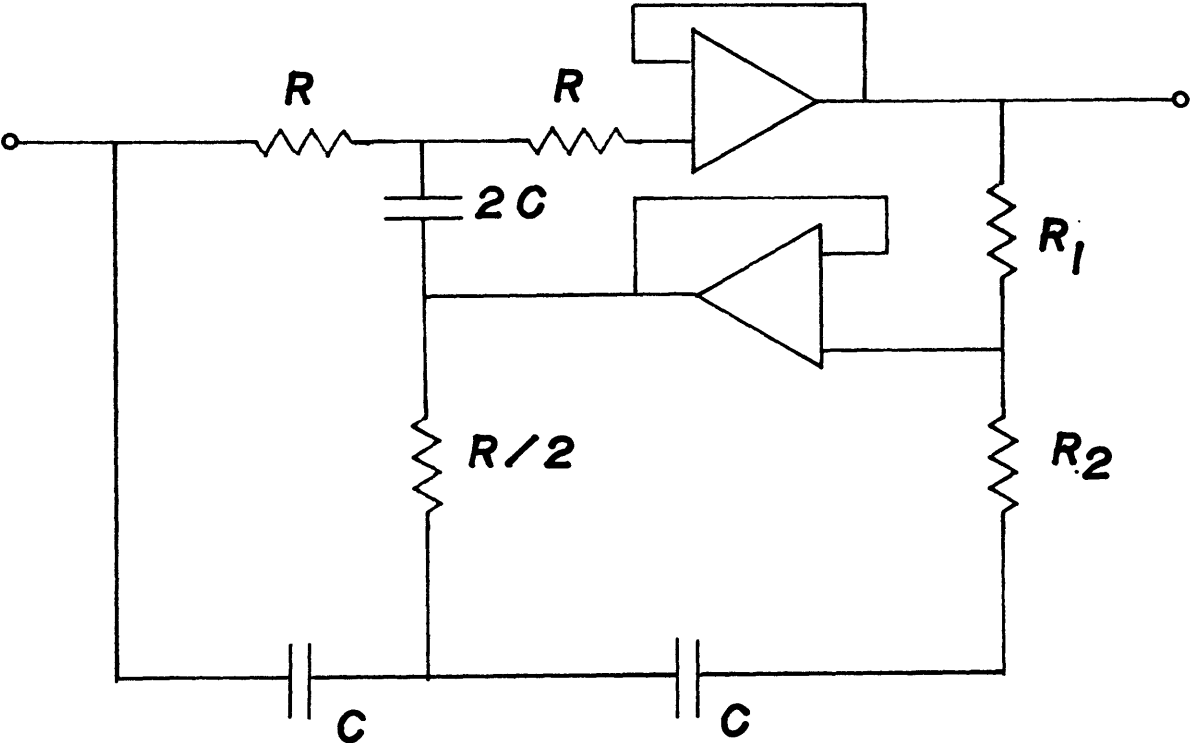


FIGURE 37

LOW PASS FILTER

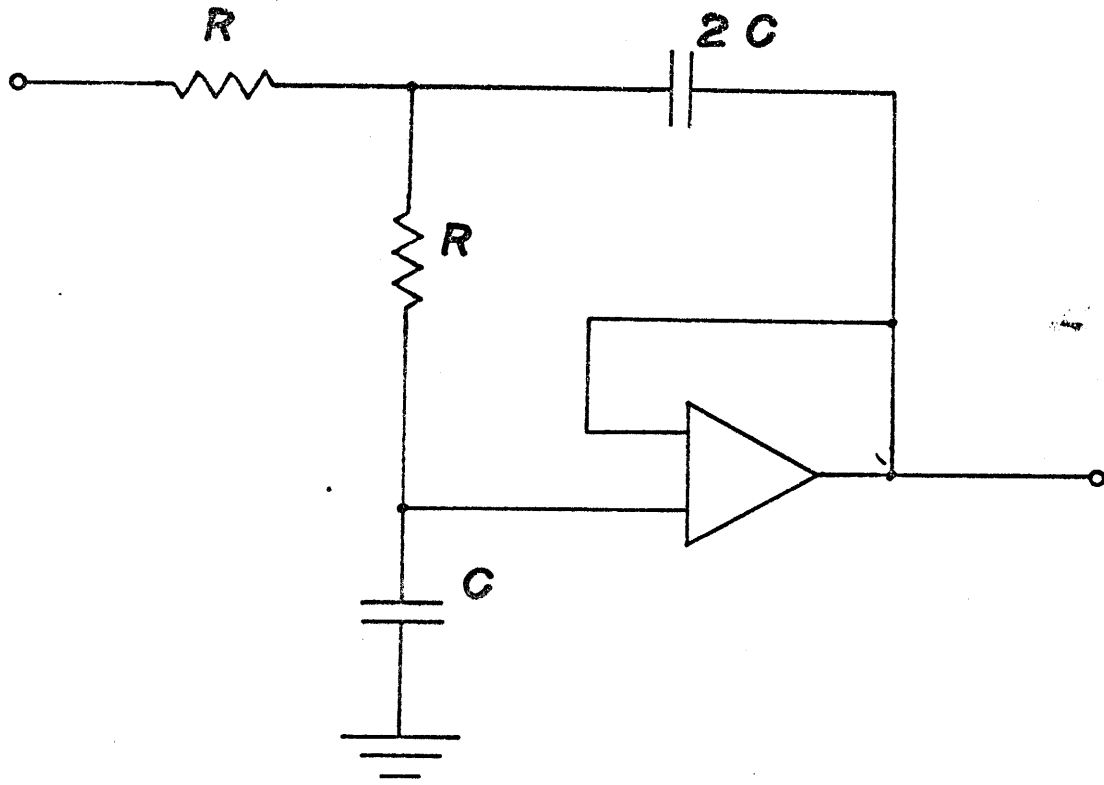
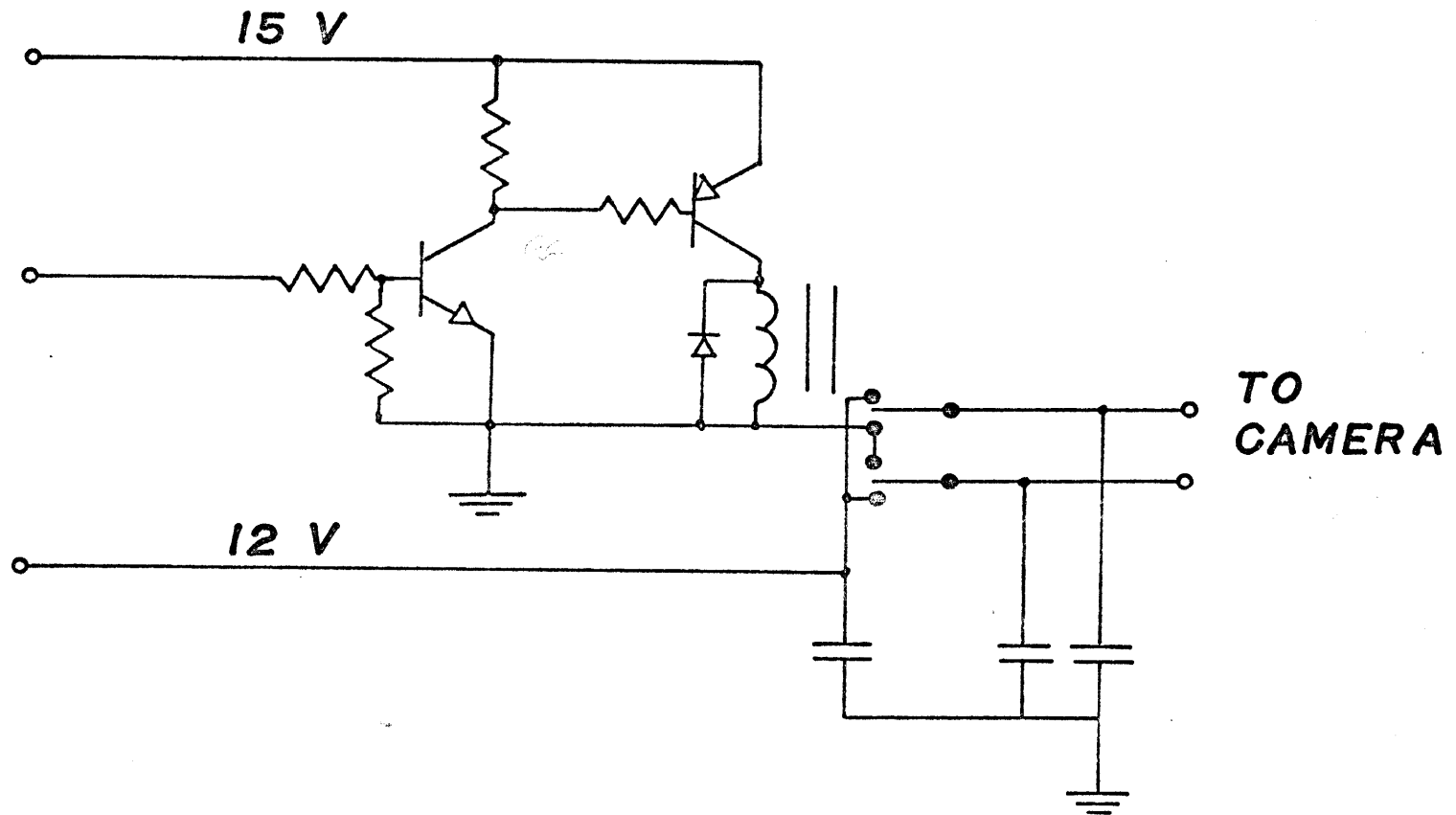


FIGURE 38

CAMERA DRIVING CIRCUITRY



66

FIGURE 39

**PERTURBATION DENSITY FIELD AT AN EARLY
STAGE OF SPIN-UP , COMPUTED FROM A
NUMERICAL MODEL**

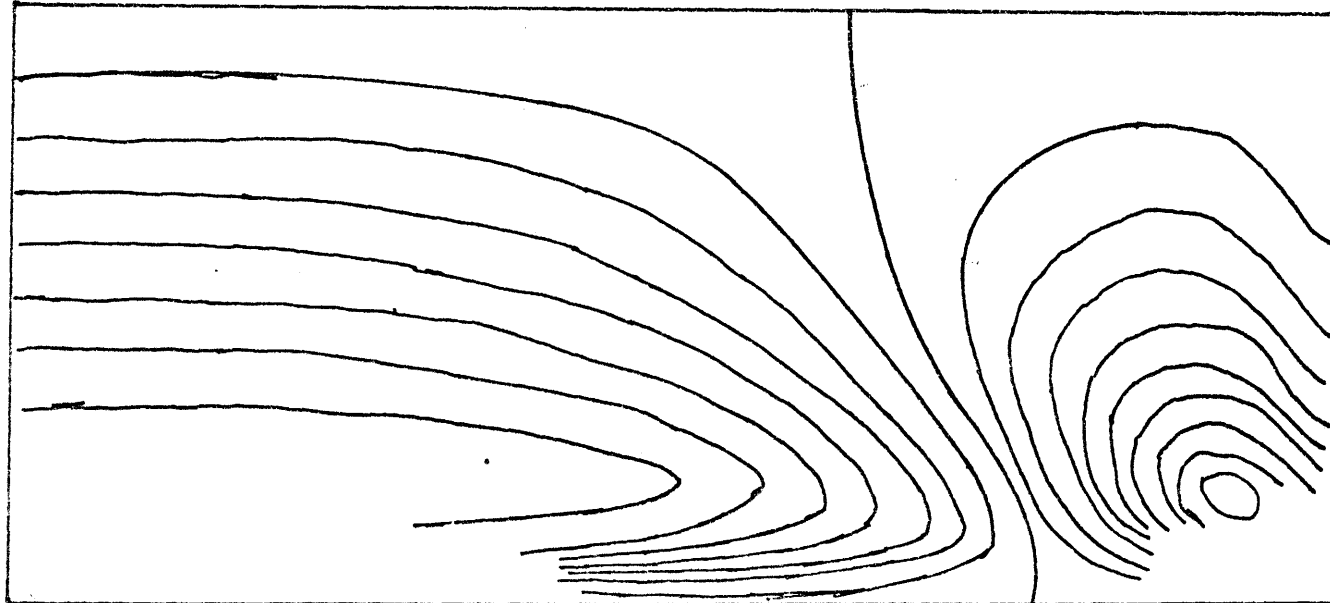


FIGURE 40

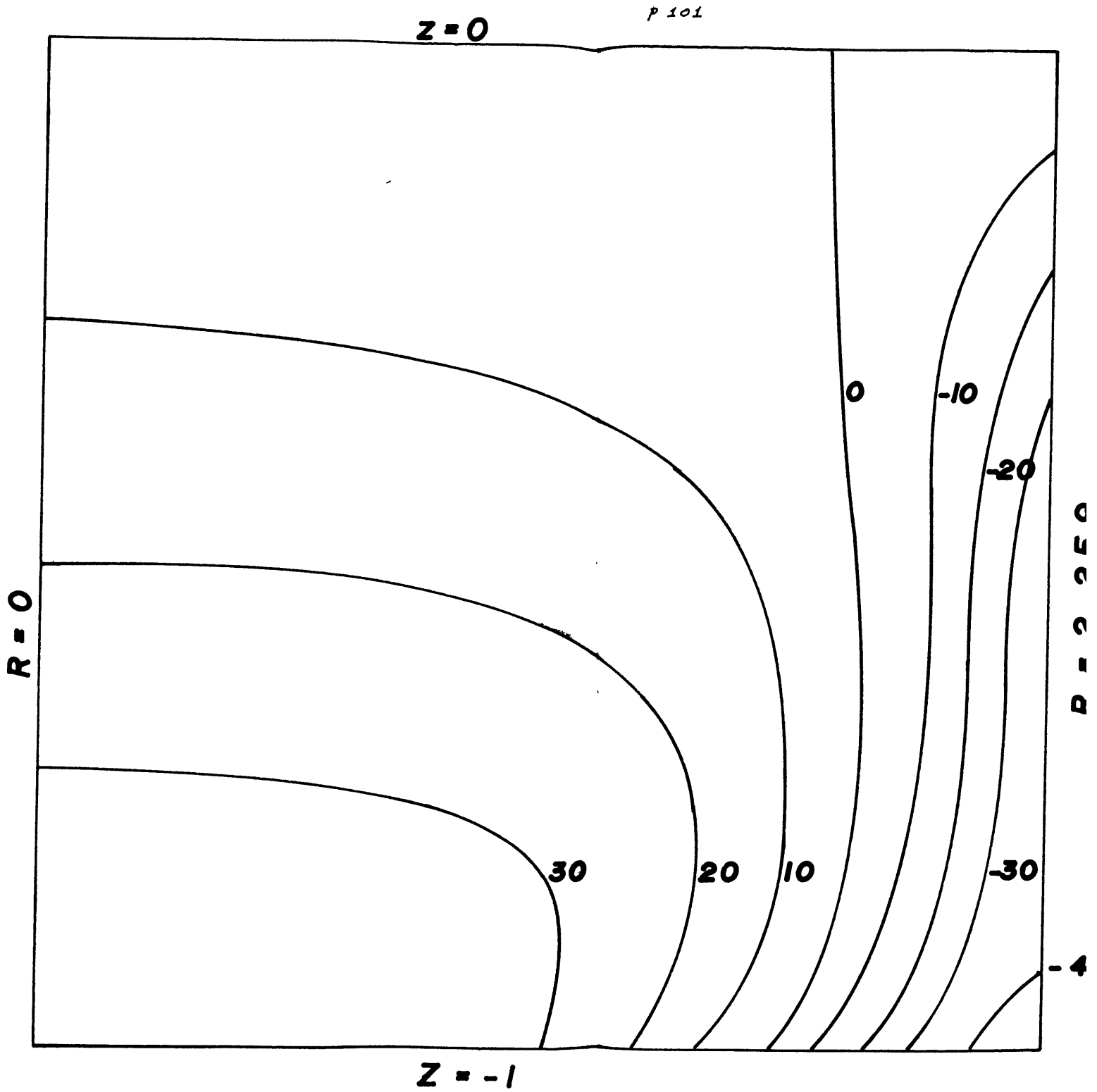


FIGURE 41

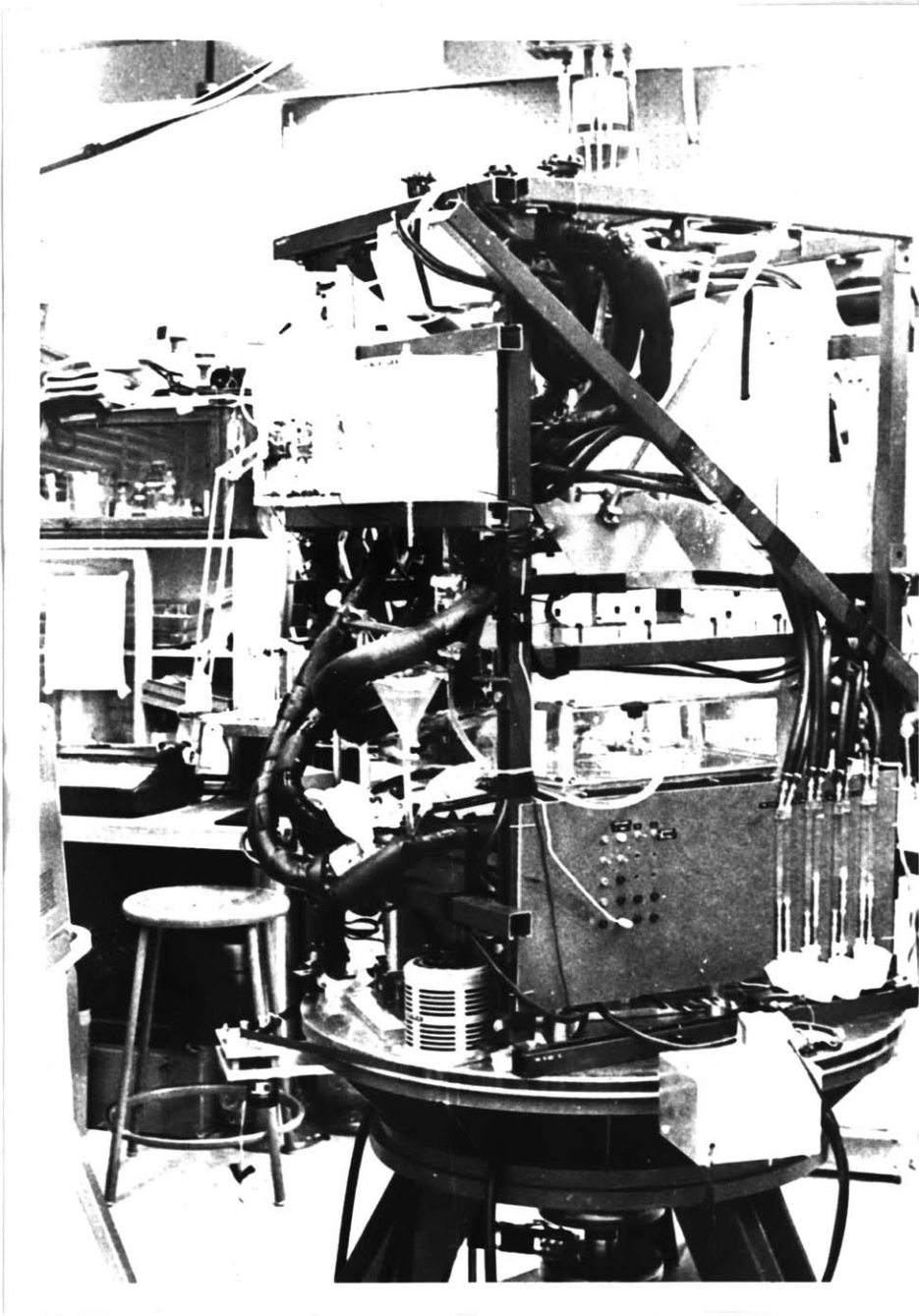


PLATE I

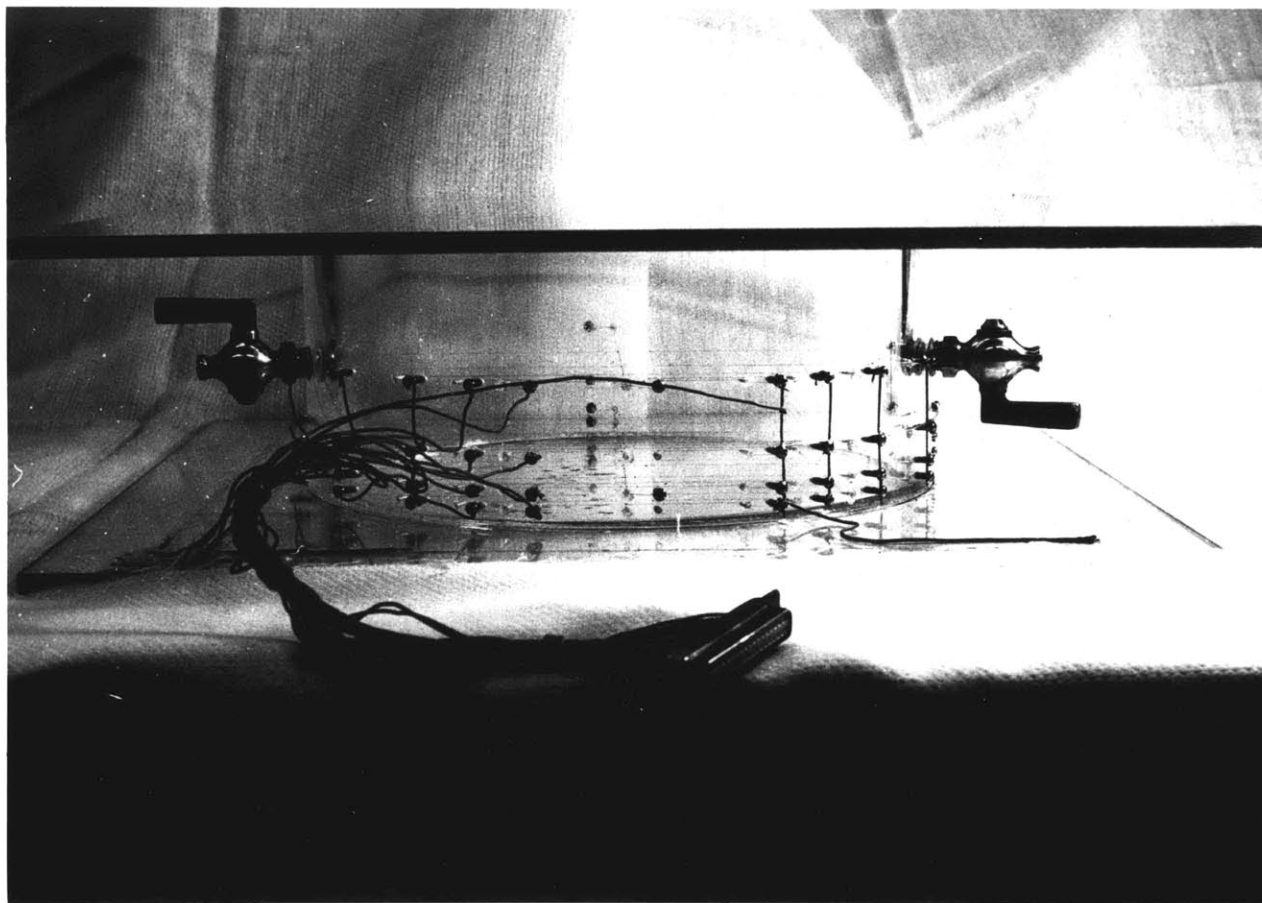
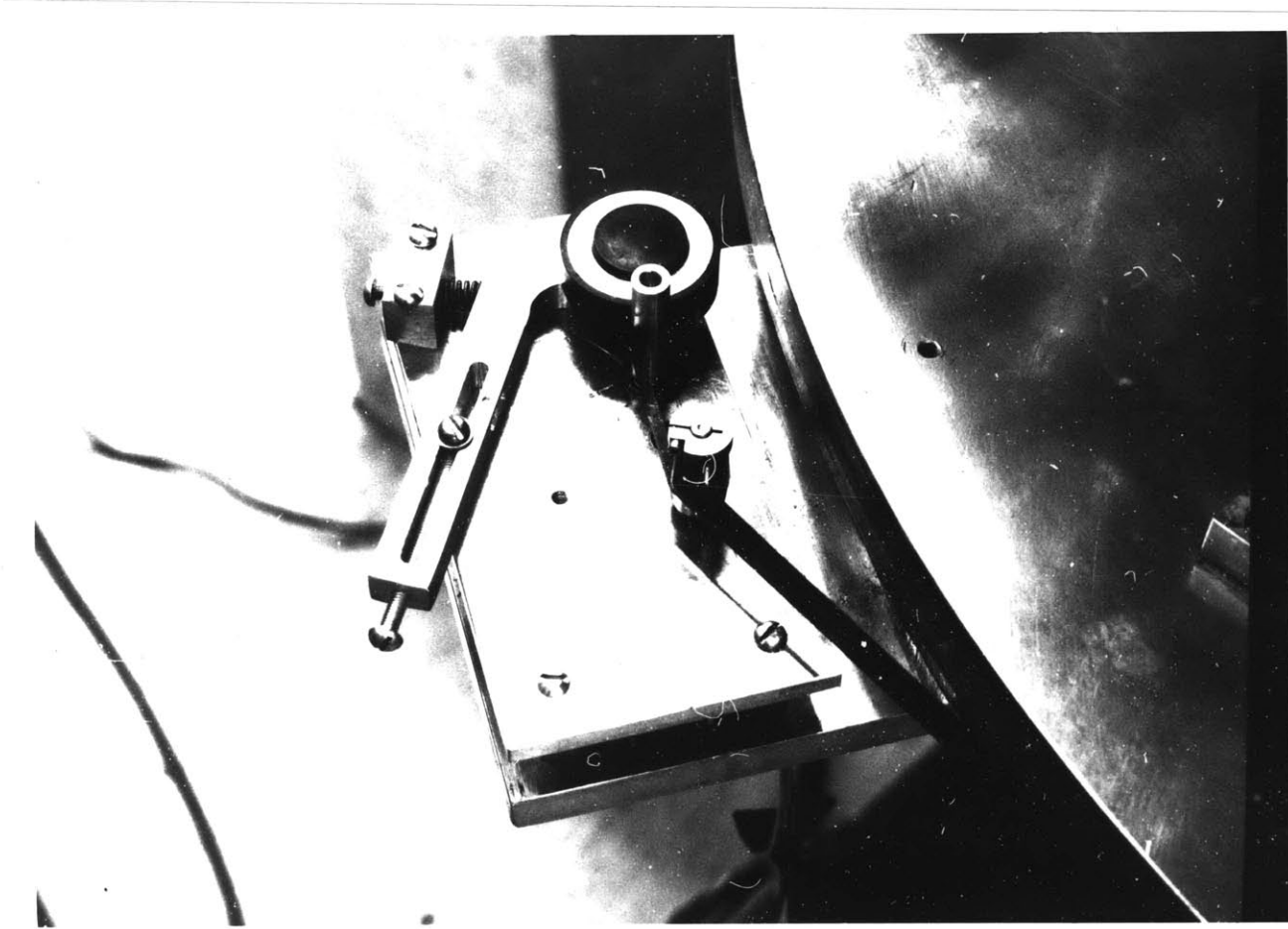
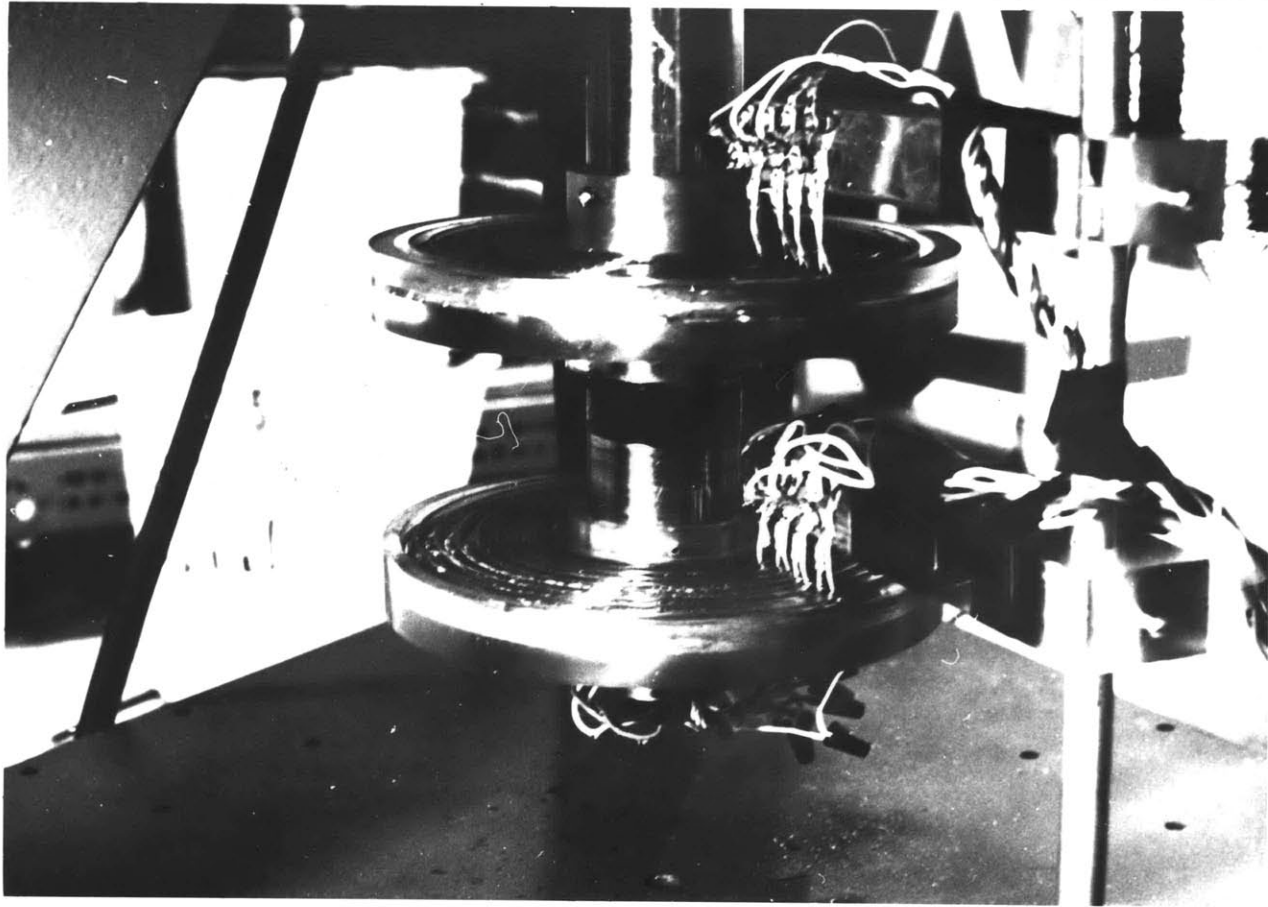


PLATE 2



104

PLATE 3



105

PLATE 4

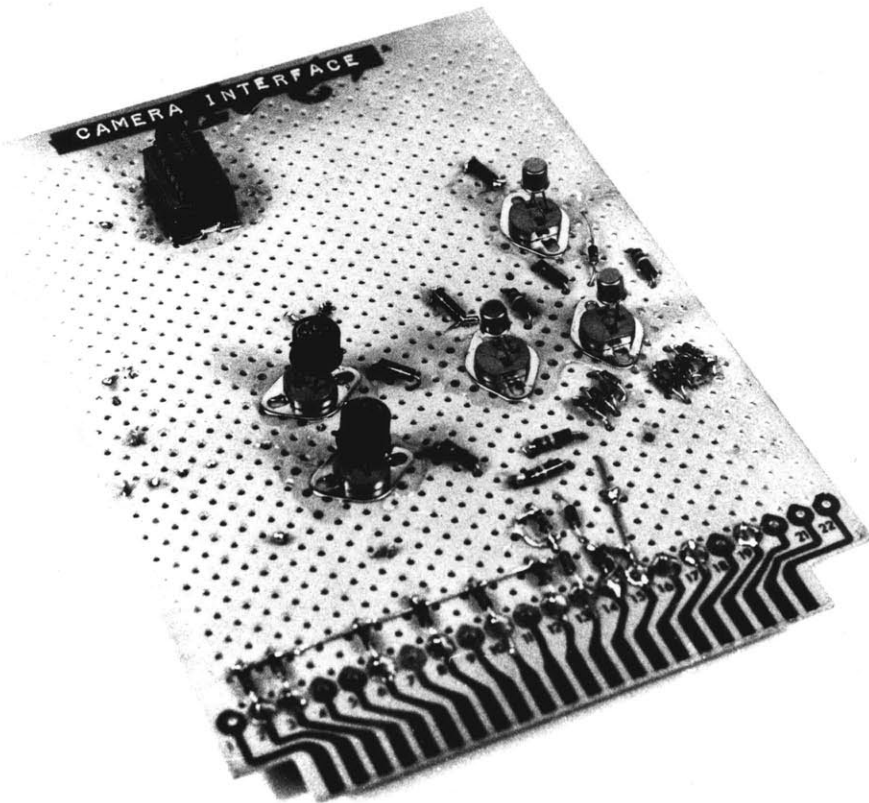


PLATE 5

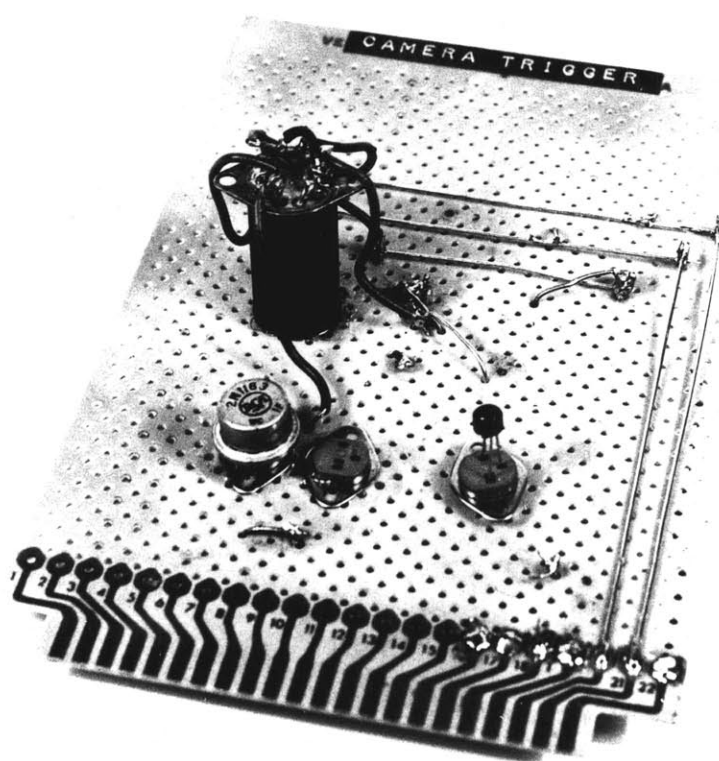


PLATE 6

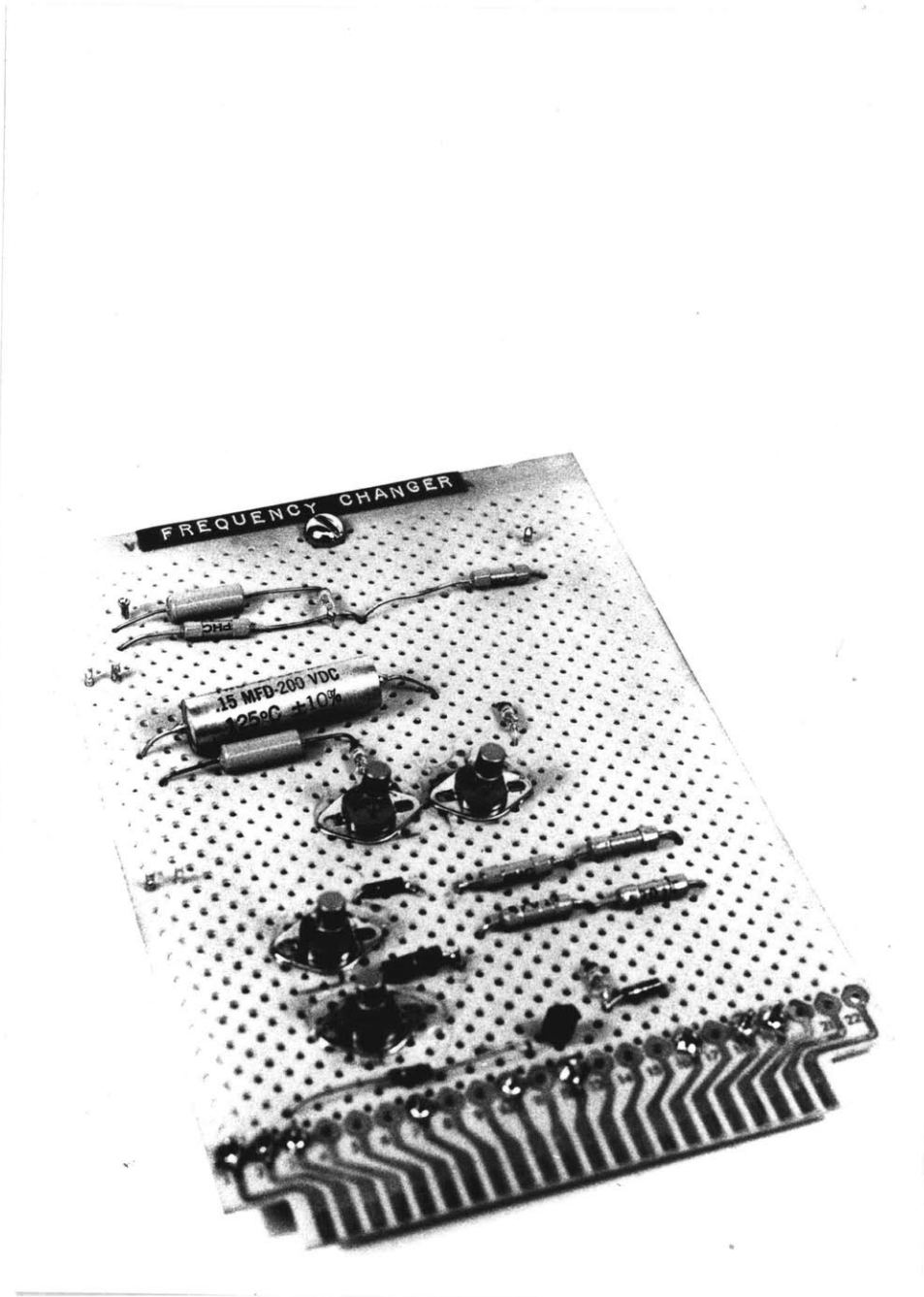


PLATE 7

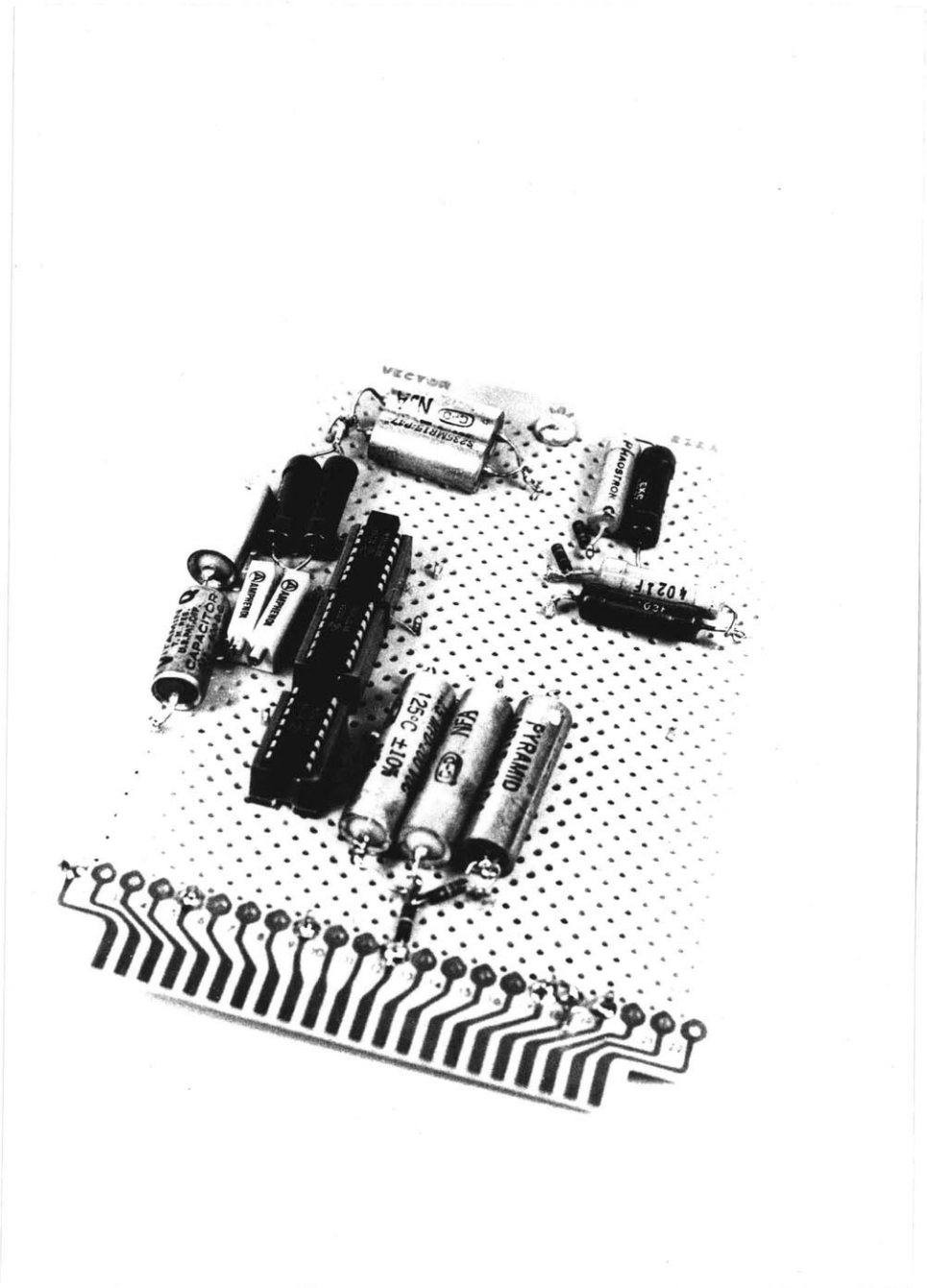


PLATE 8

APPENDIX I

DETAILS OF THE APPARATUS

Test cell configuration

The test section consists of a right circular cylinder, made from plexiglass, 8.89 cm high and 10.03 cm inner radius. The wall thickness of the cylinder is about 1 cm. The cylinder is mounted between two 0.6 cm thick glass plates. This assembly is mounted inside a large plexiglass box. (See figure 30). The space above and below the glass plates is used for heating and cooling water to maintain the temperature gradient in the cylinder.

The large box is mounted on a three point leveling system independent from the leveling system of the turntable. The mounting system also has a provision for centering the test section with that of the turntable and clamping the outer box.

The interior of the test section is filled with Dow-Corning 200 Silicone oil, 1 cs nominal viscosity grade. The region between the test section and the outer box wall is filled with Dow-Corning 200 Silicone oil, 500 cs nominal viscosity grade.

Twenty thermistors (VECO # 61A5) are located in a vertical plane along one radius in the cylinder. (See figure 2). Two thermistors are mounted on the glass plate on either side of the cylinder and two thermistors are mounted on either side of the cylinder wall.

Thermistor circuitry

All temperatures in the stratified spin-up experiments are measured by the out of null voltages of Wheatstone bridges with a thermistor in one of the arms of the bridge. There are thirty available bridges, of which twenty four are used. Twenty thermistors, two of which are broken, are mounted in the interior of the fluid. Two thermistors are mounted on either side of the cell wall and two thermistors are mounted on the upper side of the lower glass plate on either side of the cell.

A stepping switch from an ICBM guidance testing computer is used to sample the output from each of the bridges sequentially. The output is amplified by a Zeltex 132 F.E.T. operational amplifier in an amplifier-follower mode. The gain at this stage is about 240. When operating in this mode, the input impedance is above 10^{12} ohms, thus, the bridge (typical impedance 10^6 ohms) is not loaded significantly. The signal is amplified on the turntable to minimize slip-ring noise. (See figure 33 for the basic thermistor circuitry.)

The signal is sent through slip-rings and is passed through an active low pass filter and an active notch filter with a notch at 60 Hz. (See figures 36,37 for the filter design.) The signal then passes through another amplifier (used for the actual runs, but by passed when the basic field is to be measured) and a biasing circuit that changes the range from ± 15 V to 0 to +10 V to accomodate the analogue to digital converter. (See figure 35 for the bias circuit.)

The computer interfacing circuitry

The data taking process is under control of a Digital Equipment Corporation PDP 8/S computer. In order for the computer to be able to control the experiment, a number of interfacing circuits had to be built. The basic idea behind the interfaces was to allow an I/O command to set a flip-flop to a desired state. The flip-flop's state then controlled other circuitry, such as relays, which performed the tasks involved in the experiments.

As the computer operates on a -3V logic and the external logic operates on a +5V logic, an extra inverting step was needed in all the interface logic.

The PDP 8/S does all its I/O logic from a common bus. Six bits are needed to define a device and three bits exist to initiate various functions of the device. The device is selected by a diode gate defining the device and the function of the device is decided by which of the three other bits is anded with the first gate. (See the D.E.C. book The Small Computer Handbook, 1966-67, Maynard, Mass.) The three pulses, I.O.P.'s, are each 1 u sec long and separated by a few u sec. The short time of the pulse causes problems due to the capacitance of the diode gate. This is partially avoided by isolating the slow six bit portion of the gate from the I.O.P. section by a transistor network. If this network is not used, the device selector is very prone to noise. (See figures 34,39 for designs of several typical interfaces.)

Camera trigger

The schematic diagram for the camera trigger is shown in figure 39 and plate 6. The purpose of this circuit is to trigger the camera shutter and film advance motor. The principle of operation is an input signal from a flip-flop is amplified by the transistors and energises a relay which controls the current to the camera. When the input from the flip-flop is high, the camera shutter is triggered. When the level falls to ground, the film is advanced.

Frequency changer

The schematic diagram for the frequency changer is shown in figure 36 and the actual circuit is shown in plate 7. The purpose is to change the input frequency to the motor amplifier when an input pulse from a flip-flop is sensed and to lock in that mode until the circuit is manually reset. Input signals of about 5 V rms at two different frequencies are fed in at locations 1 and 2 on the diagram. Initially, the SCR is non-conducting. When a positive level from a flip-flop is sensed, the SCR conducts and continues to conduct until the circuit is broken by the opening of the switch. Before triggering, the frequency fed in at 1 is grounded by the first transistor. This means that the second frequency is output. When the trigger is set, the first transistor ceases to conduct and the first frequency is passed. The capacitor is a bias remover.

Bias and Impedance matching circuitry

The schematic diagram for this circuitry is shown in figure 35. The purpose is to transform the temperature signal from the thermistor bridge to a form acceptable by the analog to digital converter. The output from the bridge is in the range -15 to +15 V. The converter, however, only accepts signals in the range 0 to +10 V. Furthermore, the A-D converter has an input impedance of 1000 Ω . The follower circuit provides isolation of the bias circuit from the converter.

APPENDIX II

MATHEMATICAL NOTES

Note on the derivation of the thermal boundary condition

After Walin(1971), a thin wall approximation is assumed.

By the continuity of heat flux across the wall,

$$\dot{Q}_{\text{fluid}} = \dot{Q}_{\text{wall}} \quad \text{at the boundary of the wall and fluid.}$$

This is equivalent to:

$$k_{\text{fluid}} (T_{*}^{\text{fluid}})_n = k_{\text{wall}} (T_{*}^{\text{wall}})_n ,$$

where the k's are the thermal conductivities and the T_{*} 's are the temperatures in the wall and fluid. By making a thin wall approximation, the temperature gradient in the wall may be replaced by

$(T_{\text{inside}}^{\text{wall}} - T_{\text{outside}}) d_w^{-1}$, where $T_{\text{inside}}^{\text{wall}}$ is the temperature of the wall at the wall-fluid interface, and T_{outside} is the temperature outside the wall.

After non-dimensionalizing, the heat flux equation at the wall-fluid interface becomes

$$\rho_n = \frac{L k_{\text{wall}}}{d_w k_{\text{fluid}}} (\rho - \rho_o) ,$$

where L = the length scale of the experiment, d_w = the wall thickness, and ρ_o is the non-dimensionalized form of T_{outside} .

I define $\Gamma = L k_{\text{wall}} / d_w k_{\text{fluid}}$. For the experiments in this thesis, $\Gamma = 7.41$.

Fourier-Bessel analysis of the even powers of r

To determine the Fourier-Bessel modes in r, the coefficients of the Fourier-Bessel expansion of the even powers of r are required:

$$r^{2n-2} = \sum_k B_{n,k} J_0(\alpha_n r) \quad , \text{ where } J_1(\alpha_n) = 0.$$

The $B_{n,k}$ may be computed by the usual relation;

$$B_{n,k} = \frac{2}{J_0^2(\alpha_k)} \int_0^1 r^{2n-1} J_0(\alpha_k r) dr .$$

This integral may be computed by the recursion relation defined below. Let

$$\int_0^1 r^{2n+1} J_0(\alpha r) dr = u_n \text{ where } J_1(\alpha) = 0.$$

The recursion relation is then given by:

$$u_0 = 0$$

$$u_1 = \frac{2}{\alpha^2} J_0(\alpha)$$

...

$$u_n = \frac{2n}{\alpha^2} J_0(\alpha) - \frac{4n^2}{\alpha^2} u_{n-1} .$$

Note on the method of determination of the C_n

For the case where the eigenvalues of the eigenvalue equation of chapter 2 are not solutions of either $J_0(\alpha_n) = 0$ or $J_1(\alpha_n) = 0$, there is no simple inner product of the Bessel function $J_1(\alpha_n r)$ on the interval $0,1$ which gives an orthogonality relation. Therefore, an approximate method must be used to compute the C_n .

The method I have used is to define an inner product

$$(f,g) = \int_0^1 rfg \, dr$$

and form a large number of simultaneous equations

$$(J_1(\alpha_m r), r) = \sum_{n=1}^N C_n (J_1(\alpha_n r), J_1(\alpha_m r)), \quad m = 1, \dots, N,$$

and solve for the C_n . The value of N I have generally used has been about 40. This seems to give results accurate to about 1%.

Two methods for solving the set of equations have been used.

The easiest to use has been the MIT program GELB. Another method that I have used involves computing a set of Gram-Schmidt orthogonal functions recursively and using these to solve the set of equations.

Note on the boundary layer scaling

The elimination of all but one dependent variable from the equations of motion leaves

$$\frac{\partial}{\partial t} \left(B^2 \frac{\partial}{\partial r} \frac{1}{r} \frac{\partial}{\partial r} r + \frac{\partial^2}{\partial z^2} \right) v = E^{\frac{1}{2}} \left(\frac{1}{\sigma} \nabla^2 v_{zz} + \right. \\ \left. B^2 \frac{\partial}{\partial r} \frac{1}{r} \frac{\partial}{\partial r} r \cdot v \right) + EK_1 K_2 \cdot K_2 v$$

where

$$K_1 = \partial/\partial t - E^{\frac{1}{2}}/\sigma \nabla^2,$$

and

$$K_2 = \partial/\partial t - E^{\frac{1}{2}} \cdot.$$

To find if the boundary layers can exist, the stretched variables were inserted into the above equation. If no balance existed for the largest term, it was concluded that no boundary layer of that scaling existed. In this way, it was seen that only the $E^{\frac{1}{2}}$ and $E^{\frac{1}{4}}$ boundary layers could be present for B and $\sigma = O(1)$.

Detail of the solution of $\psi^{(2)}$

From the equation $B^{-2} \psi_{zz}^{(2)} + \frac{\partial}{\partial r} r \frac{\partial}{\partial r} \psi^{(2)} = 0$, we have

$$\psi^{(2)} = \sum K_n(z, t) J_1(\alpha_n r/r_0),$$

and

$$(K_n(z, t))_{zz} - \frac{\alpha_n^2 B^2}{r_0^2} K_n(z, t) = 0,$$

which, with the symmetry condition on $\psi^{(2)}$ gives

$$K_n(z, t) = F_n(t) \sinh m_n z / \sinh m_n,$$

where

$$m_n = \alpha_n B / r_0.$$

The boundary condition on $z = +1$ requires

$$F_n' + 2^{-\frac{1}{2}} m_n \coth m_n F_n = 0$$

whence

$$F_n(t) = A_n \exp(-2^{-\frac{1}{2}} m_n \coth m_n t).$$

This implies that $\psi \rightarrow 0$ as $t \rightarrow \infty$ or $v^B \rightarrow 0$ as $t \rightarrow \infty$.

Now, $v_t^{(0)} = \psi_z^{(2)}$, or

$$v^{(0)} = V(r, z) + \int_0^t \frac{\partial}{\partial z} \psi^{(2)}(r, z, t') dt'.$$

The initial condition, $v^{(0)} = r$ at $t = 0$ requires $V(r, z) = r$, and the condition on $v^{(0)}(z=1)$ as $t \rightarrow \infty$ provides the condition on the A_n .

Estimation of the effect of the wire drag on the interior flow

The method for estimating the effect of the wire drag on the interior flow will be to compare the rates of energy dissipation of the spin-up of a homogeneous fluid and the energy dissipation caused by the wire drag.

Let $v = \Omega r$ where $\Omega = \Delta\Omega e^{-t/t_s}$ where t_s is the spin-up time. The kinetic energy of the flow is

$$\begin{aligned} \text{K.E.} &= \rho H \int_0^{2\pi} d\theta \int_0^{r_{\max}} \frac{1}{2} r v^2 dr, \\ &= \pi H \rho \Delta\Omega^2 \int_0^{r_{\max}} r^3 dr, \\ &= \frac{1}{4} \rho \pi H r_{\max}^4 \Omega^2. \end{aligned}$$

The rate of dissipation is then

$$\dot{E} = - \frac{\rho \pi H r_{\max}^4 \Delta\Omega^2}{4 t_s} e^{-2t/t_s}.$$

The energy dissipation from the wire drag may be computed from Lamb's formula (Lamb, section 343, 6th ed.). The drag per unit length on a cylinder of radius a is given by

$$D = \frac{4\pi\rho\nu v}{\ln(\frac{1}{2}ka)} \quad \text{where } k = \frac{v}{2\nu}.$$

The total dissipation produced by N wires is therefore:

$$\dot{E}_w = 8N\pi\rho\nu\Delta\Omega^2 \exp(-2t/t_s) \int_0^{r_{\max}} \frac{r^2}{-\ln(\sigma r)} dr$$

where $\sigma = \frac{\Delta\Omega a e^{-t/t_s}}{4 \nu}$.

By a simple substitution the integral may be transformed as

$$\int_0^{r_{\max}} \frac{r^2}{-\ln(\sigma r)} dr = \frac{1}{\sigma^3} \int_{-3\ln(\sigma r)}^{+\infty} \frac{e^{-y}}{y} dy$$

or, asymptotically for large $(-3\ln \sigma r_{\max}) = \epsilon$,

$$\frac{r^3}{\epsilon} (1 + \epsilon^{-1} + \dots) .$$

The the energy dissipation due to the wire drag is

$$\dot{E}_w = 8N\pi\rho\nu\Delta\Omega^2 \exp(-2t/t_s) \frac{r^3}{-3 \ln \sigma r_{\max}} \left(1 + \frac{1}{-3 \ln \sigma r_{\max}} \right)$$

The ratio of the dissipation rates, \dot{E}_w / \dot{E} is given by

$$\frac{32N\nu t_s}{-3H r_{\max} \ln \sigma r_{\max}} \left(1 + \frac{1}{-3 \ln \sigma r_{\max}} \right) .$$

This gives for an upper bound on the ratio for $N = 10$, $\Delta\Omega = 0.03 \text{ sec}^{-1}$:

$$\dot{E}_w / \dot{E} < 0.05 .$$

APPENDIX III

DISCUSSION OF EXPERIMENTAL ERRORS

Section 1: Limitations of the measuring systems

1.1 Time accuracy

The time measurements for the photographs were made by recording the time each photograph was taken on a strip chart recorder. The absolute accuracy was about ± 0.15 sec.

The time measurements for the thermistor readings were computed from the stepping switch times and the photograph times measured with an oscilloscope. The absolute accuracy of these time measurements is better than ± 0.05 sec.

1.2 Accuracy of the positions of the neutrally buoyant floats

The positions of the neutrally buoyant floats were determined by photographing them with an automatic Nikon F, 35 mm camera. The positions were copied onto tracing paper. This was done on a large microfilm reader which advanced each frame to the same approximate position as the previous frame. The positions on the tracing paper were digitized on an automatic digitizer of Professor Gene Simmons. These positions were punched onto cards in terms of Cartesian coordinates. The final step in determining the positions was to transform the Cartesian positions into polar coordinates and correct for the parallax of the camera. Each of these steps contributed to the error in position.

The microfilm reader was supposed to place each frame in the same position as the previous frame. In fact this did not occur. The positions of the frames would often be shifted horizontally

a small amount, about $\frac{1}{4}$ inch on the actual scale of projection. This would amount to about 1/3 cm in the computed position. For large radii where the distance between successive points was large, this would not make much difference. For points near the center, and for points which were close together, these errors could be sizable fractions of the total differential measurement. It is for these reasons that the low Rossby number and small radius measurements are in the most error.

The errors in drawing the positions of the points were no more than about ± 0.05 in. The digitizing errors due to the digitizer alone are ± 0.001 in. These are sufficiently small that they are entirely masked by the error in the reader.

The errors due to the computing program are negligible, being about one part in 10^6 .

1.3 Accuracy of the temperature measuring system

The details of the temperature measuring system have been described in chapter 2 and appendix II . Each part of the system has an inherent error in the temperature measurement. This section will discuss the magnitude of these errors and their effect on the data. The units of temperature used in this section will be degrees Celsius or digitizing units, where one digitizing unit (d.u.) equals 0.0026 °C.

The resolution of the analog to digital converter is about 0.01 V. This corresponds to 0.0026 °C or 1 d.u. This is the absolute limit of accuracy possible with the system in the configuration used

in the experiments.

There was always the possibility of signal degradation due to electrical noise, particularly at 60 Hz. The main contribution to the 60 Hz noise was the power to the hot and cold water pumps on the turntable. These could not be eliminated, so the effect of their noise had to be removed after the signal had been contaminated. This was done by placing two active filters, one, a band-reject filter with a sharp notch at 60 Hz, and the other, a low pass filter with the cut-off at 60 Hz. These were very effective in removing any noise at 60 Hz and 120 Hz. The maximum observed error in the output signals after the filters were installed was only 2-3 d.u. The only problem the filters introduced was the requirement of a waiting time to allow the signal transients due to the step response of the filters to die out before sampling. This caused no problem, as the wait time was the same order as the maximum stepping rate of the stepping switch.

The computer, on occasion mistyped the output temperature. This was finally traced to mistriggering of the skip bus. The mistyped temperatures were corrected manually by interpolating the previous value of the thermistor and the following value of the same thermistor. This would have produced an error of no more than about 5 d.u. at any thermistor or time.

The thermistors, unfortunately, cannot measure temperatures at a mathematical point, but only give an average of the temperature over their surface. Therefore, there could be the possibility

of an error in the temperature at any thermistor equal to the diameter of the thermistor times the temperature gradient across the thermistor. The thermistors used in these experiments were about 0.025cm in diameter, and the vertical temperature gradient was about 1 deg/cm, giving a maximum error of 0.025 °C or about 10 d.u. As the maximum error observed was two to three du., it can be concluded that the thermistors can give a much more accurate reading than might be expected.

The time response of the thermistors might cause problems if the processes being investigated were varying too rapidly, but for these experiments that is no problem. The time response of the thermistors used in these experiments is about 10^{-2} sec.

There is the possibility of errors induced by the self heating of the thermistors. For this reason, the resistance of the thermistors was chosen as about 1 MΩ. The ohmic heating, E^2/R is thus about 10^{-6} Watt. This corresponds to about 0.001 °C increase.

The leads of the thermistor can conduct heat away or toward the thermistor and could constitute a source of error. To estimate the magnitude of this error, it will be assumed that the heat conducted away from the thermistor is conducted along the wire, and that the temperature gradient is determined by that of the fluid. If the thermal conductivity is that of platinum and the radius is 0.005 cm, the heat flux is about 4×10^{-7} watt which is less than the ohmic heating.

Another possible source of error is radiative transfer between the thermistor and the walls of the room. The heat flux, assuming

blackbody radiation is given by $Q = kA(T_{\text{thermistor}}^4 - T_{\text{wall}}^4)$
 or approximately $Q = 4kA \Delta T T_{\text{wall}}^3$. If $A = 12 \times 10^{-6} \text{ cm}^2$, and
 $T_{\text{wall}} = 300 \text{ }^\circ\text{K}$, $\Delta T = 5 \text{ }^\circ\text{K}$, $k = 5.7 \times 10^{-5} \text{ erg cm}^{-2} \text{ sec}^{-1}$,
 $Q = 12 \times 10^{-8} \text{ Watt}$, which is much less than either the ohmic
 heating or the lead conduction.

The secular variation in the thermistors is not known, but
 this provides no problem in the differential measurements.

The last possible problem was noise due to the slip-rings.
 This was not noticable above 1 or 2 d.u.

APPENDIX IV
COMPUTER PROGRAMS


```

DIMENSION VBAR(16,16)
COMMON ALPHA(50)
DIMENSION BB(20,20),BLOG(20,20),AAZ(4,41),BBB(20,5)
DIMENSION Q(1),S(1),FGR(16,16)
DIMENSION R(20),Z(20),F(20),FF(20),X(20),D(20,20),A(400),
1FD(16,16)
DIMENSION BAV(5)
DIMENSION BALG(5)
DIMENSION TTND(40)
DIMENSION QZ(5)
DATA QZ/5*0.0/
DATA BAV/5*0.0/
DIMENSION XXB(21,17)
DATA VBAR/256*00.0/
DATA Q(1)/' T'/,S(1)/' R'/
DATA IZZ/0/
RO = 2.259
C READ EXPERIMENTAL DATA
NUM = 0
C
N = 18
NN = 2
NNN = NN + 1
READ(5,250) NEXPT,SSS,ROSBY,EKNO ,TSPIN
BURG = SQRT(SSS)/2.
WRITE(6,251) NEXPT,BURG,ROSBY,EKNO
B = BURG
FA = 2.
ETA = .00001
SBAR = 7.41*SQRT(EKNO)
PRAND = 14.0
H = PRAND**0.250*SQRT(B/2.)
CONS = H*B*2.259*SQRT(FA)*SBAR/(SBAR - H)
CALL ALPH(ETA,CONS,SBAR,H,BURG,1.0)
WRITE(6,278)(ALPHA(I),I=1,40)
WRITE(6,200)

```

```

CALL NORTH(ALPHA,AAZ,NNN)
WRITE(6,290)(K,AAZ(1,K),AAZ(2,K),AAZ(3,K),K=1,40)
WRITE(6,200)
RR = 0.0
DO 1701 K=1,10
RR = RR + 0.1
RSUM = AAZ(2,1)
DO 1700 I = 2,40
XY= RR*ALPHA(I-1)
CALL BESJ(XY,0,BJ1,.001,IER)
RSUM = RSUM+AAZ(2,I)*BJ1
1700 CONTINUE
RRR = RR*RR
WRITE(6,291) RR,RRR,RSUM
1701 CONTINUE
WRITE(6,200)
278 FORMAT( 8(F10.4,4X))
ISW = 0
6000 CONTINUE
NUM = NUM + 1
DO 5010 KK = 1,5
5010 BAV(KK) = 0.0
DO 2000 II = 1,400
2000 A(II) = 0.0
L = 0
DO 999 I = 1,20
DJ 999 J = 1,20
D(I,J) = 0.0
Z(I) = 0.0
R(I) = 0.0
F(I) = 0.0
FF(I) = 0.0
L=L+1
A(L) = 0.0
999 CONTINUE

```

```

C      INPUT THE DATA
C
      IF(IZZ.NE.0) GO TO 6001
      READ(5,101)(R(K),Z(K),F(K),TIME,IZZ,K=1,N)
      DO 1011 K = 1,N
      R(K) = R(K) + .00001
      Z(K) = Z(K) + .00001
      F(K) = F(K) + .00001
1011 CONTINUE
C
C      PRODUCE THE 'D' MATRIX
C
      LLN = 0
      DO 1001 L = 1,NNN
      DO 1001 M = 1,NN
      LLN = LLN + 1
      LLX = 0
      DO 1001 I = 1,NNN
      DO 1001 J = 1,NN
      LLX = LLX + 1
      D(LLN,LLX) = 0.0
      IX = 2*(I+L-2)
      LX = 2*(J+M - 1)
      DO 1001 K = 1,N
1001 D(LLN,LLX) = D(LLN,LLX) + R(K)**IX*Z(K)**LX
C
C      PRODUCE THE FF MATRIX
C
      LLN = 0
      DO 1002 L = 1,NNN
      DO 1002 M = 1,NN
      LLN = LLN + 1
      FF(LLN) = 0.0
      DO 1002 K = 1,N
1002 FF(LLN) = FF(LLN) + F(K)*R(K)**(2*(L-1))*Z(K)**(2*M-1)

```

```

DO 1008 I=1,16
DO 1008 J = 1,16
FD(I,J) = 0.0
1008 FGR(I,J)=00.0
C
C PUT D INTO FORM FOR USE IN GELB
C
LLK = 0
NNK = NN*NN
DJ 1003 I = 1,NNK
DO 1003 J = 1,NNK
LLK = LLK + 1
1003 A(LLK) = C(J,I)
NNX = NNK - 1
DJ 1004 I = 1,NNK
1004 X(I) = FF(I)
CALL GELB(X,A,NNK,1,NNX,NNX,.000001,IER)
WRITE( 6,302) IER
C
C OUTPUT CCEFICIENTS
C
WRITE(6,201)
WRITE(6,202)(K,X(K),K=1,NNK)
C
C COMPUTE THE ERROR FUNCTION AND THE STD DEVIATION
C
E = 0.0
DO 1005 K = 1,N
P = 0.0
LLX = 0
DJ 1006 I = 1,NNN
DO 1006 J = 1,NN
LLX = LLX + 1
1006 P = P + X(LLX) *R(K)**(2*(I-1))*Z(K)**(2*J-1)
1005 E = E + (F(K) - P) **2
SIGMA = E/(N-1)

```

```
SIGMA = SQRT(SIGMA)
WRITE(6,200)
WRITE(6,203) E,SIGMA
```

C
C
C

```
COMPUTE THE FITTED FIELD
```

```
IF(TIME.LE.C.001) TIME = 1.40 + 4.58*(NUM - 1)
WRITE(6,252) TIME
TIMND = TIME/TSPIN
TTND(NUM) = TIMND
WRITE(6,253) TIMND
WRITE(6,208)
DR = 2.259/16.
DZ = 1./16.
DO 1009 L = 1,16
DO 1009 M = 1,16
RR = DR*(L-1) + .00001
ZZ = DZ*(M-1) + .00001
FD(L,M) = 0.0
VBAR(L,M) = 0.0
FGR(L,M) = 0.0
LLX = 0
DO 1007 I = 1,NNN
DO 1007 J = 1,NN
LLX = LLX + 1
FD(L,M) = FD(L,M) + X(LLX)*RR**(2*(I-1))*ZZ**(2*J-1)
VBAR(L,M) = VBAR(L,M) + X(LLX)*(I-1)*RR**(2*I-3)*ZZ**(2*J)/J
1007 FGR(L,M) = FGR(L,M) + 2*(I-1)*RR**(2*(I-1) - 1)*ZZ**(2*J-1)*X(LLX)
WRITE(6,209)L,M,RR,ZZ,FD(L,M),FGR(L,M), VBAR(L,M)
1009 CONTINUE
WRITE(6,200)
CALL CCNTUR(FD,16,16)
WRITE(6,200)
CALL CCNTUR(FGR,16,16)
WRITE(6,200)
CALL CCNTUR(VBAR,16,16)
```



```

WRITE(6,200)
C
C CALCULATE THE BESSEL COEFFICIENTS
C
DO 5000 NU = 1,5
NX = NU +1
DO 5000 IO = 1,16
ZZ = (IO - 1)*CZ + 0.00001
BB(NU,IO) = 0.0
LLX = 0
DO 5003 I = 1,ANN
DO 5002 J = 1,NN
LLX = LLX + 1
ANNO = ALPHA(NX)
CALL BESJ(ANNO,0,BJO,.0001,IEX)
XINT = AAZ(I,NU)
BAV(NU) = BAV(NU) + X(LLX)*2.259**((2*I)*XINT/(2.*J*BJO**2))
BBB(NUM,NU) = BAV(NU)
BB(NU,IO) = 3B(NU,IO)+X(LLX)*2.259**((2*(I-1))*XINT/BJO**2*ZZ**((2*
1J-1)*2.
5002 CONTINUE
5003 CONTINUE
BBZ = ABS(BAV(NU) )
BALG(NU) = ALOG(BBZ)
XXB(NUM,IO) = BB(1,IO)
3BX = BB(NU,IO)
BBX = ABS(BBX)
BLOG(NU,IO) = ALOG(BBX)
5000 CONTINUE
WRITE(6,200)
WRITE(6,220)
WRITE(6,221) (( I,J,BB(I,J),BLOG(I,J),I=1,5),J=1,16)
WRITE(6,200)
WRITE(6,240)
WRITE(6,241)(KK,BAV(KK),BALG(KK),KK=1,5)
WRITE(6,200)

```

```

DO 5011 KK = 1,5
QQ = BURG*ALPHA(KK+1)/RO
QA = -QQ*0.7071*TIMND*CSH(QQ)/SINH(QQ)
QZ(KK) = 1. - EXP(QA)
5011 CONTINUE
WRITE(6,254) (KK,QZ(KK),KK=1,5)
WRITE(6,200)
GO TO 6000
6001 CCNTINUE
WRITE(7,277)( TTND(K),BBB(K,1),K = 1,NUM)
WRITE(7,279)
WRITE(7,277)( TTND(K),BBB(K,2),K = 1,NUM)
WRITE(6,200)
WRITE(6,277)( TTND(K),BBB(K,1),K = 1,NUM)
WRITE(6,279)
WRITE(6,277)( TTND(K),BBB(K,2),K = 1,NUM)
DO 5100 IK = 1,16
282 FORMAT(//////////)
WRITE(7,282)
WRITE(6,282)
WRITE(7,281)( TTND(IN),XXB(IN,IK),IN,IK,NEXPT,IN=1,NUM)
WRITE(6,281)( TTND(IN),XXB(IN,IK),IN,IK,NEXPT,IN=1,NUM)
281 FORMAT(2F10.1,3I5)
5100 CONTINUE
100 FORMAT( 3I5)
101 FORMAT(4F10.5,38X,I2)
200 FORMAT(1H1)
201 FORMAT(' POLYNOMIAL COEFFICIENTS '////////)
202 FORMAT( 5X, I5,E20.8)
203 FORMAT(////' E(N) =',E20.8////' STANDARD DEVIATION =',
1E20.8////)
208 FORMAT(1H1////' L ', ' M ', ' R ', ' Z ', ' TEMPERATURE '
1' DT/DR ', ' BAROCLINIC VELOCITY'////////)
209 FORMAT( 2I5,2F8.5,4F11.5)
220 FORMAT( ' NU J B(NU,J) LOG(B(NU,J))'////////)
221 FORMAT(I5,6X,I5,2E20.8/)

```

```

240 FORMAT( '   NU           BAV(NU           LOG(BAV(NU))'/////))
241 FORMAT( I5,2E20.8)
250 FORMAT( I5,4F10.7)
251 FORMAT(1H1/' EXPERIMENT NUMBER =',I3///'          BURGER NUMBER ='F10.5
1/'          ROSSBY NUMBER ='F10.5/'          EKMANN NUMBER =' F10.7/1H1)
252 FORMAT( ' REAL TIME ='F10.5,'SEC')
253 FORMAT(' NON DIMENSIONAL TIME ='F10.5/1H1)
254 FORMAT(' NU ='I3,'          U - EXP(Q(NU)) =' , E20.8)
277 FORMAT( 2F10.2)
279 FORMAT(/////////)
290 FORMAT( I5,3E20.8)
291 FORMAT(' R = 'F10.5,'R**2 = ', F16.8,' SUM = ', F16.8)
300 FORMAT( ' MATRIX A  ')
301 FORMAT( E20.8)
302 FORMAT( ' IER = ',I5)
700 FORMAT( ' TEST POINT')
701 FORMAT(' TEST PCINT 2 ')
CALL EXIT
END

```

	SUBROUTINE GELB(R,A,M,N,MUD,MLD,EPS,IER)	GELB 700
C		GELB 690
C		GELB 710
C		GELB 720
	DIMENSION R(1),A(1)	GELB 730
C		GELB 740
C	TEST CN WRONG INPUT PARAMETERS	GELB 750
	IF(MLD)47,1,1	GELB 760
1	IF(MUD)47,2,2	GELB 770
2	MC=1+MLD+MUD	GELB 780
	IF(MC+1-M-M)3,3,47	GELB 790
C		GELB 800
C	PREPARE INTEGER PARAMETERS	GELB 810
C	MC=NUMBER OF COLUMNS IN MATRIX A	GELB 820
C	MU=NUMBER OF ZERCS TO BE INSERTED IN FIRST ROW OF MATRIX A	GELB 830
C	ML=NUMBER OF MISSING ELEMENTS IN LAST ROW OF MATRIX A	GELB 840
C	MR=INDEX OF LAST ROW IN MATRIX A WITH MC ELEMENTS	GELB 850
C	MZ=TOTAL NUMBER OF ZEROS TO BE INSERTED IN MATRIX A	GELB 860
C	MA=TOTAL NUMBER OF STORAGE LOCATIONS NECESSARY FOR MATRIX A	GELB 870
C	NM=NUMBER OF ELEMENTS IN MATRIX R	GELB 880
3	IF(MC-M)5,5,4	GELB 890
4	MC=M	GELB 900
5	MU=MC-MUD-1	GELB 910
	ML=MC-MLD-1	GELB 920
	MR=M-ML	GELB 930
	MZ=(MU*(MU+1))/2	GELB 940
	MA=M*MC-(ML*(ML+1))/2	GELB 950
	NM=N*M	GELB 960
C		GELB 970
C	MOVE ELEMENTS BACKWARD AND SEARCH FOR ABSOLUTELY GREATEST ELEMENT	GELB 980
C	(NOT NECESSARY IN CASE OF A MATRIX WITHOUT LOWER CODIAGONALS)	GELB 990
	IER=0	GELB1000
	PIV=0.	GELB1010
	IF(MLD)14,14,6	GELB1020
6	JJ=MA	GELB1030
	J=MA-MZ	GELB1040

	KST=J	GELB1050
	DO 9 K=1,KST	GELB1060
	TB=A(J)	GELB1070
	A(JJ)=TB	GELB1080
	TB=ABS(TB)	GELB1090
	IF(TB-PIV)8,8,7	GELB1100
	7 PIV=TB	GELB1110
	8 J=J-1	GELB1120
	9 JJ=JJ-1	GELB1130
C		GELB1140
C	INSERT ZEROS IN FIRST MU ROWS (NOT NECESSARY IN CASE MZ=0)	GELB1150
	IF(MZ)14,14,10	GELB1160
10	JJ=1	GELB1170
	J=1+MZ	GELB1180
	IC=1+MUD	GELB1190
	DO 13 I=1,MU	GELB1200
	DO 12 K=1,MC	GELB1210
	A(JJ)=0.	GELB1220
	IF(K-IC)11,11,12	GELB1230
11	A(JJ)=A(J)	GELB1240
	J=J+1	GELB1250
12	JJ=JJ+1	GELB1260
13	IC=IC+1	GELB1270
C		GELB1280
C	GENERATE TEST VALUE FOR SINGULARITY	GELB1290
14	TOL=EPS*PIV	GELB1300
C		GELB1310
C		GELB1320
C	START DECOMPOSITION LOOP	GELB1330
	KST=1	GELB1340
	IDST=MC	GELB1350
	IC=MC-1	GELB1360
	DO 38 K=1,M	GELB1370
	IF(K-MR-1)16,16,15	GELB1380
15	IDST=IDST-1	GELB1390
16	ID=IDST	GELB1400

	ILR=K+MLD	GELB1410
	IF(ILR-M)18,18,17	GELB1420
17	ILR=M	GELB1430
18	II=KST	GELB1440
C		GELB1450
C	PIVOT SEARCH IN FIRST COLUMN (ROW INDEXES FROM I=K UP TO I=ILR)	GELB1460
	PIV=0.	GELB1470
	DO 22 I=K,ILR	GELB1480
	TB=ABS(A(II))	GELB1490
	IF(TB-PIV)20,20,19	GELB1500
19	PIV=TB	GELB1510
	J=I	GELB1520
	JJ=II	GELB1530
20	IF(I-MR)22,22,21	GELB1540
21	ID=ID-1	GELB1550
22	II=II+ID	GELB1560
C		GELB1570
C	TEST ON SINGULARITY	GELB1580
	IF(PIV)47,47,23	GELB1590
23	IF(IER)26,24,26	GELB1600
24	IF(PIV-TCL)25,25,26	GELB1610
25	IER=K-1	GELB1620
26	PIV=1./A(JJ)	GELB1630
C		GELB1640
C	PIVOT ROW REDUCTION AND ROW INTERCHANGE IN RIGHT HAND SIDE R	GELB1650
	ID=J-K	GELB1660
	DO 27 I=K,NM,M	GELB1670
	II=I+ID	GELB1680
	TB=PIV*R(II)	GELB1690
	R(II)=R(I)	GELB1700
27	R(I)=TB	GELB1710
C		GELB1720
C	PIVOT ROW REDUCTION AND ROW INTERCHANGE IN COEFFICIENT MATRIX A	GELB1730
	II=KST	GELB1740
	J=JJ+IC	GELB1750
	DO 28 I=JJ,J	GELB1760

	TB=PIV*A(I)	GELB1770
	A(I)=A(II)	GELB1780
	A(II)=TB	GELB1790
28	II=II+1	GELB1800
C		GELB1810
C	ELEMENT REDUCTION	GELB1820
	IF(K-ILR)29,34,34	GELB1830
29	ID=KST	GELB1840
	II=K+1	GELB1850
	MU=KST+1	GELB1860
	MZ=KST+IC	GELB1870
	DO 33 I=II,ILR	GELB1880
C		GELB1890
C	IN MATRIX A	GELB1900
	ID=ID+MC	GELB1910
	JJ=I-MR-1	GELB1920
	IF(JJ)31,31,30	GELB1930
30	ID=ID-JJ	GELB1940
31	PIV=-A(ID)	GELB1950
	J=ID+1	GELB1960
	DO 32 JJ=MU,MZ	GELB1970
	A(J-1)=A(J)+PIV*A(JJ)	GELB1980
32	J=J+1	GELB1990
	A(J-1)=0.	GELB2000
C		GELB2010
C	IN MATRIX R	GELB2020
	J=K	GELB2030
	DO 33 JJ=I,NM,M	GELB2040
	R(JJ)=R(JJ)+PIV*R(J)	GELB2050
33	J=J+M	GELB2060
34	KST=KST+MC	GELB2070
	IF(ILR-MR)36,35,35	GELB2080
35	IC=IC-1	GELB2090
36	ID=K-MR	GELB2100
	IF(ID)38,38,37	GELB2110
37	KST=KST-ID	GELB2120

```

38 CONTINUE
C   END OF DECOMPOSITION LOOP
C
C   BACK SUBSTITUTION
C   IF(MC-1)46,46,39
39 IC=2
   KST=MA+ML-MC+2
   II=M
   DO 45 I=2,M
   KST=KST-MC
   II=II-1
   J=II-MR
   IF(J)41,41,40
40 KST=KST+J
41 DO 43 J=II,NM,M
   TB=R(J)
   MZ=KST+IC-2
   ID=J
   DO 42 JJ=KST,MZ
   ID=ID+1
42 TB=TB-A(JJ)*R(ID)
43 R(J)=TB
   IF(IC-MC)44,45,45
44 IC=IC+1
45 CONTINUE
46 RETURN
C
C   ERROR RETURN
C
47 IER=-1
   RETURN
   END
   FUNCTION IFAC(N)
   IX = 1
   DO 1000 J = 1,N

```

```

GELB2130
GELB2140
GELB2150
GELB2160
GELB2170
GELB2180
GELB2190
GELB2200
GELB2210
GELB2220
GELB2230
GELB2240
GELB2250
GELB2260
GELB2270
GELB2280
GELB2290
GELB2300
GELB2310
GELB2320
GELB2330
GELB2340
GELB2350
GELB2360
GELB2370
GELB2380
GELB2390
GELB2400
GELB2410
GELB2420
GELB2430
GELB2440
GELB2450

```

111


```
1000 IX = IX*J  
      IFAC = IX  
      RETURN  
      END
```

```

SUBROUTINE ALPH(ETA,CONS,SBAR,H,B,AO)
C
C
C THIS SUBROUTINE WILL FINE THE ROOTS OF THE EQUATION FOR THE ALPHAS
C
C OTHER SUBROUTINES USED: ROOT
C
C SEE 'ROOT' FOR FURTHER SUBROUTINES
C
IMPLICIT REAL*8(A-H,C-Z)
REAL*4 ALPHA
DATA NK/50/
COMMON ALPHA(50)
DIMENSION BB(6)
BB(1) = 0.0
BB(2)=2.40483
BB(3)=5.52007
BB(4) =8.65373
BB(5)=11.79153
BZZ = B/AO
C
C INITIALIZE ALPHA
C
DO 1 I = 1,50
1 ALPHA(I)=0.0
C
XQQQ = SBAR - H
IF(XQQQ.LT.0.0) GO TO 4
START THE SEQUENCE FOR FINDING THE ALPHAS
C
C
6 DO 3 I=1,3
ACC = BB(I) + .05
BOO = BB(I+1) -.05
ALPHA(I) = ROOT(AOJ,BOO,ETA,CONS,BZZ)
IF(ALPHA(I).LT.0.01) GO TO 4
3 CCNTINUE

```

```
ADD = ALPHA(3) + 3.00
BDD = ALPHA(3) + 3.30
DO 2 I = 4,50
ALPHA(I) = RCOT(ADD,BDD,ETA,CONS,BZZ)
ADD = ALPHA(I) + 3.00
BDD = ALPHA(I) + 3.30
2 CONTINUE
RETURN
4 DO 5 J=1,4
5 BB(J) = BB(J+1)
GO TO 6
END
```

```

FUNCTION ROCT(X,Y,ETA,CONS,B)
C
C SUBROUTINES USED: BESJ,COSH,SINH
C
C
IMPLICIT REAL*8(A-H,O-Z)
REAL*4 ALPHA
100 C = ( X + Y)/2.
ROOT = C
3000 FORMAT(E20.8)
IF(DABS(C- X).LE.ETA) GO TO 1000
CALL BESJ(C,0,BJO,.01,IK)
CALL BESJ(C,1,BJ1,.01,IJ)
QF = B*C
QPK = 1.0000000000
IF(QF.LT.100) QPK = DSINH(QF)/DCOSH(QF)
G = BJ1/BJO - CCNS*QPK
IF(G.GT.C.0) GO TO 2
X = C
Y = Y
GO TO 100
2 X = X
Y = C
GO TO 100
1000 RETURN
END

```

```

SUBROUTINE NORTH(ALPHA,A,MMAX)
DIMENSION ALPHA(40),A(4,41),Z(41,41),AA(164) ,ZZ(1681)
INTEGER P,PP
DO 1000 P = 1,40
CALL BESJ(ALPHA(P),1,BJ1,.0001,IE1)
CALL BESJ(ALPHA(P),0,BJO,.0001,IE0)
A(1,1) = 0.5
Z(1,1) = 1./2.
A(1,P+1)=BJ1/ALPHA(P)
Z(1,P+1) = BJO/ALPHA(P)
Z(P+1,1) = Z(1,P+1)
DO 1001 M = 2,MMAX
A(M,1) = 1./(2.*M)
MM = M - 1
1001 A(M,P+1)= BJ1/ALPHA(P) + ( 2.*MM*BJO - 4.*MM*MM*A(MM,P+1))/ALPHA(P
1)**2
PP = P - 1
IF(PP.EQ.0) GO TO 1103
DO 1002 N = 1,PP
CALL BESJ(ALPHA(N),1,BJ1N,.0001,IE2)
CALL BESJ(ALPHA(N),0,BJO,N,.0001,IE2)
Z1 = ALPHA(P)*BJ1*BJO - ALPHA(N)*BJO*BJ1N
Z2 = ALPHA(P)**2 - ALPHA(N)**2
IF(Z2.EQ.0.0) WRITE(6,7000) Z1,Z2 ,N,P
7000 FORMAT( ' Z1 = ',E20.8,5X,'Z2=',E20.8,' N=',I5,' P=',I5///)
Z(N+1,P+1) = Z1/Z2
Z(P+1,N+1) = Z(N+1,P+1)
1002 CONTINUE
1103 CONTINUE
Z(P+1,P+1) = 0.5*(BJO*BJO + BJ1*BJ1)
WRITE(6,7003)
7003 FORMAT(' TEST POINT NUMBER ZERO ')
1000 CONTINUE

```

```

C
C PUT A AND Z INTO PROPOER FORM FOR USE IN THE ROUTINE GELG
C

```

```

      NN = 0
      DO 1004 M = 1,MMAX
      WRITE(6,7001)
7001 FORMAT(' TEST POINT NUMBER ONE' )
      DO 1004 P = 1,40
      NN = NN + 1
1004 AA(NN) = A(M,P)
      NN = 0
      DO 1005 N = 1,40
      DO 1005 P=1,40
      NN = NN + 1
1005 ZZ(NN) = Z(N,P)
C
C   SOLVE FOR THE A'S
C
      CALL GELG(AA,ZZ,40,MMAX,.00001,IER)
      IF(IER.NE.0) WRITE(6,200) IER
200  FORMAT(' ERROR IN SOLUTION OF COEFFICIENT MATRIX,ERROR=',I5)
      WRITE(6,7002)
7002 FORMAT(' TEST POINT NUMBER TWO ' / 1H1)
C
C   RECCMPOSE A
C
      NN = 0
      DO 1006 M = 1,MMAX
      DO 1006 P=1,40
      NN = NN + 1
1006 A(M,P) = AA(NN)
      RETURN
      END

```

```

SUBROUTINE GELG(R,A,M,N,EPS,IER)                                GELG 520
THE ABOVE CARD SHOULD BE PLACED IN PROPER SEQUENCE
BEFORE COMPILING THIS UNDER IBM FORTRAN G.

.....
SUBROUTINE GELG                                              GELG 10
PURPOSE                                                      GELG 20
  TO SOLVE A GENERAL SYSTEM OF SIMULTANEOUS LINEAR EQUATIONS. GELG 30
USAGE                                                         GELG 40
  CALL GELG(R,A,M,N,EPS,IER)                                GELG 50
DESCRIPTION OF PARAMETERS                                     GELG 60
  R      - THE M BY N MATRIX OF RIGHT HAND SIDES. (DESTROYED) GELG 70
          ON RETURN R CONTAINS THE SOLUTION OF THE EQUATIONS. GELG 80
  A      - THE M BY M COEFFICIENT MATRIX. (DESTROYED)       GELG 90
  M      - THE NUMBER OF EQUATIONS IN THE SYSTEM.           GELG 100
  N      - THE NUMBER OF RIGHT HAND SIDE VECTORS.           GELG 110
  EPS    - AN INPUT CONSTANT WHICH IS USED AS RELATIVE     GELG 120
          TOLERANCE FOR TEST ON LOSS OF SIGNIFICANCE.       GELG 130
  IER    - RESULTING ERROR PARAMETER CODED AS FOLLOWS      GELG 140
          IER=0 - NO ERROR,                                  GELG 150
          IER=-1 - NO RESULT BECAUSE OF M LESS THAN 1 OR    GELG 160
                   PIVOT ELEMENT AT ANY ELIMINATION STEP  GELG 170
                   EQUAL TO 0,                              GELG 180
          IER=K - WARNING DUE TO POSSIBLE LOSS OF SIGNIFI-  GELG 190
                   CANCE INDICATED AT ELIMINATION STEP K+1, GELG 200
                   WHERE PIVOT ELEMENT WAS LESS THAN OR    GELG 210
                   EQUAL TO THE INTERNAL TOLERANCE EPS TIMES GELG 220
                   ABSOLUTELY GREATEST ELEMENT OF MATRIX A. GELG 230
REMARKS                                                       GELG 240
  INPUT MATRICES R AND A ARE ASSUMED TO BE STORED COLUMNWISE GELG 250
  IN M*N RESP. M*M SUCCESSIVE STORAGE LOCATIONS. ON RETURN  GELG 260

```

C	SOLUTION MATRIX R IS STORED COLUMNWISE TOO.	GELG 340
C	THE PROCEDURE GIVES RESULTS IF THE NUMBER OF EQUATIONS M IS	GELG 350
C	GREATER THAN 0 AND PIVOT ELEMENTS AT ALL ELIMINATION STEPS	GELG 360
C	ARE DIFFERENT FROM 0. HOWEVER WARNING IER=K - IF GIVEN -	GELG 370
C	INDICATES POSSIBLE LOSS OF SIGNIFICANCE. IN CASE OF A WELL	GELG 380
C	SCALED MATRIX A AND APPROPRIATE TOLERANCE EPS, IER=K MAY BE	GELG 390
C	INTERPRETED THAT MATRIX A HAS THE RANK K. NO WARNING IS	GELG 400
C	GIVEN IN CASE M=1.	GELG 410
C		GELG 420
C	SUBROUTINES AND FUNCTION SUBPROGRAMS REQUIRED	GELG 430
C	NCNE	GELG 440
C		GELG 450
C	METHOD	GELG 460
C	SOLUTION IS DONE BY MEANS OF GAUSS-ELIMINATION WITH	GELG 470
C	COMPLETE PIVOTING.	GELG 480
C		GELG 490
C	GELG 500
C		GELG 510
C		GELG 530
C		GELG 540
C	DIMENSION A(1),R(1)	GELG 550
C	IF(M)23,23,1	GELG 560
C		GELG 570
C	SEARCH FOR GREATEST ELEMENT IN MATRIX A	GELG 580
1	IER=0	GELG 590
	PIV=0.	GELG 600
	MM=M*M	GELG 610
	NM=N*M	GELG 620
	DO 3 L=1,MM	GELG 630
	TB=ABS(A(L))	GELG 640
	IF(TB-PIV)3,3,2	GELG 650
2	PIV=TB	GELG 660
	I=L	GELG 670
3	CONTINUE	GELG 680
	TOL=EPS*PIV	GELG 690
C	A(I) IS PIVOT ELEMENT. PIV CONTAINS THE ABSOLUTE VALUE OF A(I).	GELG 700

C		GELG 710
C		GELG 720
C	START ELIMINATION LOOP	GELG 730
	LST=1	GELG 740
	DO 17 K=1,M	GELG 750
C		GELG 760
C	TEST ON SINGULARITY	GELG 770
	IF(PIV)23,23,4	GELG 780
4	IF(IER)7,5,7	GELG 790
5	IF(PIV-TCL)6,6,7	GELG 800
6	IER=K-1	GELG 810
7	PIVI=1./A(I)	GELG 820
	J=(I-1)/M	GELG 830
	I=I-J*M-K	GELG 840
	J=J+1-K	GELG 850
C	I+K IS ROW-INDEX, J+K COLUMN-INDEX OF PIVOT ELEMENT	GELG 860
C		GELG 870
C	PIVOT ROW REDUCTION AND ROW INTERCHANGE IN RIGHT HAND SIDE R	GELG 880
	DO 8 L=K,NM,M	GELG 890
	LL=L+I	GELG 900
	TB=PIVI*R(LL)	GELG 910
	R(LL)=R(L)	GELG 920
8	R(L)=TB	GELG 930
C		GELG 940
C	IS ELIMINATION TERMINATED	GELG 950
	IF(K-M)9,18,18	GELG 960
C		GELG 970
C	COLUMN INTERCHANGE IN MATRIX A	GELG 980
9	LEND=LST+M-K	GELG 990
	IF(J)12,12,10	GELG1000
10	II=J*M	GELG1010
	DO 11 L=LST,LEND	GELG1020
	TB=A(L)	GELG1030
	LL=L+II	GELG1040
	A(L)=A(LL)	GELG1050
11	A(LL)=TB	GELG1060

C		GELG1070
C	ROW INTERCHANGE AND PIVOT ROW REDUCTION IN MATRIX A	GELG1080
	12 DO 13 L=LST,MM,M	GELG1090
	LL=L+I	GELG1100
	TB=PIVI*A(LL)	GELG1110
	A(LL)=A(L)	GELG1120
	13 A(L)=TB	GELG1130
C		GELG1140
C	SAVE COLUMN INTERCHANGE INFORMATION	GELG1150
	A(LST)=J	GELG1160
C		GELG1170
C	ELEMENT REDUCTION AND NEXT PIVOT SEARCH	GELG1180
	PIV=0.	GELG1190
	LST=LST+1	GELG1200
	J=0	GELG1210
	DO 16 II=LST,LEND	GELG1220
	PIVI=-A(II)	GELG1230
	IST=II+M	GELG1240
	J=J+1	GELG1250
	DO 15 L=IST,MM,M	GELG1260
	LL=L-J	GELG1270
	A(L)=A(L)+PIVI*A(LL)	GELG1280
	TB=ABS(A(L))	GELG1290
	IF(TB-PIV)15,15,14	GELG1300
	14 PIV=TB	GELG1310
	I=L	GELG1320
	15 CONTINUE	GELG1330
	DO 16 L=K,MM,M	GELG1340
	LL=L+J	GELG1350
	16 R(LL)=R(LL)+PIVI*R(L)	GELG1360
	17 LST=LST+M	GELG1370
C	END OF ELIMINATION LOOP	GELG1380
C		GELG1390
C		GELG1400
C	BACK SUBSTITUTION AND BACK INTERCHANGE	GELG1410
	18 IF(M-1)23,22,19	GELG1420

```

19 IST=MM+M
   LST=M+1
   DO 21 I=2,M
     II=LST-I
     IST=IST-LST
     L=IST-M
     L=A(L)+.5
     DO 21 J=II,NM,M
       TB=R(J)
       LL=J
       DO 20 K=IST,MM,M
         LL=LL+1
20  TB=TB-A(K)*R(LL)
     K=J+L
     R(J)=R(K)
21  R(K)=TB
22  RETURN
C
C
C   ERROR RETURN
23  IER=-1
   RETURN
   END

```

```

GELG1430
GELG1440
GELG1450
GELG1460
GELG1470
GELG1480
GELG1490
GELG1500
GELG1510
GELG1520
GELG1530
GELG1540
GELG1550
GELG1560
GELG1570
GELG1580
GELG1590
GELG1600
GELG1610
GELG1620
GELG1630
GELG1640
GELG1650

```

SUBROUTINE GAUSHA (NPROB,FOF,NDB,Y,NQ,TH,DIFZ,SIGNS,EP1S,
1 EP2S,MIT,FLAM,FNU)

GAUS0010
GAUS0020

VERSION MIT/1

THIS VERSION OF GAUSHA HAS BEEN CONVERTED FOR USE ON THE MIT-IBM
360/65
KIM DAVID SAUNDERS DEPARTMENT OF METEOROLOGY

SUBROUTINES REQUIRED:
GAUS6C (SPECIAL)
SIMQ (SSP)
MINV (SSP)
ALLMAT (MATHLIB)

THE CALLING SEQUENCE IS:
CALL GAUSHA(NPROB,FOF,NDB,Y,NP,TH,DIFF,SIGNS,EP1,EP2,MIT,FLAM,
FNU,SCTRAT)

DESCRIPTION OF THE INPUT PARAMETERS

NPROB	INTEGER CONSTANT GIVING THE PROBLEM NUMBER
FOF	THE NAME OF THE USER SUPPLIED SUBRPOGRAM. IT MUST BE DECLARED EXTERNAL IN THE MAIN PROGRAM.
NDB	NUMBER OF OBSERVATIONS
Y	ONE DIMENSIONAL ARRAY CONTAINING THE OBSERVED

C FUNCTION VALUES.
 C NP NUMBER OF UNKNOWN PARAMETERS.
 C TH ONE DIMENSIONAL ARRAY CONTAINING THE PARAMETER VALUES
 C BEFORE THE SUBPROGRAM IS EXECUTED, TH MUST CONTAIN
 C AN INITIAL GUESS, WHICH MAY HAVE NO ZERO COMPONENT.
 C DIFF ONE DIMENSIONAL ARRAY CONTAINING A VECTOR OF
 C PROPORTIONS USED IN CALCULATING THE DIFFERENCE QUO-
 C IENTS. DIFF(I) MUST BE GT.0 AND LT.1
 C SIGNS IF SET = 0 , THERE IS NO RESTRICTION ON THE SIGNS OF
 C THE PARAMETERS. IF .GT. 0, THE SIGNS MUST REMAIN THE
 C SAME AS THOSE OF THE INITIAL GUESS.
 C EPS1 REAL CONSTANT WHICH IS THE SUM OF SQUARES CONVERGENCE
 C CRITERION. IF EPS1 = 0 , THIS FEATURE IS DISABLED.
 C EPS2 A REAL CONSTANT WHICH IS THE PARAMETER CONVERGENCE
 C CRITERION. IF EPS2 = 0, THIS FEATURE IS DISABLED.
 C MIT MAXIMUM NUMBER OF ITERATIONS.
 C FLAM STARTING VALUE FOR LAMDA. (.01 USUALLY WORKS WELL)
 C FNU STARTING VALUE FOR NU. IT MUST BE .GT.1
 C SCTRAT A WORKING VECTOR. IT MUST BE LARGER THAN:
 C 5*NP+2*NP**2+2*NOB+NP*NOB

C
 C IF THERE ARE ANY QUESTIONS, SEE KIM DAVID SAUNDERS
 C 54-1310
 C EXT 5938

C *****

C
 C DIMENSION A(10,10),D(10,10),DELZ(300,10)
 C DIMENSION LLCL(10),LLDM(10)
 C DIMENSION AXX(100)
 C DIMENSION TH(10),DIFZ(10),SIGNS(10),Y(50)
 C DIMENSION VECTR(50)
 C COMPLEX AAA(10,10),PPP(10)

COMMON Q(10),P(10),E(10),PHI(10),TB(10)	GAUS0040
COMMON F(300),R(300)	GAUS0050
COMMON /BLK1/X	
DATA DET/1./	
DATA LP/6/	GAUS0070
NP=NQ	GAUS0080
NPROB=NPRB0	
NOB=NBJ	
EPS1=EP1S	
EPS2=EP2S	
WRITE(LP,1000) NPRJB,NOB,NP	GAUS0090
WRITE(LP,1001)	GAUS0100
CALL GAUS60 (1,NP,TH,TEMP,TEMP)	
WRITE(LP,1002)	GAUS0120
CALL GAUS60 (1,NP,DIFZ,TEMP,TEMP)	
IF(NP.LT.1 .OR. NP.GT.50 .OR. NOB.LT.NP) GO TO 99	GAUS0140
IF(MIT.LT.1 .OR. MIT.GT.999 .OR. FNU .LT. 1) GO TO 99	GAUS0150
DO 19 I=1,NP	GAUS0160
TEMP = DIFZ(I)	GAUS0170
IF(TEMP) 17,99,18	GAUS0180
17 TEMP = -TEMP	GAUS0190
18 IF(TEMP .GE. 1 .OR. TH(I) .EQ. 0) GO TO 99	GAUS0200
19 CONTINUE	GAUS0210
GA = FLAM	GAUS0220
NIT = 1	GAUS0230
ASSIGN 225 TO IRAN	GAUS0240
ASSIGN 265 TO JORDAN	GAUS0250
ASSIGN 180 TO KUWAIT	GAUS0260
IF(EPS1 .GE. 0) GO TO 10	GAUS0270
EPS1 = 0	GAUS0280
10 IF(EPS2 .GT. 0) GO TO 30	GAUS0290
IF(EPS1 .GT. 0) GO TO 50	GAUS0300
ASSIGN 270 TO IRAN	GAUS0310
GO TO 70	GAUS0320
50 ASSIGN 265 TO IRAN	GAUS0330
GO TO 70	GAUS0340

30	IF(EPS1 .GT. 0) GO TO 70	GAUS0350
	ASSIGN 270 TO JORDAN	GAUS0360
70	SSQ = 0	GAUS0370
	CALL FOF(NPROB,TH,F,NOB,NP)	GAUS0380
	DO 90 I=1,NOB	GAUS0390
	R(I) = Y(I) - F(I)	GAUS0400
90	SSQ = SSQ + R(I)*R(I)	GAUS0410
	WRITE(LP,1003) SSQ	GAUS0420
	GO TO 105	GAUS0430
C		GAUS0440
C	** BEGIN ITERATION	GAUS0450
C		GAUS0460
100	WRITE(LP,1004) NIT	GAUS0470
105	GA = GA/FNU	GAUS0480
	INTCOU = 0	
	DO 130 J=1,NP	GAUS0500
	TEMP = TH(J)	GAUS0510
	P(J) = DIFZ(J)*TH(J)	GAUS0520
	TH(J) = TH(J) + P(J)	GAUS0530
	Q(J) = 0	GAUS0540
	CALL FOF(NPROB,TH,VECTR,NCB,NP)	
	DO 5010 I = 1,NOB	
5010	DELZ(I,J) = VECTR(I)	GAUS0560
	DO 120 I=1,NOB	GAUS0570
	DELZ(I,J) = DELZ(I,J) - F(I)	GAUS0580
120	Q(J) = Q(J) + DELZ(I,J)*R(I)	GAUS0590
	Q(J) = Q(J)/P(J)	GAUS0600
C		GAUS0610
C	** Q=XT*R (STEEPEST DESCENT)	GAUS0620
C		GAUS0630
130	TH(J) = TEMP	GAUS0640
	DO 150 I=1,NP	GAUS0650
	DO 151 J=1,I	GAUS0660
	SUM = 0.0	GAUS0670
	DO 160 K=1,NOB	GAUS0680
160	SUM = SUM + DELZ(K,I)*DELZ(K,J)	

TEMP = SUM/(P(I)*P(J))	GAUS0690
D(J,I) = TEMP	GAUS0700
151 D(I,J) = TEMP	GAUS0710
C	GAUS0720
C ** D=XT*X (MOMENT MATRIX)	GAUS0730
C	GAUS0740
150 E(I) = SQRT(D(I,I))	GAUS0750
GO TO KUWAIT,(180,666)	
C	GAUS0770
C ** ITERATION 1 ONLY	GAUS0780
C	GAUS0790
180 DO 200 I=1,NP	GAUS0800
DO 200 J=1,I	GAUS0810
SUM = D(I,J)	GAUS0820
A(J,I) = SUM	GAUS0830
200 A(I,J) = SUM	GAUS0840
WRITE(6,5003)	
WRITE(6,5004)((A(I,J),I=1,NP),J=1,NP)	
WRITE(6,5003)	
5003 FORMAT(1H1)	
5004 FORMAT(E20.8)	
DO 5000 IKX = 1,NP	
DO 5000 JKX = 1,NP	
PPP(IKX) = P(IKX)	
5000 AAA(IKX,JKX) = A(IKX,JKX)	
CALL ALLMAT(AAA,PPP,NP,10,NCALL)	
DO 5001 IKX = 1,NP	
DO 5001 IKJ = 1,NP	
P(IKX) = REAL(PPP(IKX))	
5001 A(IKX,IKJ) = REAL(AAA(IKX,IKJ))	
WRITE(LP,1006)	GAUS0860
WRITE(LP,2001) (P(I),I=1,NP)	GAUS0870
WRITE(LP,1004) NIT	GAUS0880
ASSIGN 666 TO KUWAIT	GAUS0890
C	GAUS0900
C ** END ITERATION 1 ONLY	GAUS0910

C	666	DO 153 I=1,NP	GAUS0920
		DO 153 J=1,I	GAUS0930
		A(I,J) = D(I,J)/(E(I)*E(J))	GAUS0940
	153	A(J,I) = A(I,J)	GAUS0950
C			GAUS0960
C	**	A = SCALED MOMENT MATRIX	GAUS0970
C			GAUS0980
		DO 155 I=1,NP	GAUS0990
		P(I) = Q(I)/E(I)	GAUS1000
		PHI(I) = P(I)	GAUS1010
	155	A(I,I) = A(I,I) + GA	GAUS1020
		I = 1	GAUS1030
		IKK = 0	GAUS1040
		DO 8000 I = 1,NP	
		DO 8000 J = 1,NP	
		IKK = IKK + 1	
		AXXX(IKK) = A(I,J)	
	8000	CONTINUE	
		CALL SIMQ(AXXX,P,NP,KKS)	
C			GAUS1060
C	**	P/E = CORRECTICN VECTOR	GAUS1070
C			GAUS1080
		STEP = 1.0	GAUS1100
		SUM1 = 0.0	
		SUM2 = 0.0	
		SUM3 = 0.0	
		DO 231 I=1,NP	GAUS1120
		SUM1 = P(I)*PHI(I) + SUM1	GAUS1130
		SUM2 = P(I)*P(I) + SUM2	GAUS1140
	231	SUM3 = PHI(I)*PHI(I) + SUM3	GAUS1150
		TEMP = SUM1/SQRT(SUM2*SUM3)	GAUS1160
		IF(TEMP .LE. 1.0) GO TO 233	GAUS1170
		TEMP = 1.0	GAUS1180
	233	TEMP = 57.295* COS(TEMP)	
		WRITE(LP,1041) TEMP	GAUS1200

170	DO 220 I=1,NP	GAUS1210
220	TB(I) = P(I)*STEP/E(I) + TH(I)	GAUS1220
	WRITE(LP,7000)	GAUS1230
7000	FORMAT('0TEST POINT PARAMETER VALUES')	GAUS1240
	WRITE(LP,2006) (TB(I),I=1,NP)	GAUS1250
	DO 2401 I=1,NP	GAUS1260
	IF(SIGNS(I).GT.0.0 .AND. TH(I)*TB(I).LE.0.0) GO TO 663	GAUS1270
2401	CONTINUE	GAUS1280
	SUMB = 0.0	GAUS1290
	CALL FOF(NPROB,TB,F,NCB,NP)	GAUS1300
	DO 230 I=1,NOR	GAUS1310
	R(I) = Y(I) - F(I)	GAUS1320
230	SUMB = SUMB + R(I)*R(I)	GAUS1330
	WRITE(LP,1043) SUMB	GAUS1340
	IF(SUMB/SSQ-1.0 .LE. EPS1) GO TO 662	GAUS1350
663	IF(TEMP .GT. 30.0) GO TO 664	GAUS1360
	STEP = STEP/2.0	GAUS1370
	INTCOU = INTCOU +1	
	IF(INTCOU - 36) 170,2700,2700	
664	GA = GA*FNU	GAUS1400
	INTCOU = INTCOU +1	
	IF(INTCOU - 36) 666,2700,2700	
662	WRITE(LP,1007)	GAUS1430
	DO 669 I=1,NP	GAUS1440
669	TH(I) = TB(I)	GAUS1450
	CALL GAUS60 (1,NP,TH,TEMP,TEMP)	
	WRITE(LP,1040) GA,SUMB	GAUS1470
	GO TO IRAN,(225,265,270)	
225	DO 240 I=1,NP	GAUS1490
	IF(ABS(P(I)*STEP/E(I))/(1.0E-20+ABS(TH(I)))-EPS2) 240,240,250	GAUS1500
240	CONTINUE	GAUS1510
	WRITE(LP,1009) EPS2	GAUS1520
	GO TO 280	GAUS1530
250	GO TO JORDAN,(265,270)	
265	IF(ABS((SUMB-SSQ)/SSQ) .GT. EPS1) GO TO 270	GAUS1550
260	WRITE(LP,1010) EPS1	GAUS1560

GO TO 28C		GAUS1570
270 SSQ = SUMB		GAUS1580
NIT = NIT+1		GAUS1590
IF(NIT - MIT) 100,100,280		GAUS1600
2700 WRITE(LP,2710)		GAUS1610
2710 FORMAT(//'0**** THE SUM OF SQUARES CANNOT BE REDUCED TO THE SUM OF	1 SQUARES AT THE END OF THE LAST ITERATION - ITERATING STOPS' //)	GAUS1620
C		GAUS1630
C ** END ITERATION		GAUS1640
C		GAUS1650
280 WRITE(LP,1011)		GAUS1660
WRITE(LP,2001) (F(I),I=1,NDB)		GAUS1670
WRITE(LP,1012)		GAUS1680
WRITE(LP,2001) (R(I),I=1,NDB)		GAUS1690
SSQ = SUMB		GAUS1700
IDF = NCB-NP		GAUS1710
WRITE(LP,1015)		GAUS1720
I = 0		GAUS1730
IKK = 0		GAUS1740
DO 8001 I = 1,NP		
DO 8001 J = 1,NP		
IKK = IKK + 1		
AXXX(IKK) = D(I,J)		
8001 CJNTINUE		
CALL MINV(AXXX,NP,DET,LLQL,LLCM)		
IKK = 0		
DO 8002 I = 1,NP		
DO 8002 J = 1, NP		
IKK = IKK + 1		
D(I,J) = AXXX(IKK)		
8002 CJNTINUE		
DO 7692 I=1,NP		GAUS1760
7692 E(I) = SQRT(D(I,I))		GAUS1770
DO 340 I=1,NP		GAUS1780
DO 340 J=I,NP		GAUS1790
A(J,I) = D(J,I)/(E(I)*E(J))		GAUS1800

	D(J,I) = D(J,I)/(DIFZ(I)*TH(I)*DIFZ(J)*TH(J))	GAUS1810
	D(I,J) = D(J,I)	GAUS1820
340	A(I,J) = A(J,I)	GAUS1830
	CALL GAUS60 (3,NP,TEMP,TEMP,A)	
7057	WRITE(LP,1016)	GAUS1850
	CALL GAUS60 (1,NP,E,TEMP,TEMP)	
	IF(IDF .LE. 0) GO TO 410	GAUS1870
	SDEV = SSQ/IDF	GAUS1880
	WRITE(LP,1014) SDEV, IDF	GAUS1890
	SDEV = SQRT(SDEV)	GAUS1900
	DO 391 I=1,NP	GAUS1910
	P(I) = TH(I) + 2.0*E(I)*SDEV	GAUS1920
391	TB(I) = TH(I) - 2.0*E(I)*SDEV	GAUS1930
	WRITE(LP,1029)	GAUS1940
	CALL GAUS60 (2,NP,TB,P,TEMP)	
	DO 415 K=1,NCB	GAUS1960
	TEMP = 0.0	GAUS1970
	DO 420 I=1,NP	GAUS1980
	DO 420 J=1,NP	GAUS1990
420	TEMP = TEMP + DELZ(K,I)*DELZ(K,J)*D(I,J)	GAUS2000
	TEMP = 2.0*SQRT(TEMP)*SDEV	GAUS2010
	R(K) = F(K) + TEMP	GAUS2020
415	F(K) = F(K) - TEMP	GAUS2030
	WRITE(LP,1008)	GAUS2040
	IE = 0	GAUS2050
	DO 425 I=1,NOB,10	GAUS2060
	IE = IE + 10	GAUS2070
	IF(NOB-IE) 430,435,435	GAUS2080
430	IE = NOB	GAUS2090
435	WRITE(LP,2001) (R(J),J=I,IE)	GAUS2100
425	WRITE(LP,2006) (F(J),J=I,IE)	GAUS2110
410	WRITE(LP,1033) NPROB	GAUS2120
	RETURN	GAUS2130
99	WRITE(LP,1034)	GAUS2140
	GO TO 410	GAUS2150
1000	FORMAT('1NON-LINEAR ESTIMATION, PROBLEM NUMBER ',I3// I5,	GAUS2160

```

1 ' OBSERVATIONS ',15,' PARAMETERS') GAUS2170
1001 FORMAT(''0INITIAL PARAMETER VALUES') GAUS2180
1002 FORMAT(''0PROPORTIONS USED IN CALCULATING DIFFERENCE QUOTIENTS') GAUS2190
1003 FORMAT(''0INITIAL SUM OF SQUARES = ',E12.4) GAUS2200
1004 FORMAT(''0ITERATION NO. ',I4) GAUS2210
1005 FORMAT(''0DETERMINANT = ',E12.4) GAUS2220
1006 FORMAT(''0EIGENVALUES OF MOMENT MATRIX - PRELIMINARY ANALYSIS') GAUS2230
1007 FORMAT(''0PARAMETER VALUES VIA REGRESSION') GAUS2240
1008 FORMAT(''0APPROXIMATE CONFIDENCE LIMITS FOR EACH FUNCTION VALUEGAUS2250
1 ' ') GAUS2260
1009 FORMAT(''0ITERATION STOPS - RELATIVE CHANGE IN EACH PARAMETER LESSGAUS2270
1 THAN ',E12.4) GAUS2280
1010 FORMAT(''0ITERATION STOPS - RELATIVE CHANGE IN SUM OF SQUARES LESSGAUS2290
1 THAN ',E12.4) GAUS2300
1011 FORMAT(''1FINAL FUNCTION VALUES ') GAUS2310
1012 FORMAT(''0RESIDUALS') GAUS2320
1014 FORMAT(''0VARIANCE OF RESIDUALS = ',E12.4,' ',I4,
' ' DEGREES OF FREEDOM') GAUS2330
1015 FORMAT(''0CORRELATION MATRIX') GAUS2340
1016 FORMAT(''0NORMALIZING ELEMENTS') GAUS2350
1033 FORMAT(''0END OF PROBLEM NO. ',I3) GAUS2370
1034 FORMAT(''0PARAMETER ERROR') GAUS2380
1039 FORMAT(''0INDIVIDUAL CONFIDENCE LIMITS FOR EACH PARAMETER (ON LINEGAUS2390
1AR HYPOTHESIS)') GAUS2400
1040 FORMAT(''0LAMBDA = ',E10.3,40X,'SUM OF SQUARES AFTER REGRESSION ='GAUS2410
1 E17.7) GAUS2420
1041 FORMAT(''0ANGLE IN SCALED COORD. = ',F5.2, ' DEGREES') GAUS2430
1043 FORMAT(''0TEST POINT SUM OF SQUARES = ',E12.4) GAUS2440
2001 FORMAT(/10E12.4) GAUS2450
2006 FORMAT(10E12.4) GAUS2460
END GAUS2470

```

```

SUBROUTINE GAUS60(ITYPE,NQ,A,B,C)
DIMENSION A(NQ),B(NQ),C(NQ,NQ)
DATA LP/6/
NP = NQ
NR = NP/10
LOW = 1
LUP = 10
10 IF(NR) 15,20,30
15 RETURN
20 LUP = NP
30 WRITE(LP,500)(J,J=LOW,LUP)
GO TO (40,60,80),ITYPE
40 WRITE(LP,600)(A(J),J=LOW,LUP)
GO TO 100
60 WRITE(LP,600)(B(J),J=LOW,LUP)
GO TO 40
80 DO 90 I = LOW,LUP
90 WRITE(LP,720) I,(C(J,I),J=LOW,LUP)
LOW2 = LUP + 1
DO 95 I = LOW2,NP
95 WRITE(LP,720)I,(C(J,I),J=LOW,LUP)
100 LOW = LOW + 10
LUP = LUP + 10
NR = NR - 1
GO TO 10
500 FORMAT(/I8,9I12)
600 FORMAT(1CE12.4)
720 FORMAT(1H0,I3,1X,F7.4,9F12.4)
END

```

SUBROUTINE BESJ(X,N,BJ,D,IER)	
IER = 0	
Z = X/3.	KB002
IF(N.EQ.0) GO TO 1	KB003
IF(N.EQ.1) GO TO 2	KB004
IER = 5	KB005
GO TO 7000	KB006
1 IF(Z.GE.1.) GO TO 3	KB007
BJ = 1. - 2.2499997*Z*Z + 1.2656208*Z**4 - .3163866*Z**6	KB008
1 + .0444479*Z**8 - .0039444*Z**10 + .0002100*Z**12	KB009
GO TO 7000	
3 Z = 1./Z	KB011
FU = (((((10.00014476*Z - .00072805)*Z + .00137237)*Z - .00009512)	KB012
1 *Z - .00552740)*Z - .00000077)*Z + .79788456	KB013
THETA=X-.78539816 + (((((.00013558*Z - .00029333)*Z - .00054125)	
1 *Z + .00262573)*Z - .00003954)*Z - .04166397)*Z	KB015
BJ = FU*COS(THETA)/SQRT(X)	KB016
GO TO 7000	
2 IF(Z.GE.1.) GO TO 4	KB018
Z = Z*Z	KB019
BJ=X*(((((((0.0001109*Z - .00031761)*Z + .00443319)*Z - .0394289)	KB020
1 *Z + .21093573)*Z - .5624985)*Z + .5)	
GO TO 7000	KB022
4 Z = 1./Z	KB023
F1=(((((((-0.00020033*Z+.00113653)*Z - .00249511)*Z+ .00017105)*Z	KB024
1 + .01659667)*Z + .00000156)*Z + .79788456	
THET1 = X+(((((((-0.00029166*Z+.00079824)*Z+.00074348)*Z -	KB026
1 .00637879)*Z + .000565)*Z+.12499612)*Z - 2.35619449	KB027
BJ=F1*COS(THET1)/SQRT(X)	
7000 RETURN	KB029
END	

```

C   TEMPERATURE INTERPOLATION PROGRAM FOR DATA COLLECTED ON THE PDP/8S
C   KIM DAVID SAUNDERS MIT 54-1310
C
C   VERSION 2 / 13 JANUARY 1971
C
C
C   DIMENSION THETA(30,20),TEMP(30,20)
C   DIMENSION T(30)
C   DATA T/30*0.0/
C   DATA THETA/600*0.0/,TEMP/600*0.0/,LP,LU/5,6/
C
C   INPUT TEMPERATURE DATA
C
C   10 READ(5,100) NS,NT,THETA(NS,NT),IQQQ
C   100 FORMAT( 2I5,F10.5,58X,I2)
C   IF(IQQQ.EQ.0) GO TO 10
C   NMAX = NS
C
C   REDUCE THE DATA TO DIFFERENCE FORM
C
C   NOT: NS = 1 CORRESPONDS TO TIME = 0.0
C
C   PAGE 2
C
C   WRITE(LC,200)
C   200 FORMAT(1H1)
C   DO 1000 I = 2,NMAX
C   DO 1000 J = 1,20
C   K = I - 1
C   THETA(I,J) = THETA(I,J) - THETA(1,J)
C   1000 WRITE(LO,201) K,J,THETA(I,J)
C   DO 1004 J = 1,20
C   1004 THETA(1,J) = 0.0
C   201 FORMAT(' SERIES NO. = ',I5,5X,' THERMISTOR NO. = ',I5,5X,' DT = ',F

```



```

16.1/)
WRITE(LC,200)
C
C   PERFORM THE INTERPOLATION ON SERIES 1
C
DT = 1.40
DO 1001 J = 1,20
TN1 = 1.40 + (J-1)*0.106
TEMP(2,J) = THETA(2,J)*DT/TN1
1001 CONTINUE
C
C   PAGE 3
C
C
C   COMPUTE THE REST OF THE INTERPOLATED TEMPERATURES
C
DO 1002 I = 2,NMAX
DO 1002 J = 1,20
TN1 = 4.58
DT = (J-1)*0.106
TEMP(I ,J) = (THETA(I+1,J) - THETA(I,J))*DT/TN1 + THETA(I,J)
1002 CONTINUE
DO 1003 I = 2,10
1003 T(I) = (I-2)*4.58 + 1.40
C
C   OUTPUT THE CORRECTED FIELD
C
C
C   PAGE 4
C
WRITE(LC,200)
WRITE(LC,202)
202 FORMAT(' SERIES TIME THERMISTOR CORRECTED TEMPERATURE'//////)
203 FURMAT( 14,3X,F7.3,3X,14,20X,F6.1/)
WRITE(LC,203)((I, T(I),J,TEMP(I,J),J=1,20),I=1,NMAX)
RU = 2.259

```

```
DO 2000 IO = 1, NMAX
LLX = 0
DO 2000 I = 1, 5
DO 2000 J = 1, 4
LLX = LLX + 1
R = RO*(1.-1./2.** (5-I))
Z = 1. - 1./2.** (4-J)
IF (LLX.EQ.3) GO TO 2000
IF (LLX.EQ.9) GO TO 2000
IP = IO - 1
WRITE (7, 204) R, Z, TEMP(IO, LLX), T(IO), IP, LLX
2000 CONTINUE
204 FORMAT( 4F10.4, 2I5)
CALL EXIT
END
```

```

C PROGRAM TO CONVERT POINT DATA INTO POLAR COORDINATES AND CALCULATE
C RADIAL AND AZIMUTHAL VELOCITIES FOR THE STRATIFIED SPIN-UP EXPT.
C KIM DAVID SAUNDERS
C MIT
C OCTOBER 1970
C
C THE MAIN INPUT DATA FOR THE PROGRAM IS FROM THE DIGITIZER
C ON THE THIRD FLOOR OF THE EARTH AND PLANETARY SCIENCE BLDG.
C DEFINITION OF OTHER PARAMETERS:
C RO IS THE RADIUS OF THE CYLINDER IN CM
C H IS THE RATIO OF THE DISTANCE THE PLANE OF LIGHT IS FROM THE
C TOP OF THE CYLINDER TO THE TOTAL HEIGHT OF THE CYLINDER.
C THIS IS NEEDED FOR PARALLAX CORRECTION.
C PSI IS THE PARALLAX CORRECTION FACTOR
C
C DIMENSION R(20,37),THETA(20,36),DR(20,36),DTHET(20,36),TIME(36) ,
1 X(36),Y(36) ,U(20,36),V(20,36)
C DIMENSION TIMP(36) ,HEADR(20)
C DIMENSION EU(20,36),EV(20,36)
C DIMENSION RPLT(36),UPLT(36),VPLT(36),UMGPT(36),TIMK(36)
C READ(5,102) ( HEADR(I),I=1,20)
C READ(5,100) XO,YO,X1,Y1,X2,Y2,H,RO,N
C READ(5,112) EX,ET,IDEX
C READ(5,113) DCMEG,TSPIN
C N = NUMBER OF SERIES IN CURRENT RUN
C INITIALIZE EVERYTHING
C DO 10 I = 1,20
C R(I,37) = 0.0
C DO 10 J=1,36
C EU(I,J) = 0.0
C EV(I,J) = 0.0
C R(I,J) = 0.0
C THETA(I,J) = 0.0
C DR(I,J) = 0.0
C DTHET(I,J) = 0.0
C TIMP(J) = 0.0

```

```

RPLT(J) = 0.0
UPLT(J) = 0.0
VPLT(J) = 0.0
CMGPT(J) = 0.0
TIMK(J) = 0.0
10 TIME(J) = 0.0
R11 = SQRT((X2 - X0)**2 + ( Y2 - Y0)**2)
R00 = SQRT( (X1 - X0)**2 + ( Y1 - Y0)**2)
R0R = R0/R11
PSI = 1. + H*( R11/RCC - 1.)
WRITE(6,105)
WRITE(6,102)( HEADR(I),I=1,20)
WRITE(6,104)
DO 1000 I=1,N
C FIRST CARD IN EACH SERIES MUST HAVE THE FOLLOWING INFORMATION:
C SERIES NO., NO. OF FIRST PICTURE, NO. OF CARDS IN SERIES IN THE
C FORMAT: NSER          NPNOO          NCARD
READ(5,101) NSER, NPNOO, NCARD
NN = NCARD - 1
NNC = NPNOO + NN
DO 1001 J = 1,36
X(J) = 0.0
1001 Y(J) = 0.0
READ( 5,103)(X(J),Y(J),J=NPNOO,NNC )
DO 1002 J = NPNOO,NNC
XP = X(J) - XC
YP = Y(J) - YC
IF(IDEX.EQ.0) GO TO 3000
XP = -XP
3000 CONTINUE
R(NSER,J) = R0R*PSI*SQRT(XP*XP + YP*YP)
THETA(NSER,J) = ATAN2(YP,XP)
1002 IF( THETA(NSER,J).LT.0.0) THETA(NSER,J) = 2.*3.14159+THETA(NSER,J)
1000 CONTINUE
DO 1004 I=1,20
DO 1004 J=1,35

```

```

IF(R(I,J).LE..1) GO TO 1004
DR(I,J) = R(I,J+1) - R(I,J)
DTHET(I,J) = THETA(I,J+1) - THETA(I,J)
IF(DTHET(I,J).LT.0.0) DTHET(I,J) = DTHET(I,J) + 2.*3.14159
1004 CONTINUE
READ(5,110) ( TIME(J),J=1,36)
DO 1006 I = 1,20
DU 1006 J=1,35
IF( ABS(DR(I,J)). LT. .00001) GO TO 1006
DT = TIME(J+1) - TIME(J)
TIMP(J) = 0.5*(TIME(J) + TIME(J+1))
U(I,J) = DR(I,J)/DT
V(I,J) = (DTHET(I,J)/DT)*(R(I,J) + R(I,J+1))/2.
EU(I,J) = ABS(EX/DT)+ABS(ET*DR(I,J)/(DT*DT))
EV(I,J) = ABS(EX/DT) + ABS(ET*V(I,J)/DT)
1006 CONTINUE
WRITE(6,109)
DO 1007 I=1,20
WRITE(6,111)
DU 1007 J = 1,36
IF(R(I,J).GT..1)WRITE(6,107) I ,J,R(I,J),THETA(I,J),TIME(J)
IF( R(I,J).GT..1.AND.R(I,J+1).GT..1) WRITE(6,108)DR(I,J),DTHET(I,J
1),U(I,J),V(I,J) , TIMP(J),EU(I,J) , EV(I,J)
1007 CONTINUE
WRITE(6,105)
CALL EXIT
100 FORMAT( 3(2F5.3, 6X),2F10.5,I5)
101 FORMAT( 5X,I5,10X,I5,5X,I5)
102 FORMAT(20A4)
103 FORMAT( 5(2F5.3, 6X))
104 FORMAT(1H , ////)
105 FORMAT( 1H1)
107 FORMAT( 2I5,3F10.5)
108 FORMAT( 40X,5F15.5/77X,2F10.6)
109 FORMAT(' SERIES PN R THETA TIME DR
1 DTHETA U V TIME'/80X,' ERROR

```

```
      2IN U      ERROR IN V*////)
110 FORMAT(8F10.5)
111 FCRMAT( 1H ,///)
112 FCRMAT( 2F10.5,I5)
113 FORMAT( 2F10.5)
      END
```

C	SUBROUTINE SIMQ(A,B,N,KS)	SIMQ 490
C	THE ABOVE CARD SHOULD BE PLACED IN PROPER SEQUENCE	
C	BEFORE COMPILING THIS UNDER IBM FORTRAN G.	
C	SIMQ 10
C		SIMQ 20
C	SUBROUTINE SIMQ	SIMQ 30
C		SIMQ 40
C	PURPOSE	SIMQ 50
C	OBTAIN SOLUTION OF A SET OF SIMULTANEOUS LINEAR EQUATIONS,	SIMQ 60
C	AX=B	SIMQ 70
C		SIMQ 80
C	USAGE	SIMQ 90
C	CALL SIMQ(A,B,N,KS)	SIMQ 100
C		SIMQ 110
C		SIMQ 120
C	DESCRIPTION OF PARAMETERS	SIMQ 130
C	A - MATRIX OF COEFFICIENTS STORED COLUMNWISE. THESE ARE	SIMQ 140
C	DESTROYED IN THE COMPUTATION. THE SIZE OF MATRIX A IS	SIMQ 150
C	N BY N.	SIMQ 160
C	B - VECTOR OF ORIGINAL CONSTANTS (LENGTH N). THESE ARE	SIMQ 170
C	REPLACED BY FINAL SOLUTION VALUES, VECTOR X.	SIMQ 180
C	N - NUMBER OF EQUATIONS AND VARIABLES. N MUST BE .GT. ONE.	SIMQ 190
C	KS - OUTPUT DIGIT	SIMQ 200
C	0 FOR A NORMAL SOLUTION	SIMQ 210
C	1 FOR A SINGULAR SET OF EQUATIONS	SIMQ 220
C		SIMQ 230
C	REMARKS	SIMQ 240
C	MATRIX A MUST BE GENERAL.	SIMQ 250
C	IF MATRIX IS SINGULAR , SOLUTION VALUES ARE MEANINGLESS.	SIMQ 260
C	AN ALTERNATIVE SOLUTION MAY BE OBTAINED BY USING MATRIX	SIMQ 270
C	INVERSION (MINV) AND MATRIX PRODUCT (GMPRD).	SIMQ 280
C		SIMQ 290
C	SUBROUTINES AND FUNCTION SUBPROGRAMS REQUIRED	SIMQ 300
C	NCNE	SIMQ 310
C		SIMQ 320
C	METHOD	SIMQ 330

```

C      METHOD OF SOLUTION IS BY ELIMINATION USING LARGEST PIVOTAL SIMQ 340
C      DIVISOR. EACH STAGE OF ELIMINATION CONSISTS OF INTERCHANGING SIMQ 350
C      ROWS WHEN NECESSARY TO AVOID DIVISION BY ZERO OR SMALL SIMQ 360
C      ELEMENTS. SIMQ 370
C      THE FORWARD SOLUTION TO OBTAIN VARIABLE N IS DONE IN SIMQ 380
C      N STAGES. THE BACK SOLUTION FOR THE OTHER VARIABLES IS SIMQ 390
C      CALCULATED BY SUCCESSIVE SUBSTITUTIONS. FINAL SOLUTION SIMQ 400
C      VALUES ARE DEVELOPED IN VECTOR B, WITH VARIABLE 1 IN B(1), SIMQ 410
C      VARIABLE 2 IN B(2),....., VARIABLE N IN B(N). SIMQ 420
C      IF NO PIVOT CAN BE FOUND EXCEEDING A TOLERANCE OF 0.0, SIMQ 430
C      THE MATRIX IS CONSIDERED SINGULAR AND KS IS SET TO 1. THIS SIMQ 440
C      TOLERANCE CAN BE MODIFIED BY REPLACING THE FIRST STATEMENT. SIMQ 450
C      SIMQ 460
C      ..... SIMQ 470
C      DIMENSION A(1),B(1) SIMQ 480
C      SIMQ 500
C      FORWARD SOLUTION SIMQ 510
C      SIMQ 520
C      SIMQ 530
C      TOL=0.0 SIMQ 540
C      KS=0 SIMQ 550
C      JJ=-N SIMQ 560
C      DO 65 J=1,N SIMQ 570
C      JY=J+1 SIMQ 580
C      JJ=JJ+N+1 SIMQ 590
C      BIGA=0 SIMQ 600
C      IT=JJ-J SIMQ 610
C      DO 30 I=J,N SIMQ 620
C      SIMQ 630
C      SEARCH FOR MAXIMUM COEFFICIENT IN COLUMN SIMQ 640
C      SIMQ 650
C      IJ=IT+I SIMQ 660
C      IF(ABS(BIGA)-ABS(A(IJ))) 20,30,30 SIMQ 670
20  BIGA=A(IJ) SIMQ 680
C      IMAX=I SIMQ 690
30  CONTINUE SIMQ 700

```


C		SIMQ 710
C	TEST FOR PIVOT LESS THAN TOLERANCE (SINGULAR MATRIX)	SIMQ 720
C		SIMQ 730
	IF (ABS(BIGA)-TOL) 35,35,40	SIMQ 740
	35 KS=1	SIMQ 750
	RETURN	SIMQ 760
C		SIMQ 770
C	INTERCHANGE ROWS IF NECESSARY	SIMQ 780
C		SIMQ 790
	40 I1=J+N*(J-2)	SIMQ 800
	IT=IMAX-J	SIMQ 810
	DO 50 K=J,N	SIMQ 820
	I1=I1+N	SIMQ 830
	I2=I1+IT	SIMQ 840
	SAVE=A(I1)	SIMQ 850
	A(I1)=A(I2)	SIMQ 860
	A(I2)=SAVE	SIMQ 870
C		SIMQ 880
C	DIVIDE EQUATION BY LEADING COEFFICIENT	SIMQ 890
C		SIMQ 900
	50 A(I1)=A(I1)/BIGA	SIMQ 910
	SAVE=B(IMAX)	SIMQ 920
	B(IMAX)=B(J)	SIMQ 930
	B(J)=SAVE/BIGA	SIMQ 940
C		SIMQ 950
C	ELIMINATE NEXT VARIABLE	SIMQ 960
C		SIMQ 970
	IF (J-N) 55,70,55	SIMQ 980
	55 IQS=N*(J-1)	SIMQ 990
	DO 65 IX=JY,N	SIMQ1000
	IXJ=IQS+IX	SIMQ1010
	IT=J-IX	SIMQ1020
	DO 60 JX=JY,N	SIMQ1030
	IXJX=N*(JX-1)+IX	SIMQ1040
	JJX=IXJX+IT	SIMQ1050
	60 A(IXJX)=A(IXJX)-(A(IXJ)*A(JJX))	SIMQ1060

```
65 B(IX)=B(IX)-(B(J)*A(IXJ))
C
C      BACK SOLUTION
C
70 NY=N-1
   IT=N*N
   DO 80 J=1,NY
     IA=IT-J
     IB=N-J
     IC=N
     DO 80 K=1,J
       B(IB)=B(IB)-A(IA)*B(IC)
       IA=IA-N
80 IC=IC-1
   RETURN
   END
```

```
SIMQ1070
SIMQ1080
SIMQ1090
SIMQ1100
SIMQ1110
SIMQ1120
SIMQ1130
SIMQ1140
SIMQ1150
SIMQ1160
SIMQ1170
SIMQ1180
SIMQ1190
SIMQ1200
SIMQ1210
SIMQ1220
```